Chemistry–A European Journal

Supporting Information

Soft Scorpionate Hydridotris(2-mercapto-1-methylimidazolyl) borate) Tungsten-Oxido and -Sulfido Complexes as Acetylene Hydratase Models

Carina Vidovič, Ferdinand Belaj, and Nadia C. Mösch-Zanetti*[a]

TABLE OF CONTENTS:

1 Experimental Section 2

2 NMR spectra 3

3 High-resolution mass spectra 26

4 Crystal Structure Determinations 47

4.1 Stereoscopic ORTEP plots 55

4.2 Selected bond lengths and angels 64

5 References 71

1 EXPERIMENTAL SECTION

Table S1: Behavior of Complexes 1,2 and 4-15 in wet solvents.

	Complex	*Time*	*Behavior*
1	$[W(CO)(C_2H_2)(Tm^{Me})Br]$	24 h	20% oxidation to **4**
4	$[WO(C_2H_2)(Tm^{Me})Br]$	5 days	30% decomposition to free 2-butyne
6	$[WS(C_2H_2)(Tm^{Me})Br]$	5 h 24 h	Formation of 60% of **4** full decomposition
7	$[WS(C_2Me_2)(Tm^{Me})Br]$	24 h	full conversion to **13**
8	$[W_2O(\mu\text{-}O)(C_2Me_2)_2(Tm^{Me})_2](OTf)_2$	24 h	decomposition to beige precipitate but majority of complex still present
9	$[W_2(\mu\text{-}S)_2(C_2Me_2)(Tm^{Me})_2](OTf)_2$	7 days	no changes
10	$[W(CO)(C_2H_2)(MeCN)(Tm^{Me})](OTf)$	24 h	minor decomposition to **4**
11	$[W(CO)(C_2Me_2)(MeCN)(Tm^{Me})](OTf)$	24 h	no changes
12	$[WO(C_2H_2)(MeCN)(Tm^{Me})](OTf)$	24 h 10 days	no significant changes complex still present
13	$[WO(C_2Me_2)(MeCN)(Tm^{Me})](OTf)$	24 h 10 days	13% decomposition complex still present
14	$[WS(C_2H_2)(MeCN)(Tm^{Me})](OTf)$	2 h	46% conversion to **12** and decomposition
15	$[WS(C_2Me_2)(MeCN)(Tm^{Me})](OTf)$	1 h	full conversion to **13**

2 NMR SPECTRA

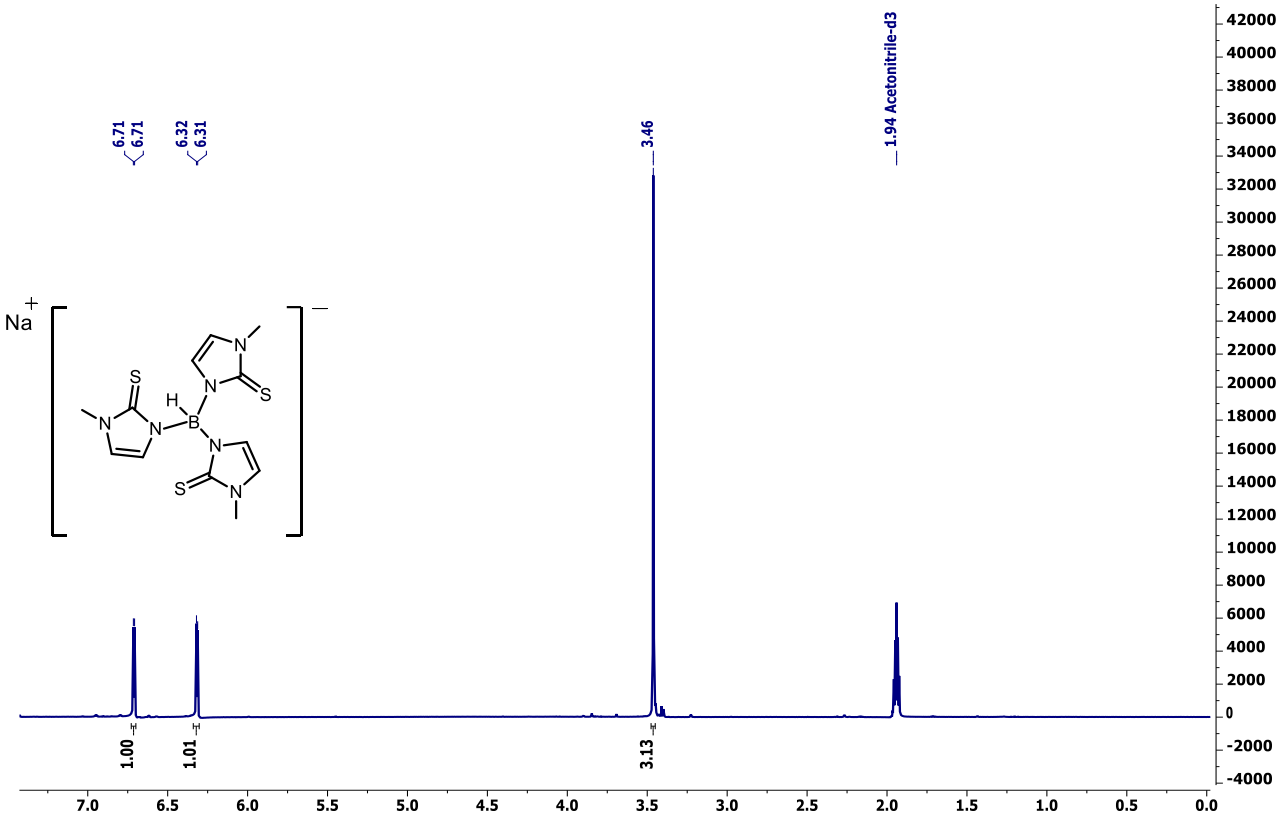

Figure S1: ^{1}H NMR spectrum of NaTm^{Me} in CD_3CN.

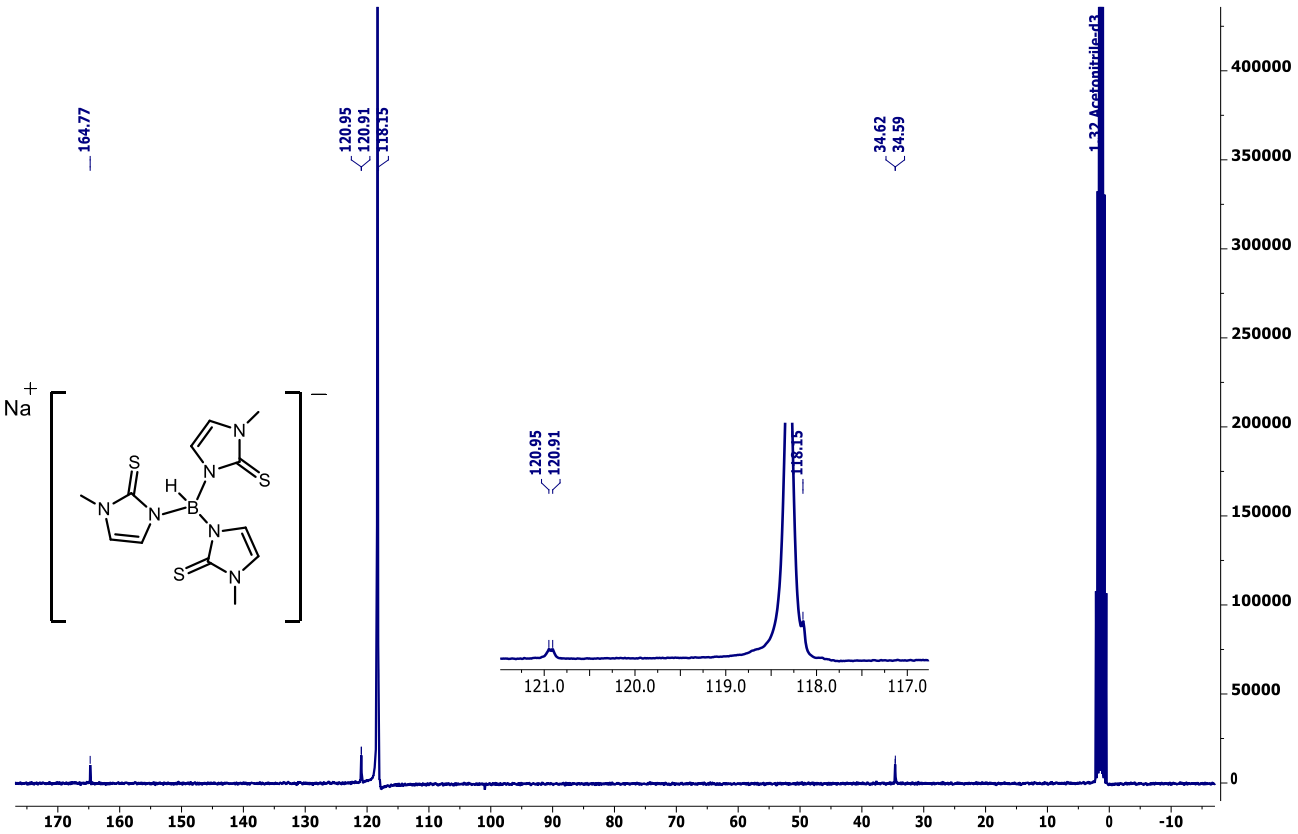

Figure S2: ^{13}C NMR spectrum of NaTm^{Me} in CD_3CN.

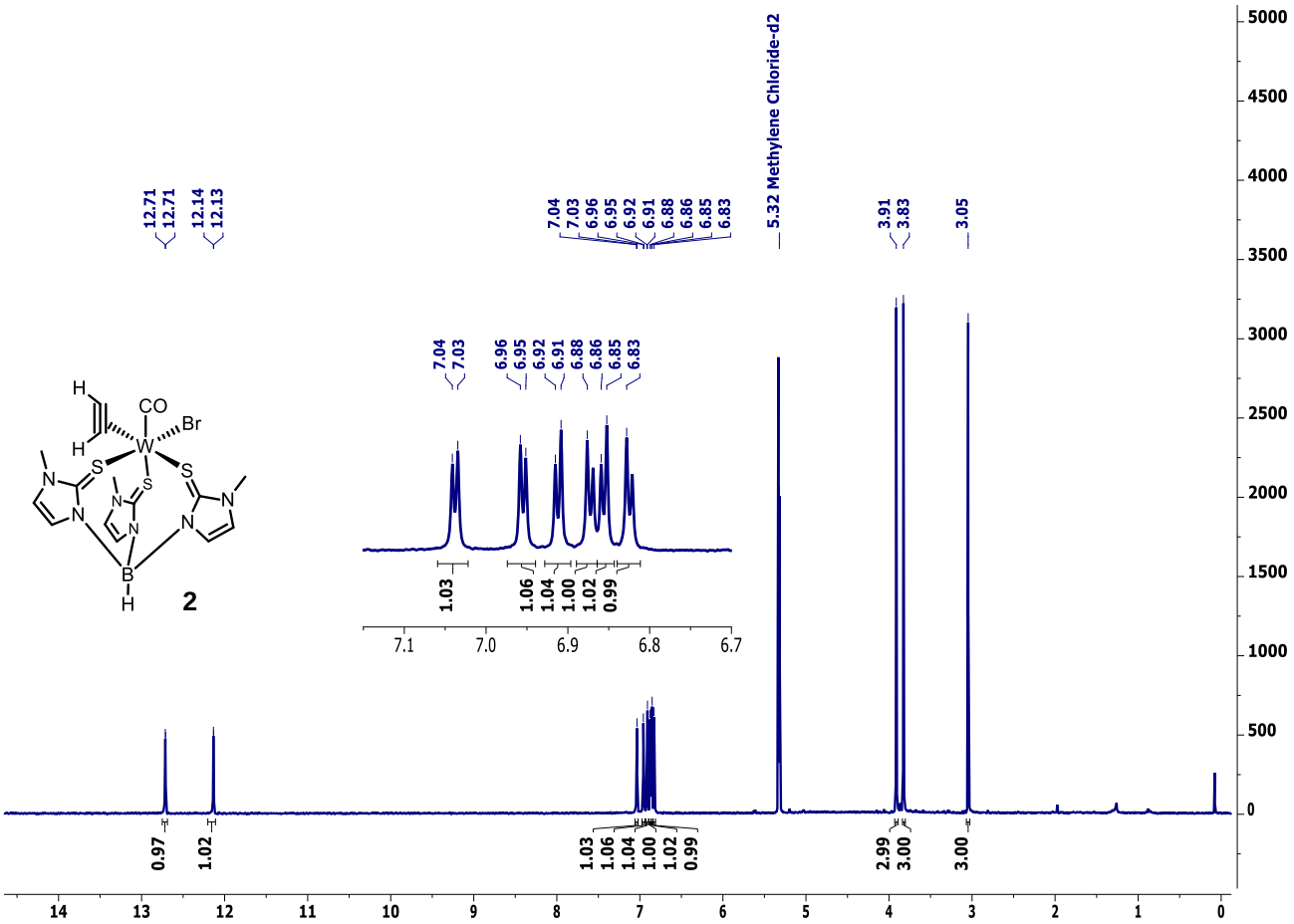

Figure S3: ^{1}H NMR spectrum of [W(CO)(C_2H_2)(Tm^{Me})Br] (**1**) in CD_2Cl_2.

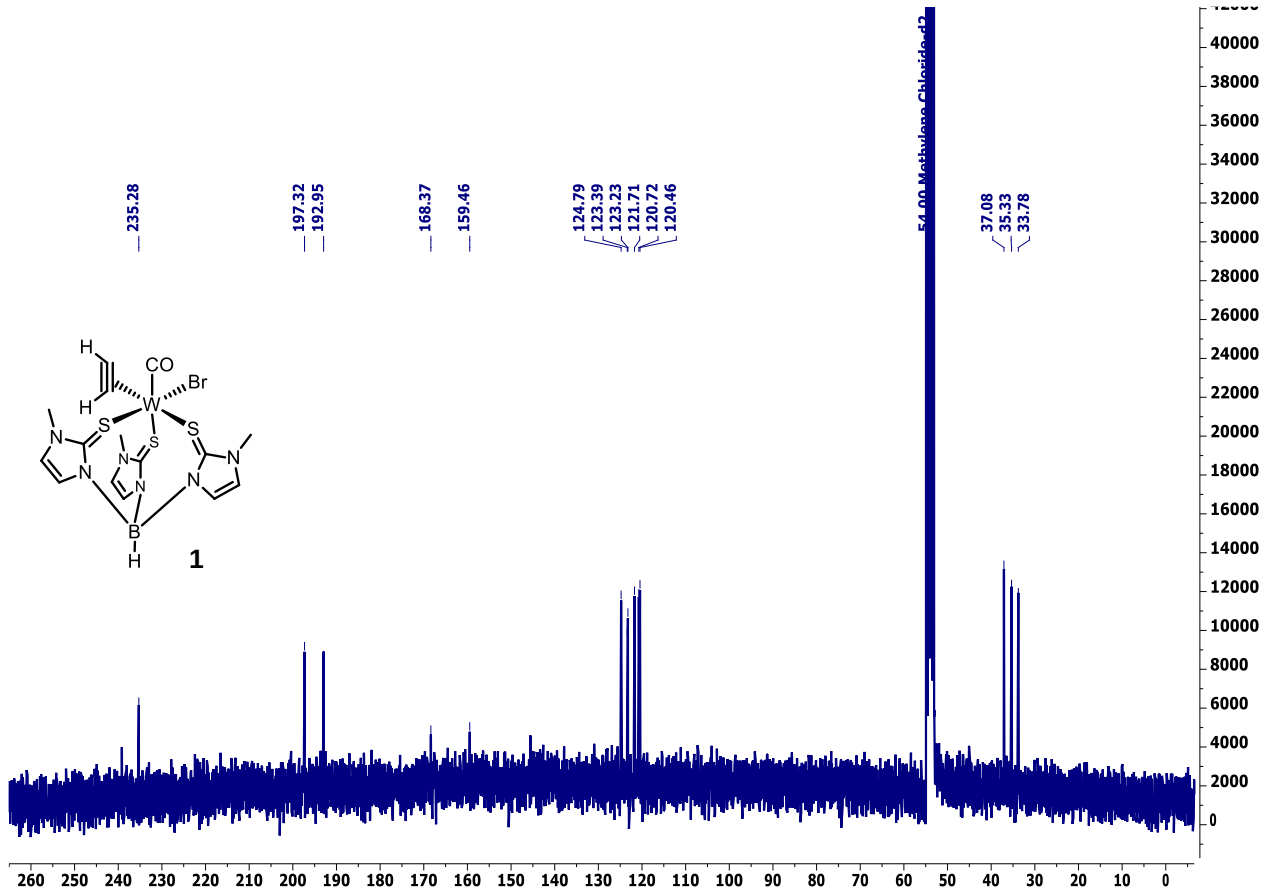

Figure S4: ^{13}C NMR spectrum of [W(CO)(C_2H_2)(Tm^{Me})Br] (**1**) in CD_2Cl_2.

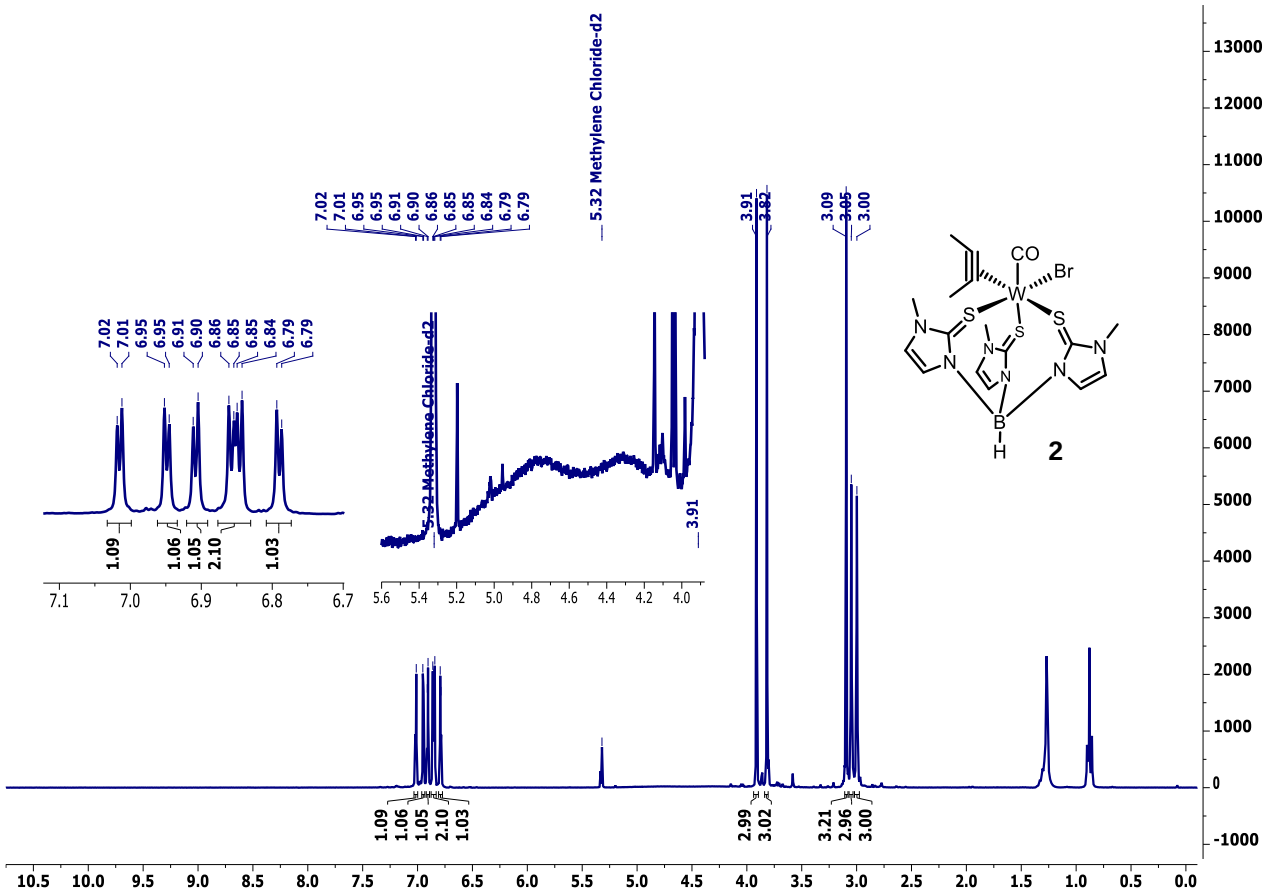

Figure S5: ^{1}H NMR spectrum of [W(CO)(C_2Me_2)(Tm^{Me})Br] (**2**) in CD_2Cl_2.

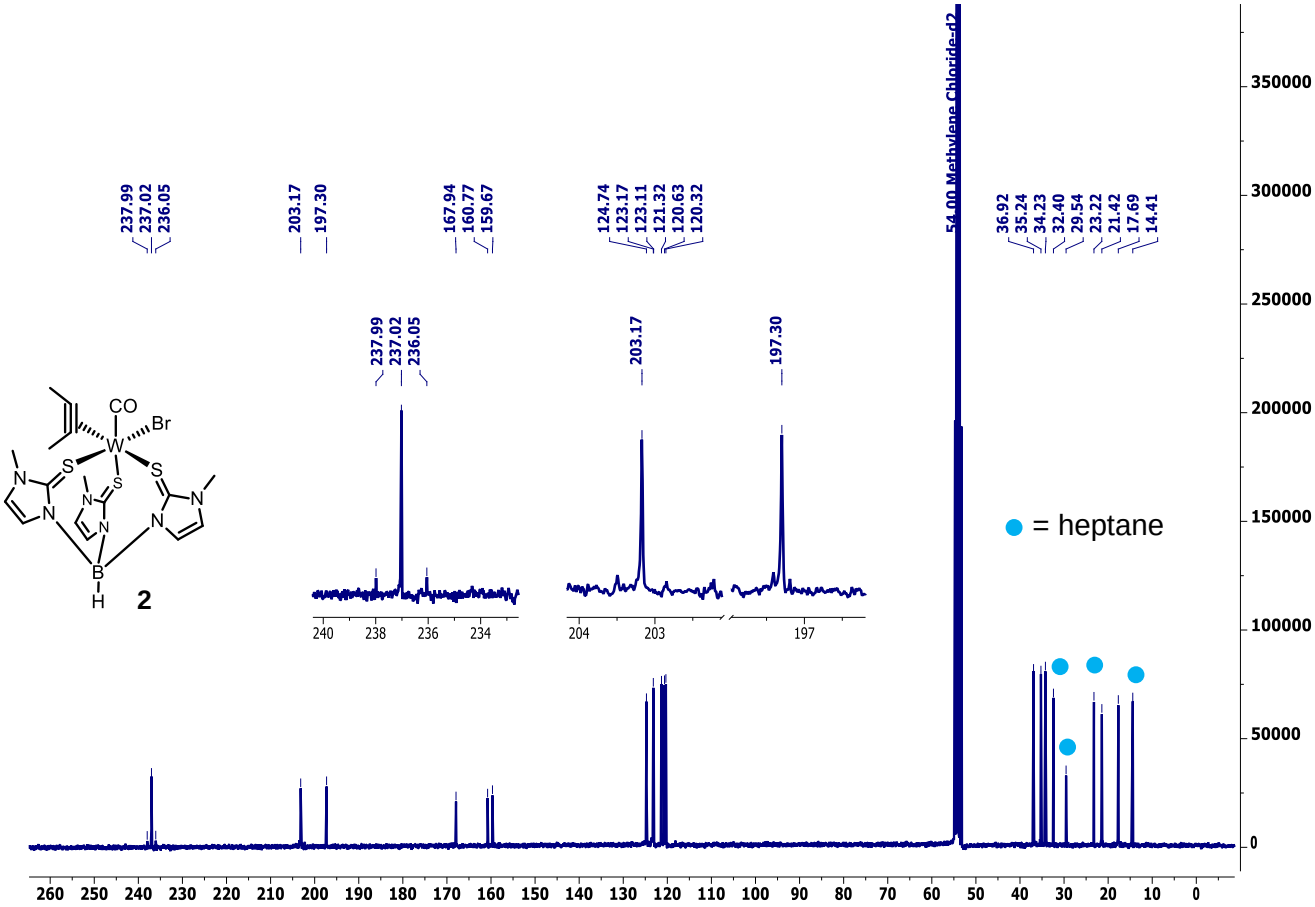

Figure S6: ^{13}C NMR spectrum of [W(CO)(C_2Me_2)(Tm^{Me})Br] (**2**) in CD_2Cl_2.

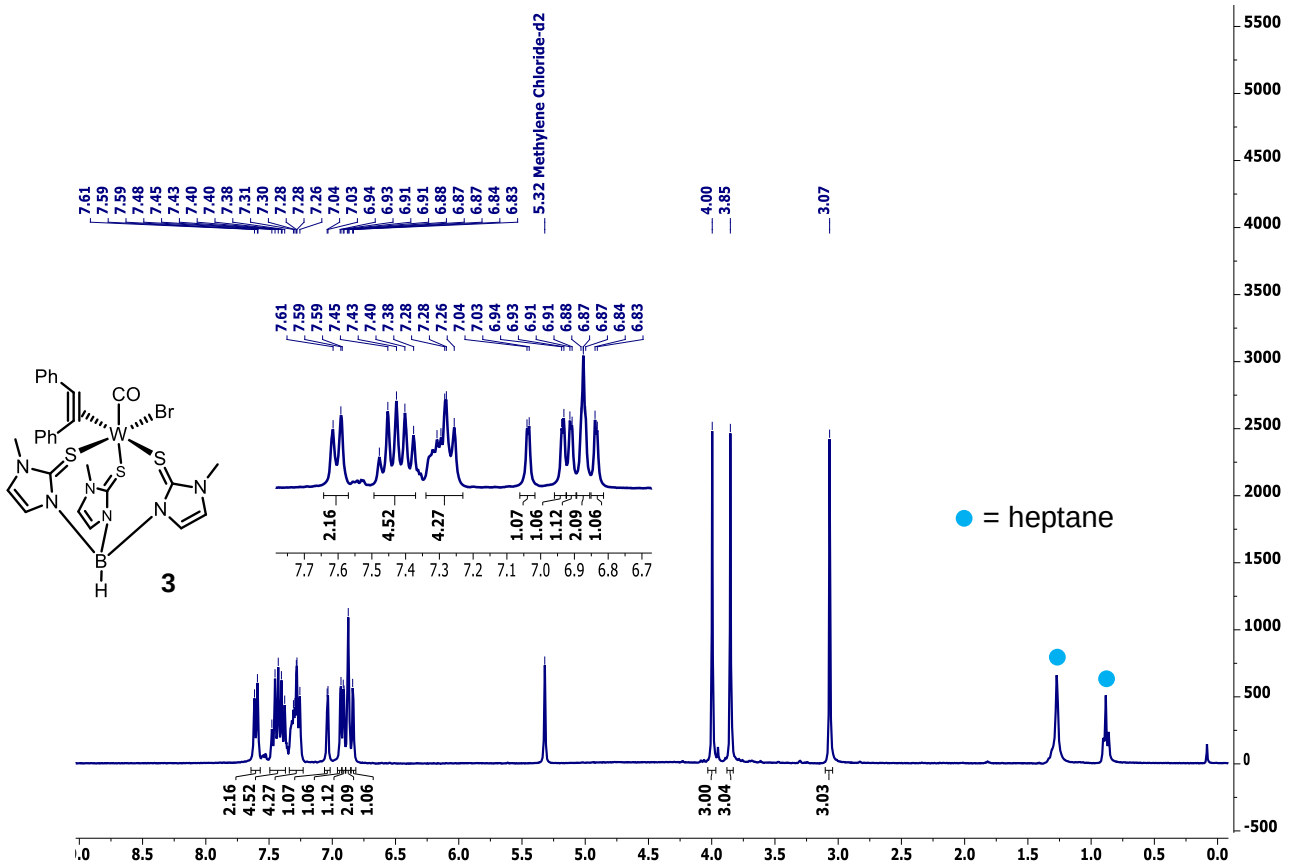

Figure S7: ^{1}H NMR spectrum of [W(CO)(C_2Ph_2)(Tm^{Me})Br] (**3**) in CD_2Cl_2.

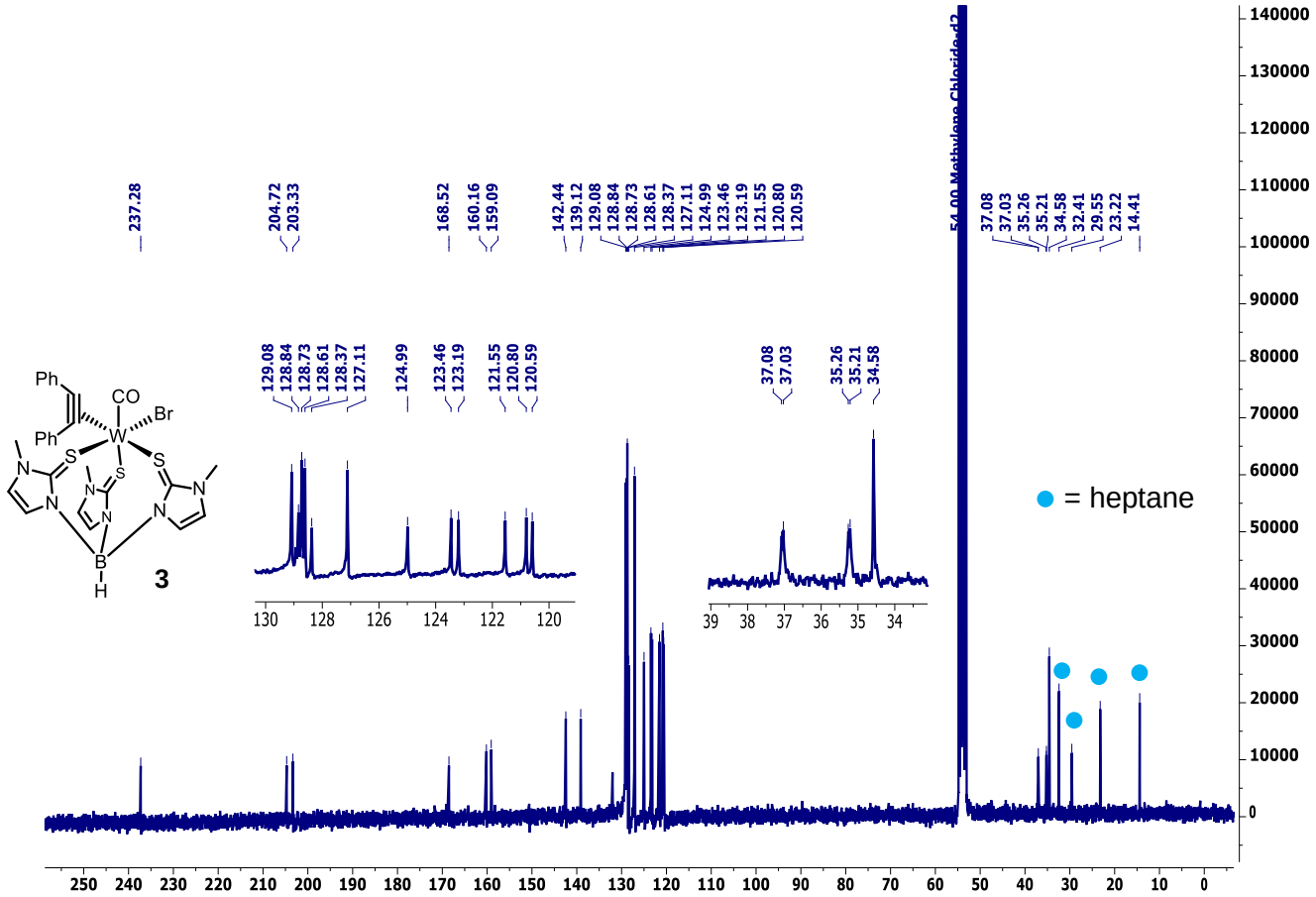

Figure S8: ^{13}C NMR spectrum of [W(CO)(C_2Ph_2)(Tm^{Me})Br] (**3**) in CD_2Cl_2.

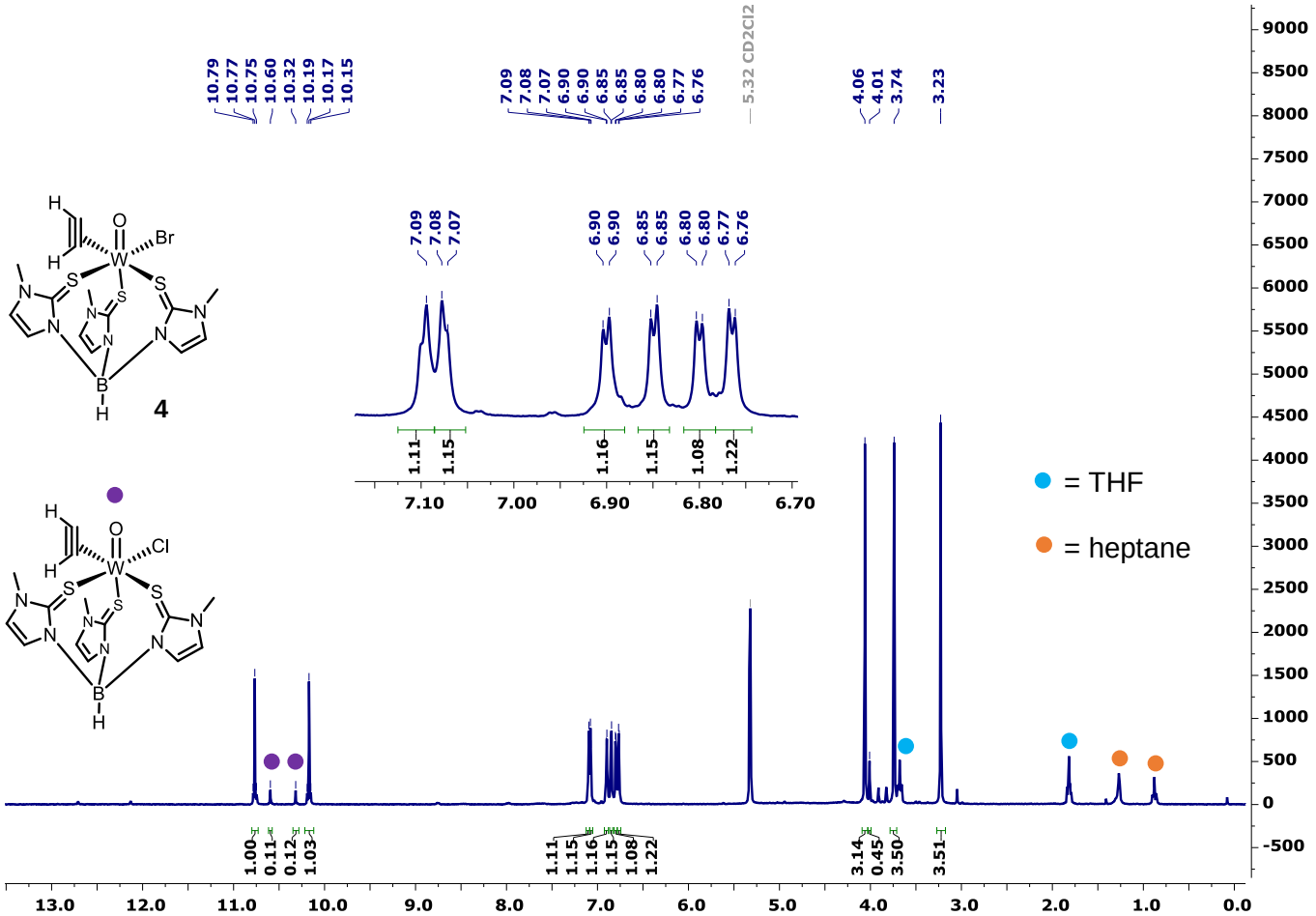

Figure S9: ^{1}H NMR spectrum of [WO(C_2H_2)(Tm^{Me})Br] (**4**) in CD_2Cl_2.

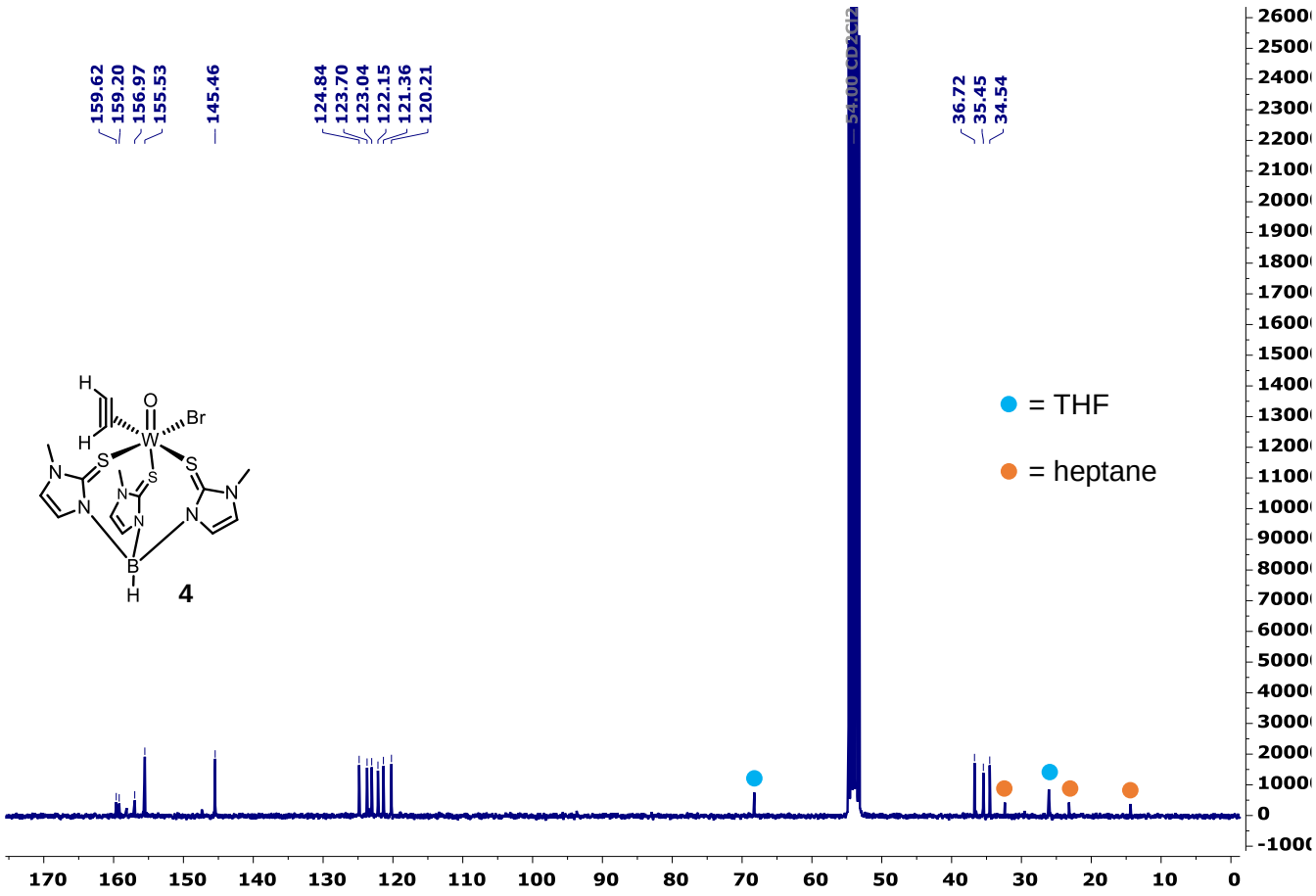

Figure S10: ^{13}C NMR spectrum of [WO(C_2H_2)(Tm^{Me})Br] (**4**) in CD_2Cl_2.

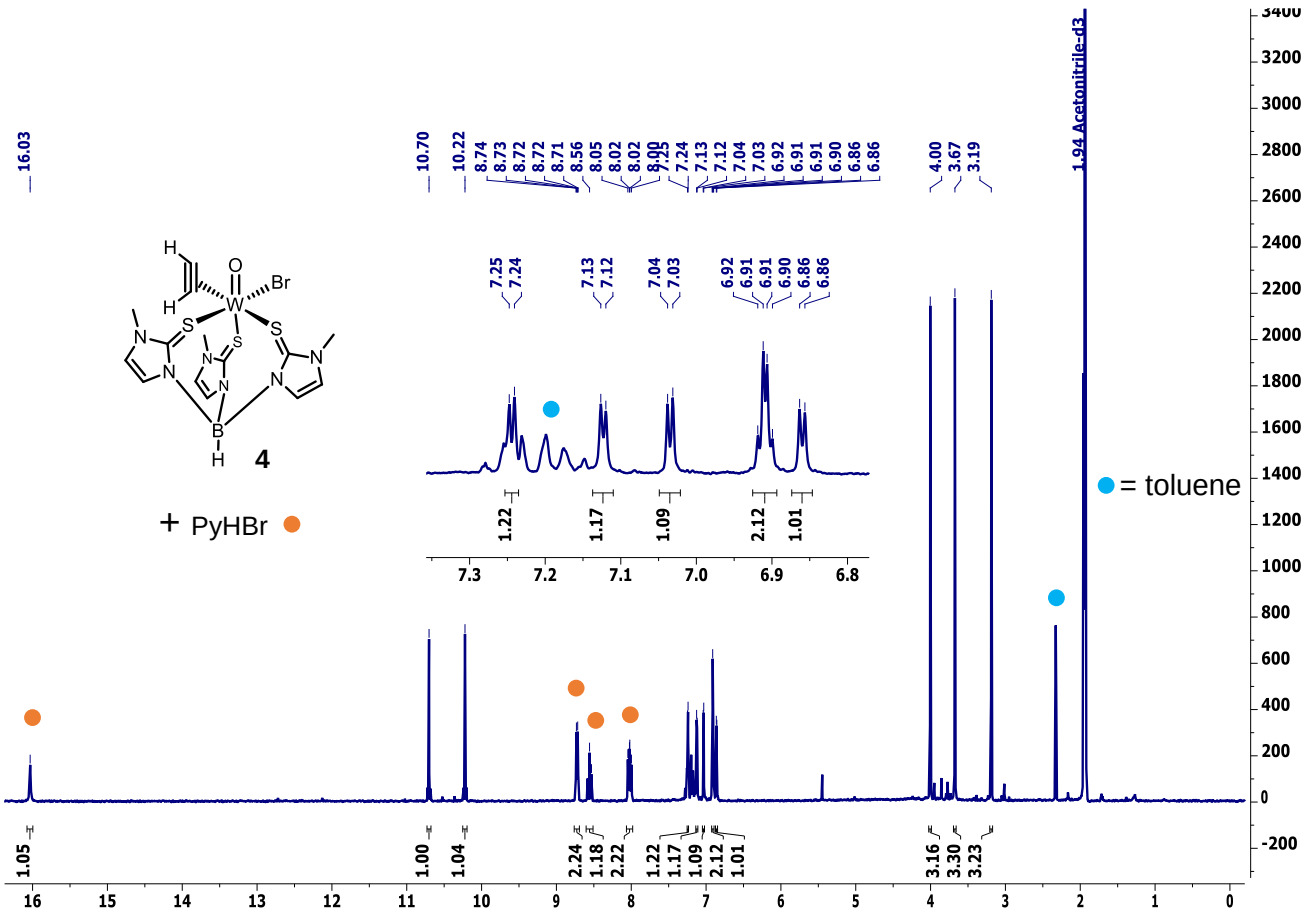

Figure S11: ^{1}H NMR spectrum of [WO(C_2H_2)(Tm^{Me})Br] · PyHBr (**4**) in CD_3CN.

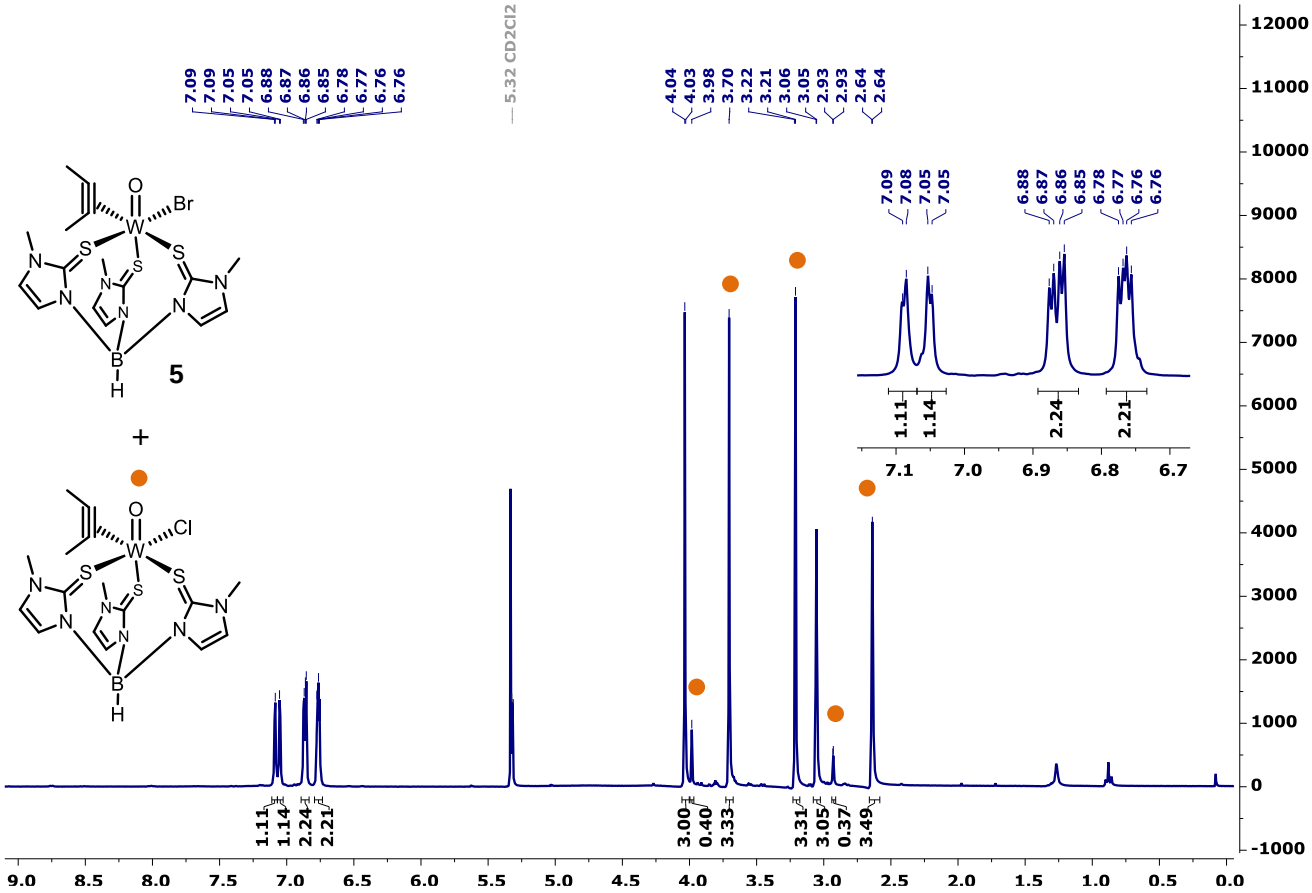

Figure S12: ^{1}H NMR spectrum of [WO(C_2Me_2)(Tm^{Me})Br] (**5**) with small amounts of [WO(C_2Me_2)(Tm^{Me})Cl] in CD_2Cl_2.

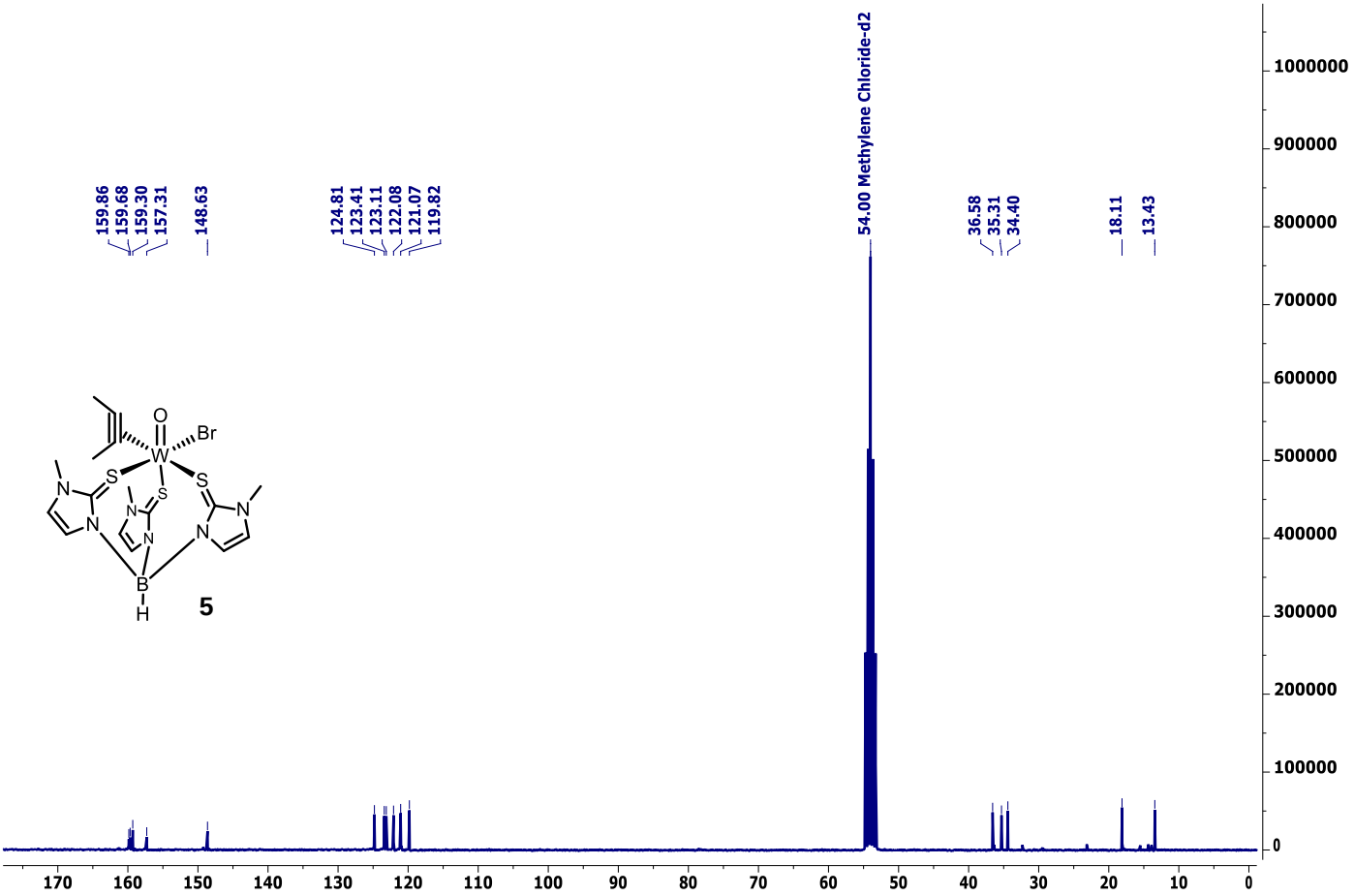

Figure S13: ^{13}C NMR spectrum of [WO(C_2Me_2)(Tm^{Me})Br] (**5**) in CD_2Cl_2.

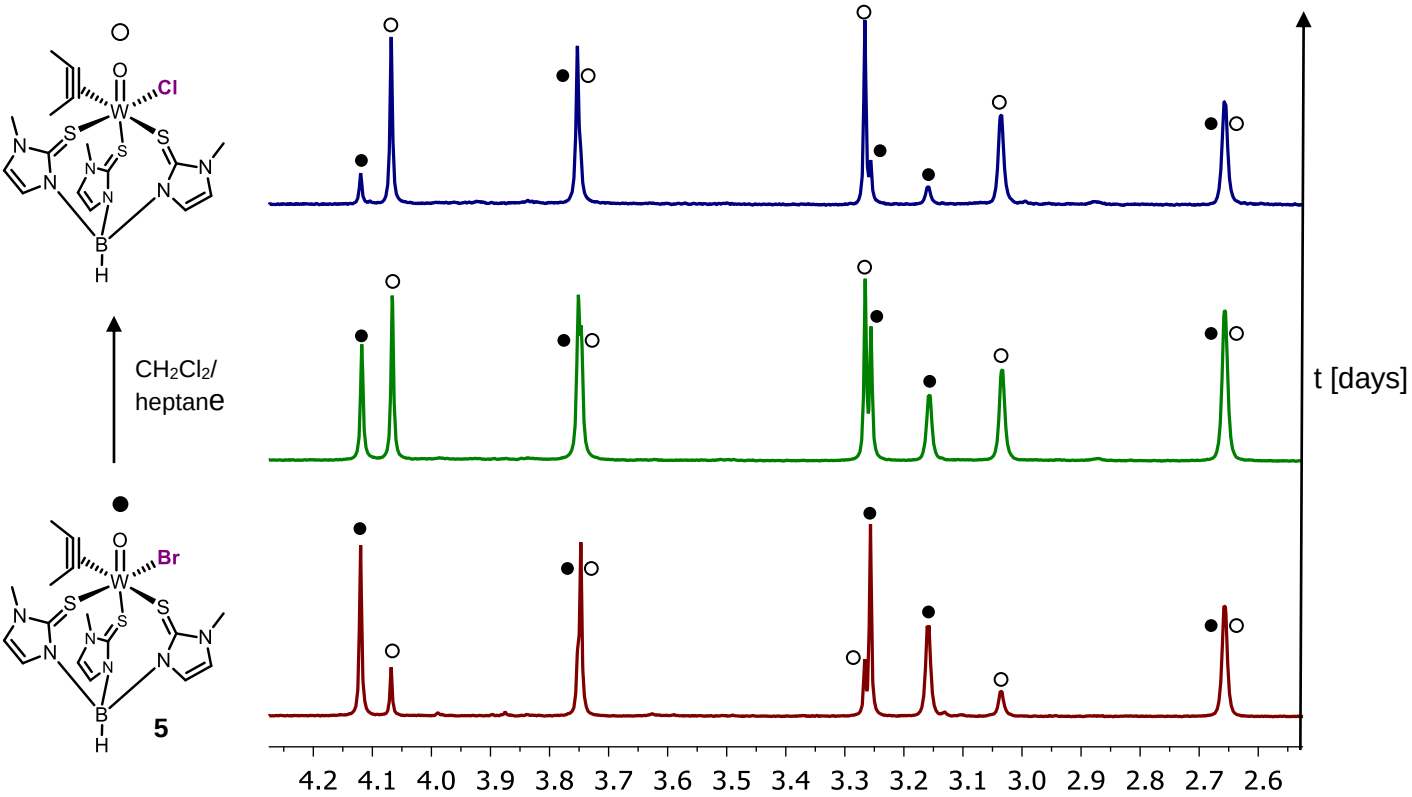

Figure S14: ^{1}H NMR spectra in $CDCl_3$ of crystal fractions of complex [WO(C_2Me_2)(Tm^{Me})Br] (**5**, black points) from re-peated recrystallization (CH_2Cl_2/heptane) with increasing amount of [WO(C_2Me_2)(Tm^{Me})Cl] (white circles) from bottom to top.

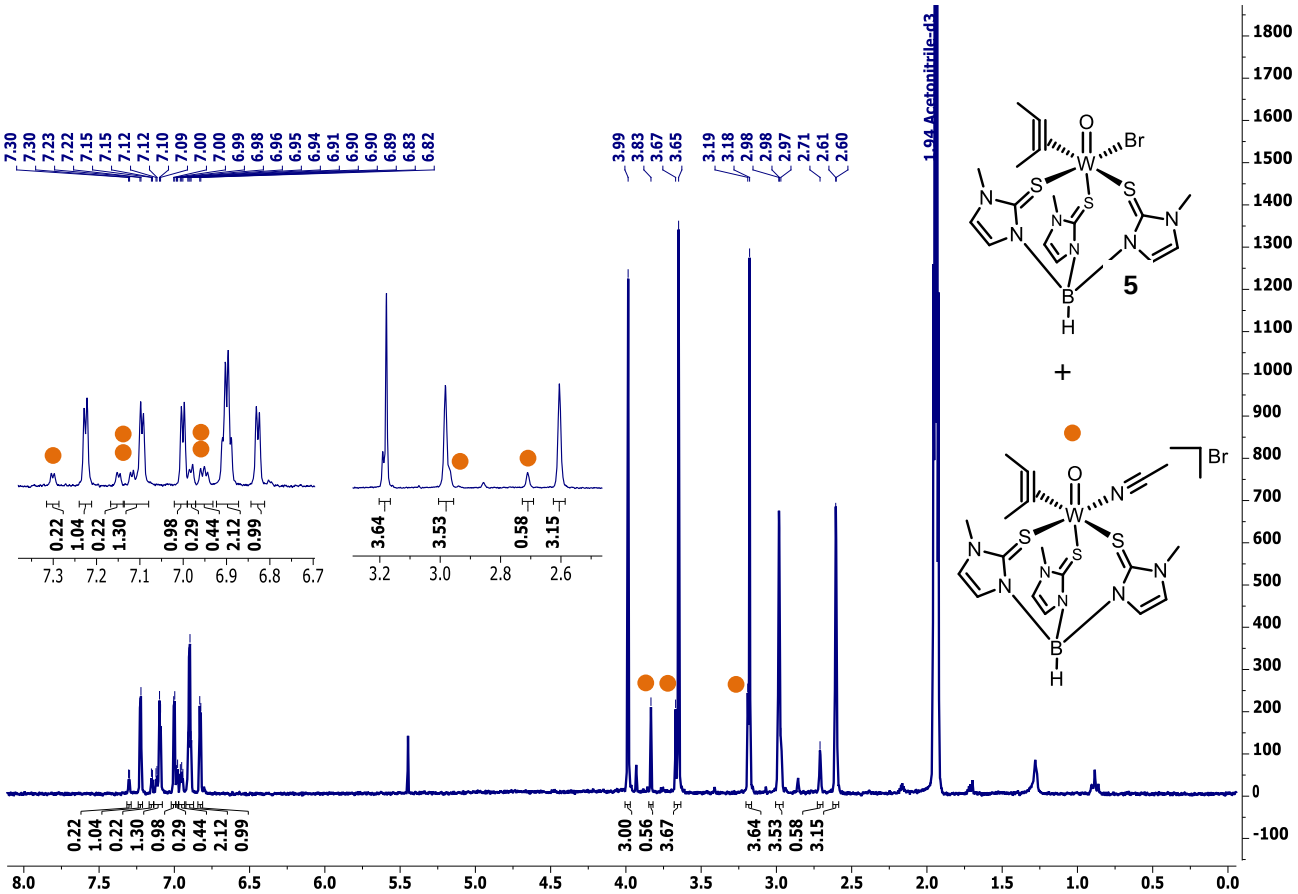

Figure S15: ^{1}H NMR spectrum of [WO(C_2Me_2)(Tm^{Me})Br] (**5**) with small amounts of [WO(C_2Me_2)(MeCN)(Tm^{Me})]Br in $MeCN_{d3}$.

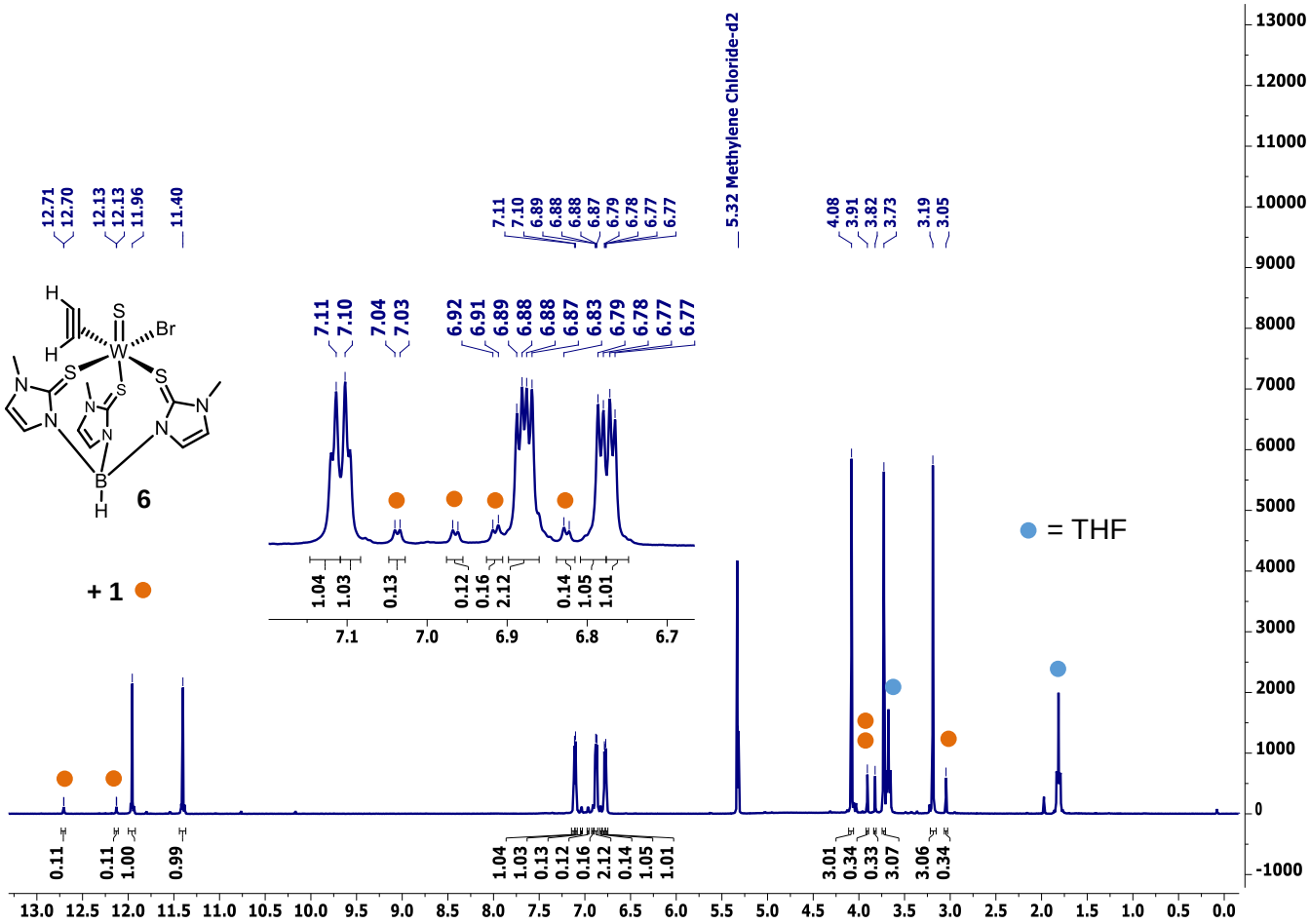

Figure S16: ^{1}H NMR spectrum of [WS(C_2H_2)(Tm^{Me})Br] (**6**) in CD_2Cl_2.

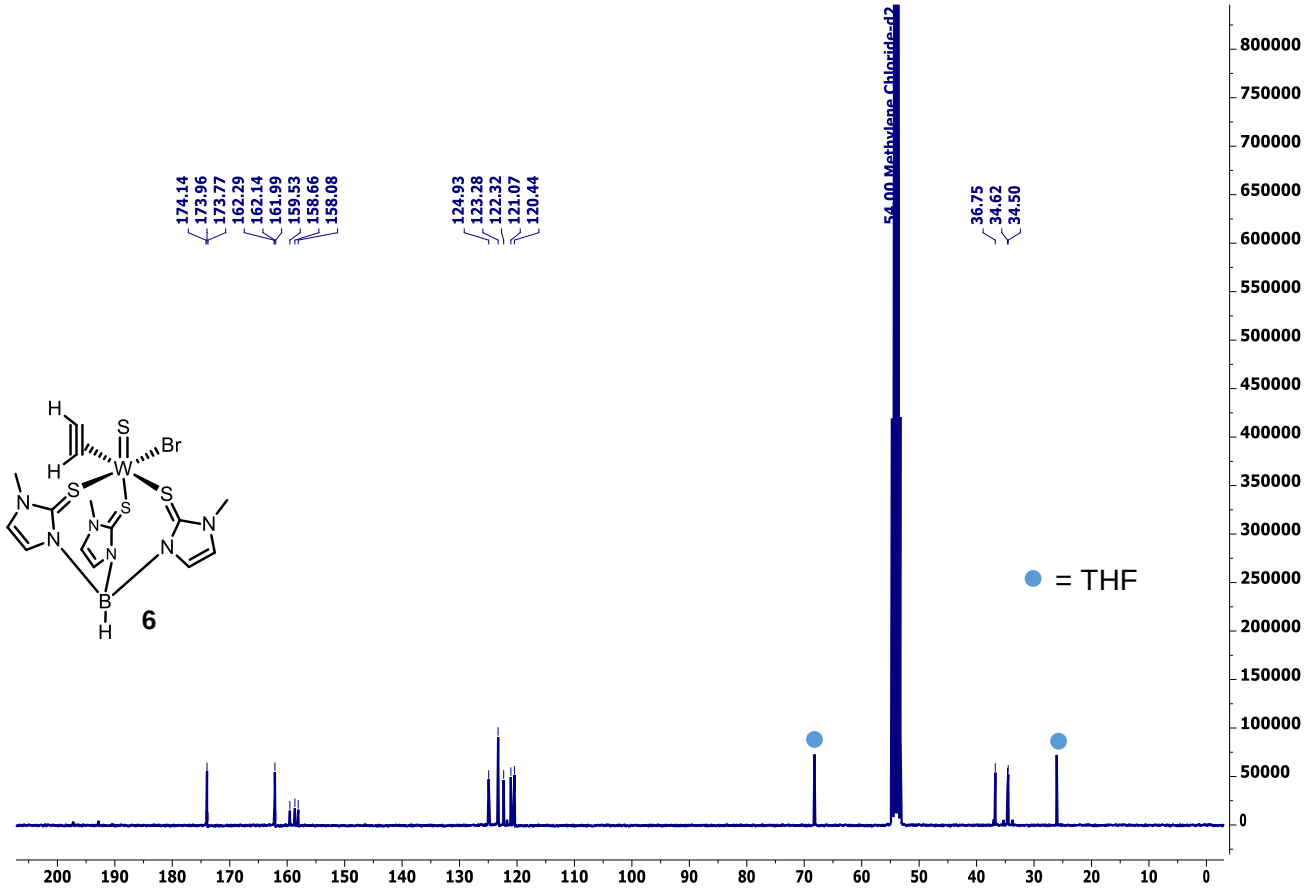

Figure S17: ^{13}C NMR spectrum of $[WS(C_2H_2)(Tm^{Me})Br]$ (**6**) in CD_2Cl_2.

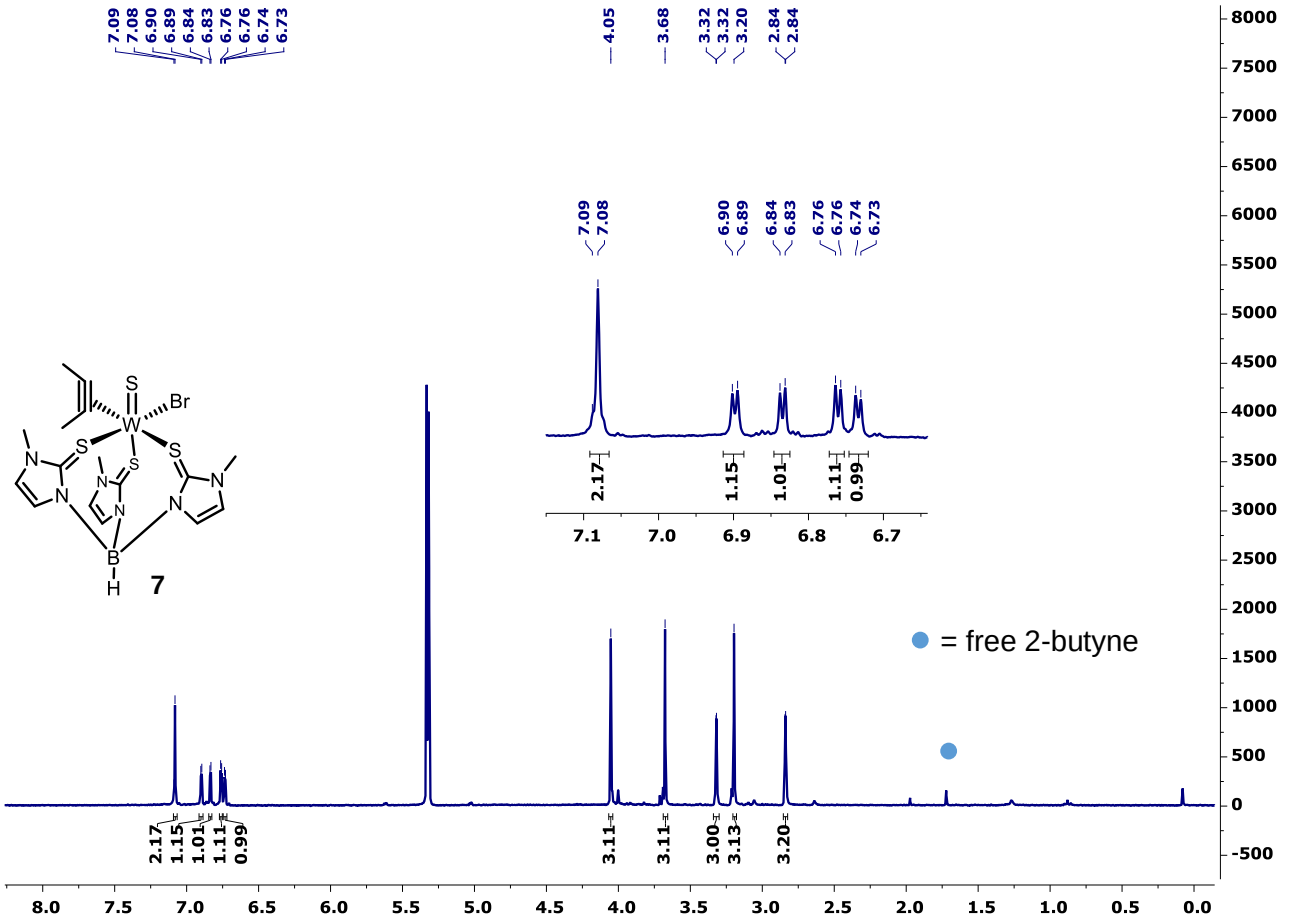

Figure S18: ^{1}H NMR spectrum of $[WS(C_2Me_2)(Tm^{Me})Br]$ (**7**) in CD_2Cl_2.

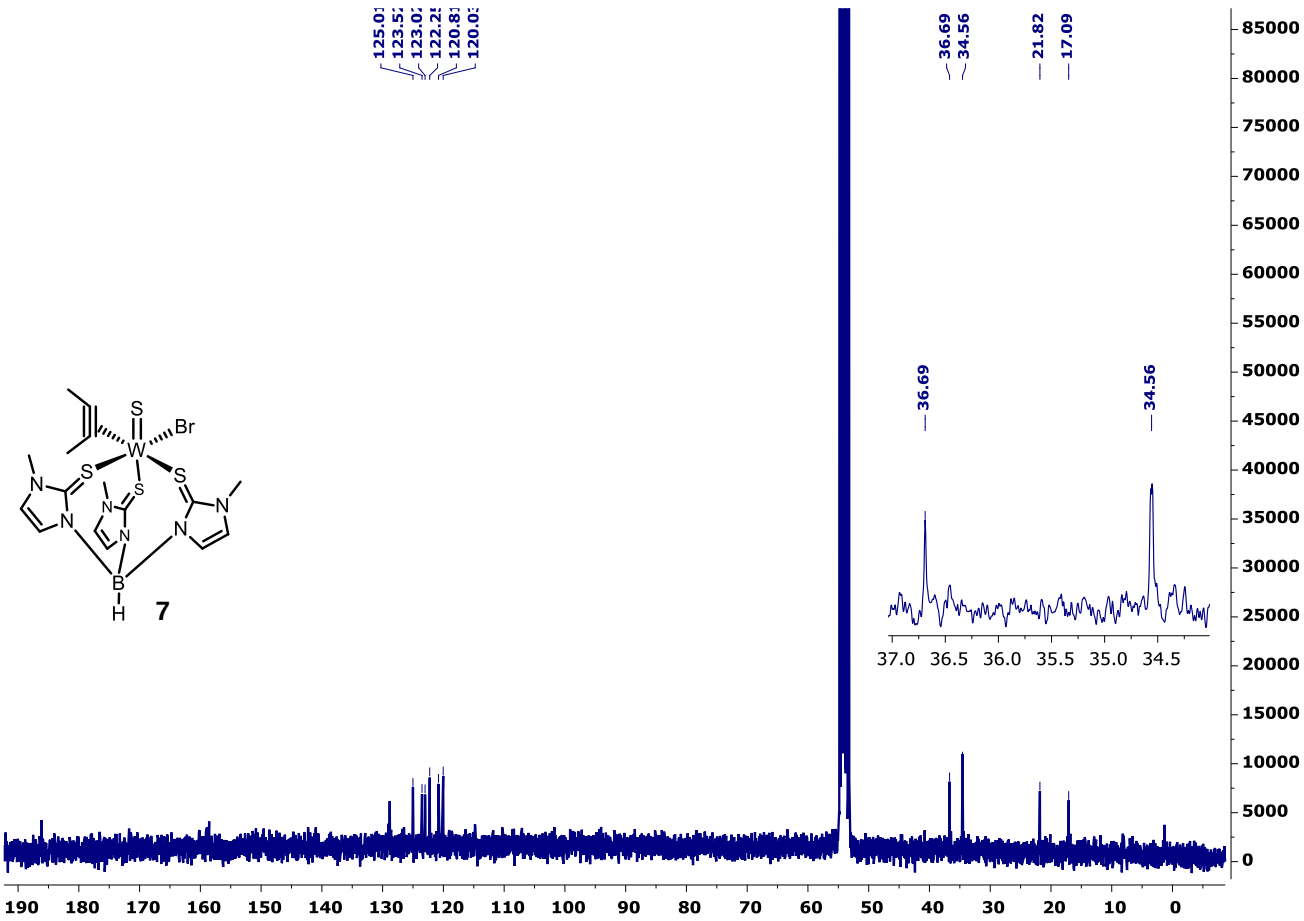

Figure S19: ^{13}C NMR spectrum of [WS(C_2Me_2)(Tm^{Me})Br] (**7**) in CD_2Cl_2.

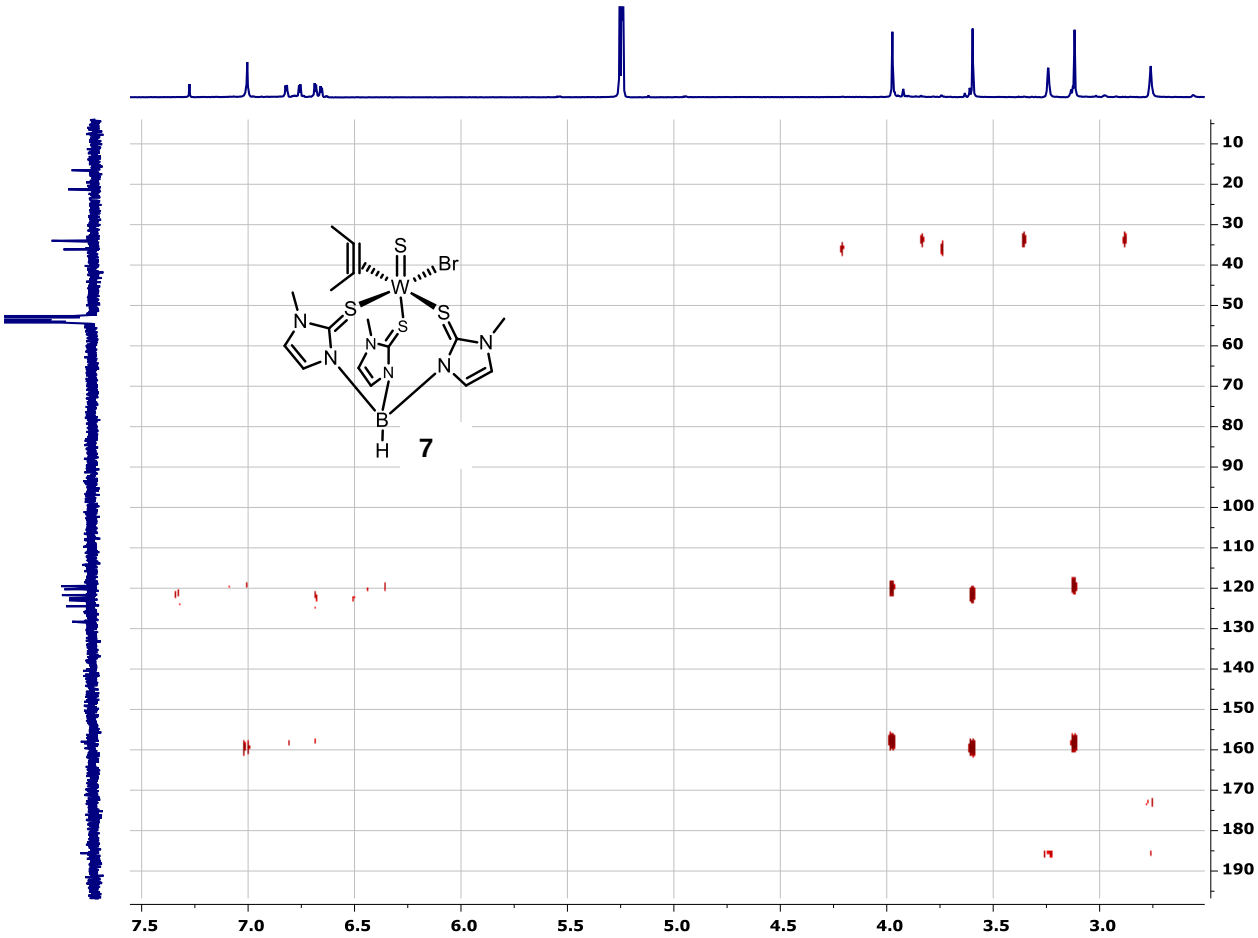

Figure S20: HMBC NMR spectrum of [WS(C_2Me_2)(Tm^{Me})Br] (**7**) in CD_2Cl_2.

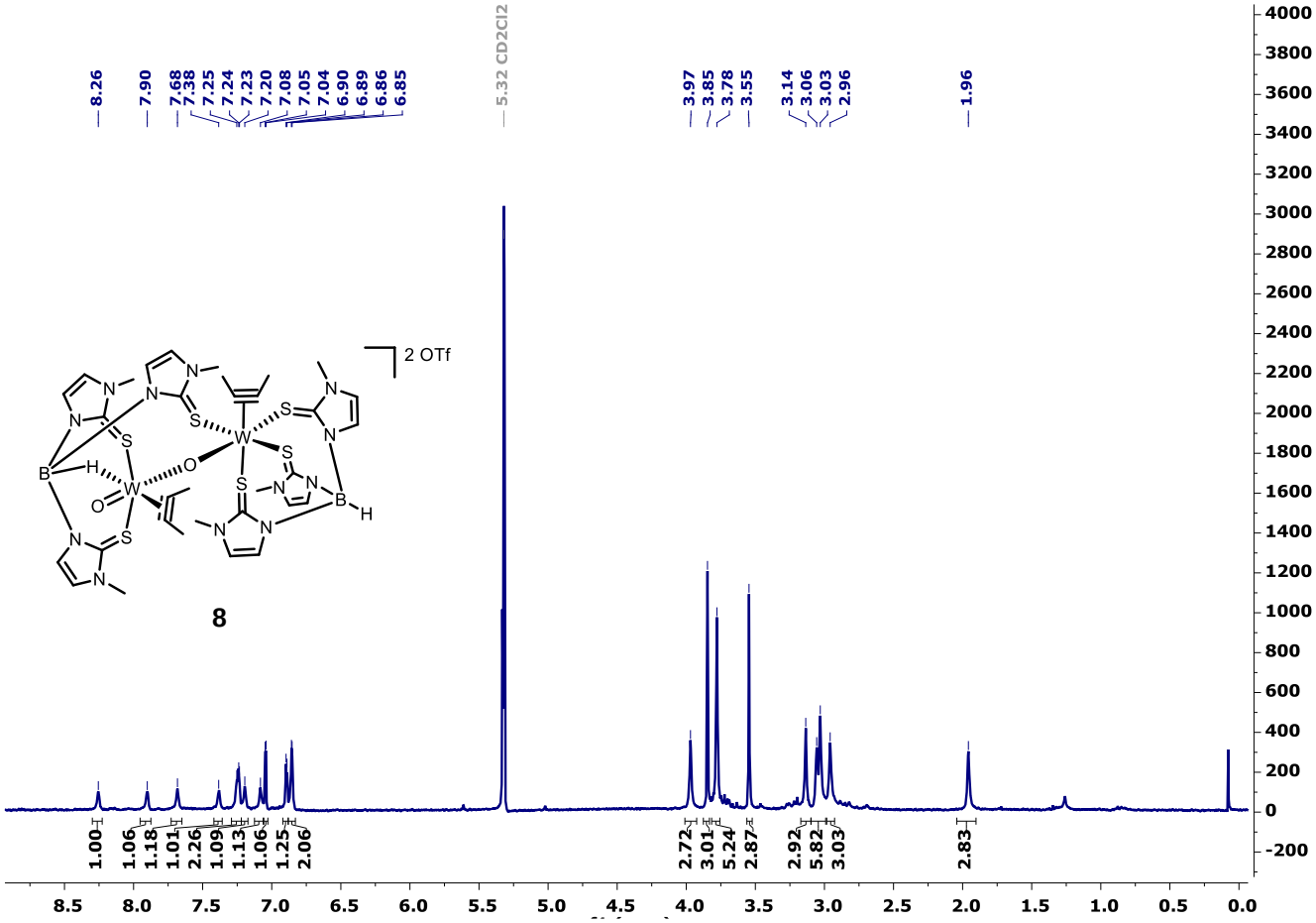

Figure S21: ^{1}H NMR spectrum of $[W_2O(\mu\text{-}O)(C_2Me_2)_2(Tm^{Me})_2](OTf)_2$ (**8**) in CD_2Cl_2.

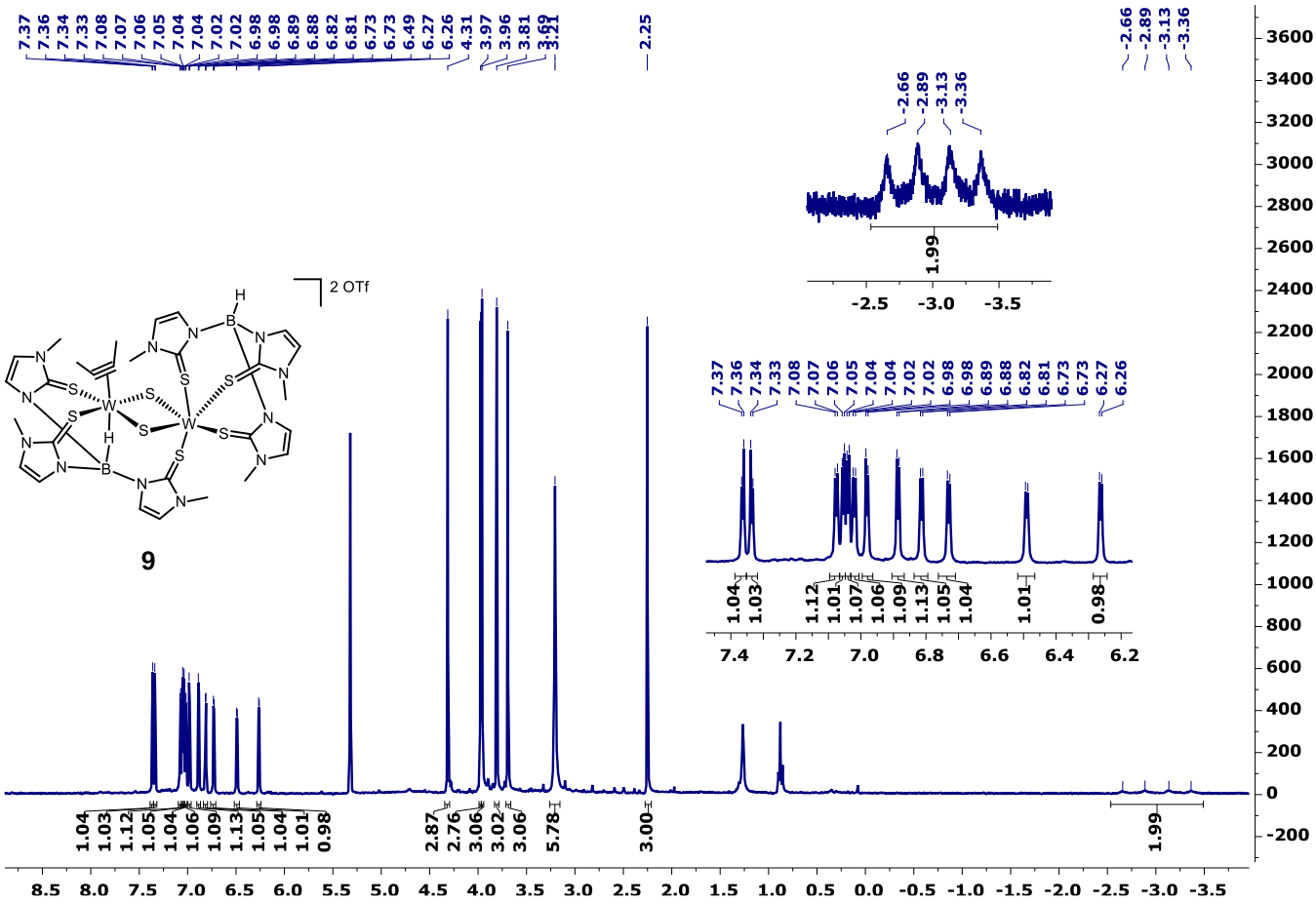

Figure S22: ^{1}H NMR spectrum of $[W_2(\mu\text{-}S)_2(C_2Me_2)(Tm^{Me})_2](OTf)_2$ (**9**) in CD_2Cl_2.

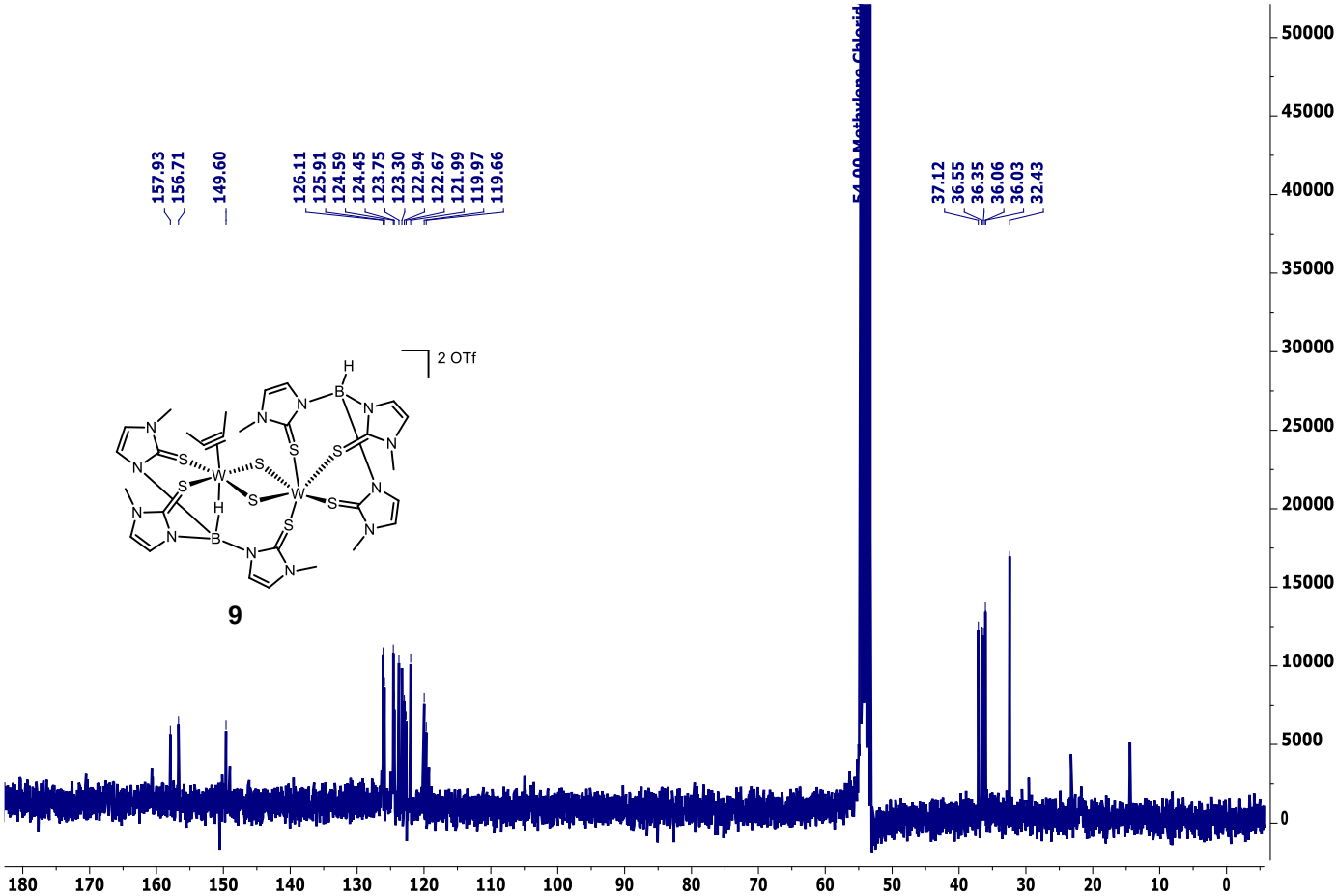

Figure S23: ^{13}C NMR spectrum of $[W_2(\mu\text{-}S)_2(C_2Me_2)(Tm^{Me})_2](OTf)_2$ (**9**) in CD_2Cl_2.

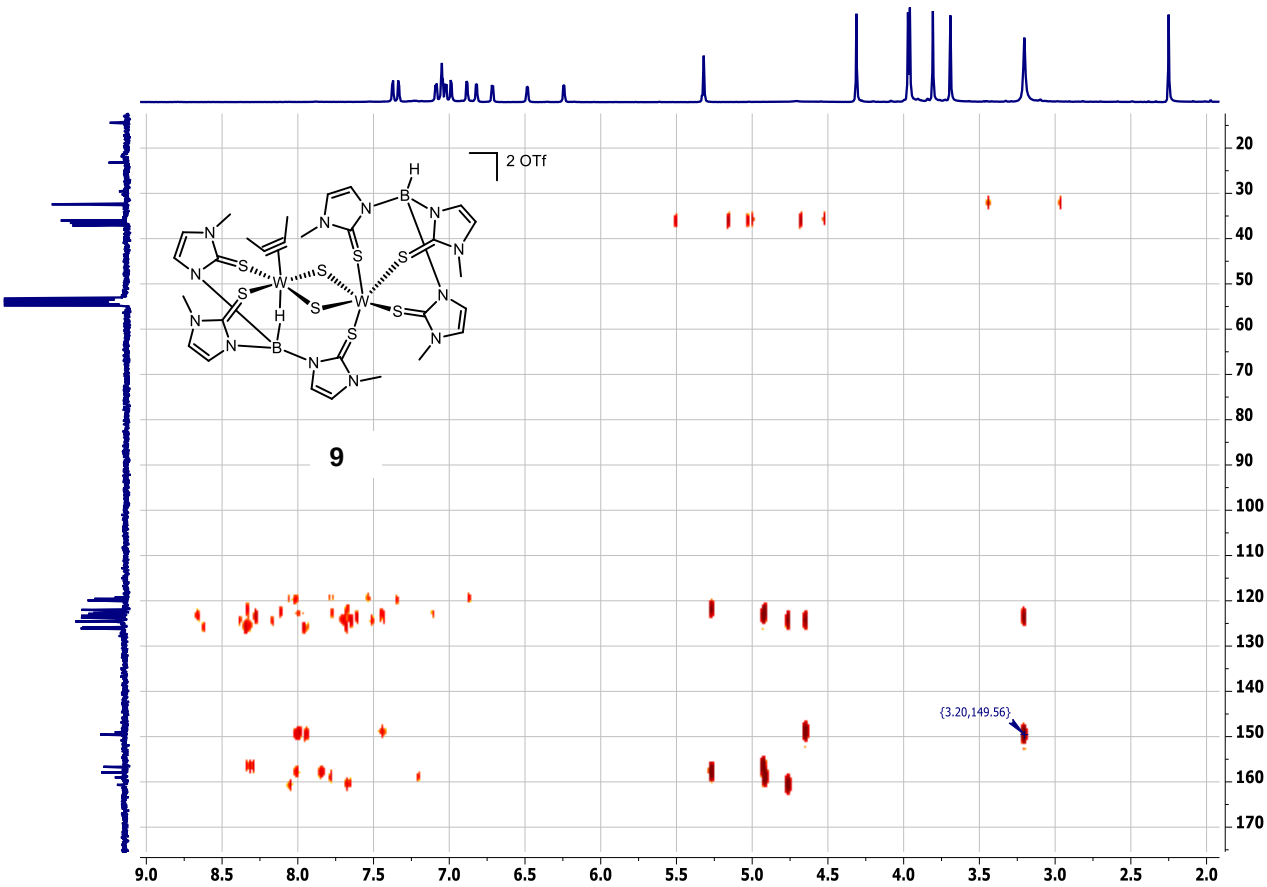

Figure S24: HMBC NMR spectrum of $[W_2(\mu\text{-}S)_2(C_2Me_2)(Tm^{Me})_2](OTf)_2$ (**9**) in CD_2Cl_2.

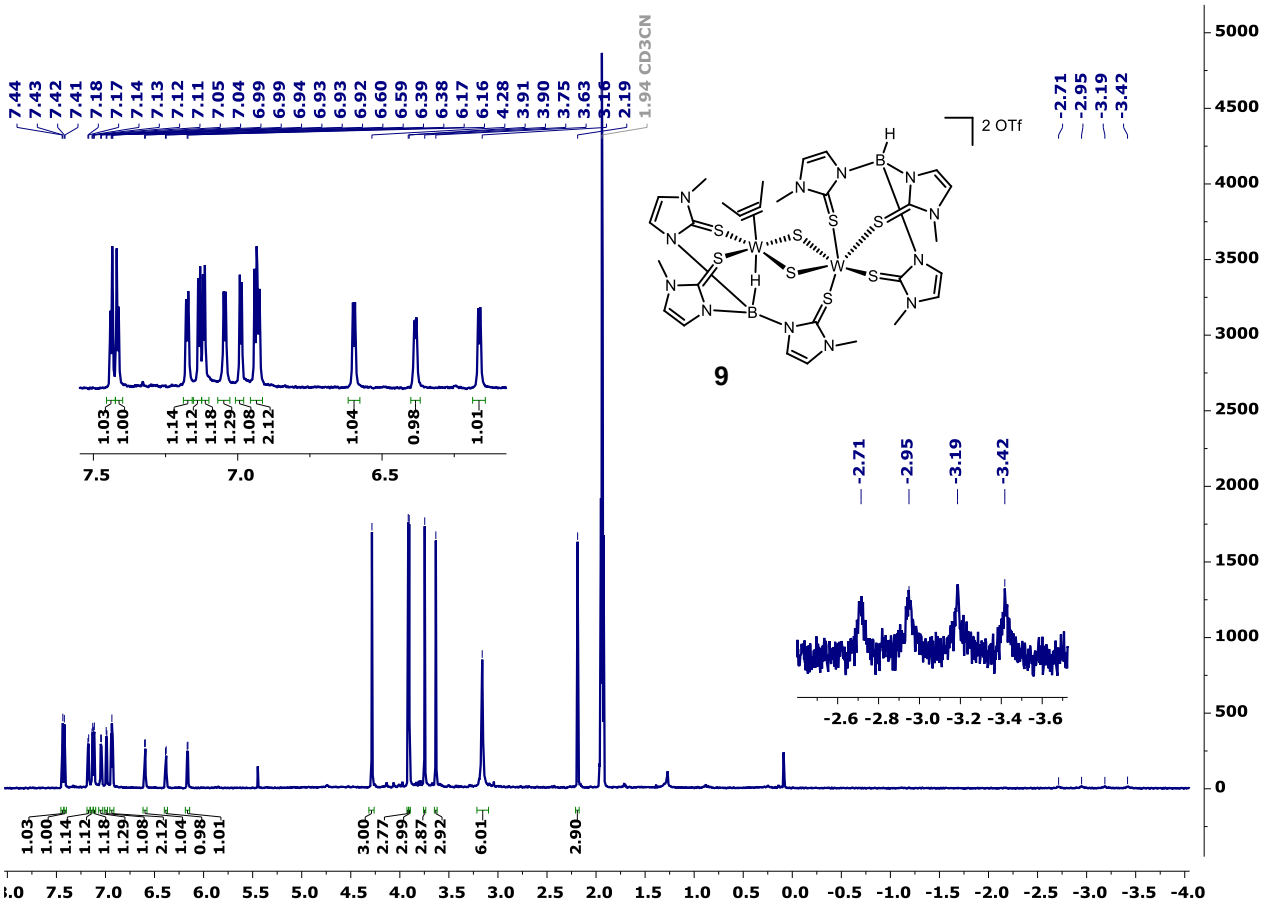

Figure S25: ^{1}H NMR spectrum of $[W_2(\mu\text{-}S)_2(C_2Me_2)(Tm^{Me})_2](OTf)_2$ (**9**) in CD_3CN.

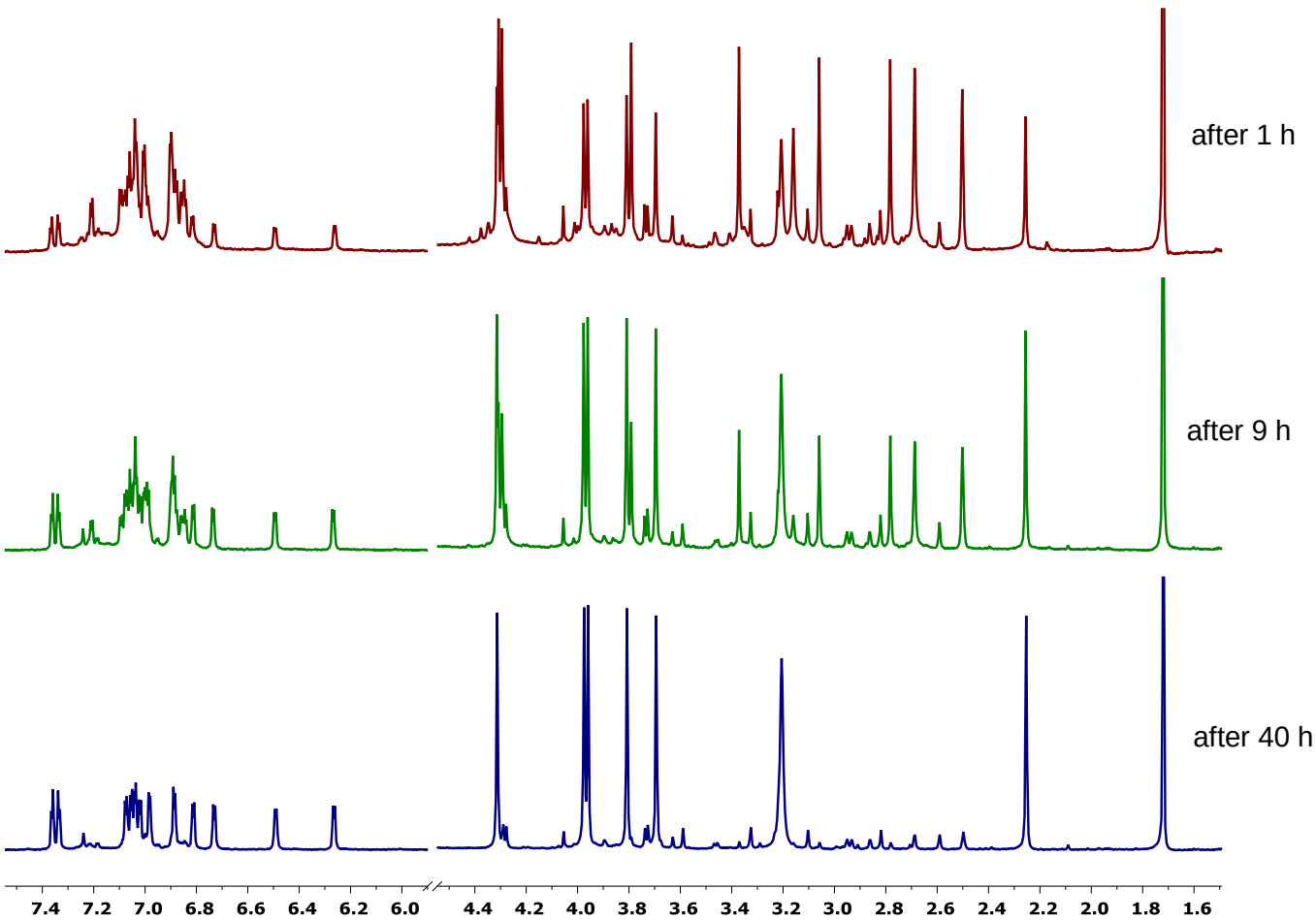

Figure S26: ^{1}H NMR spectra of the formation of $[W_2(\mu\text{-}S)_2(C_2Me_2)(Tm^{Me})_2](OTf)_2$ (**9**) in CD_2Cl_2 over 40h.

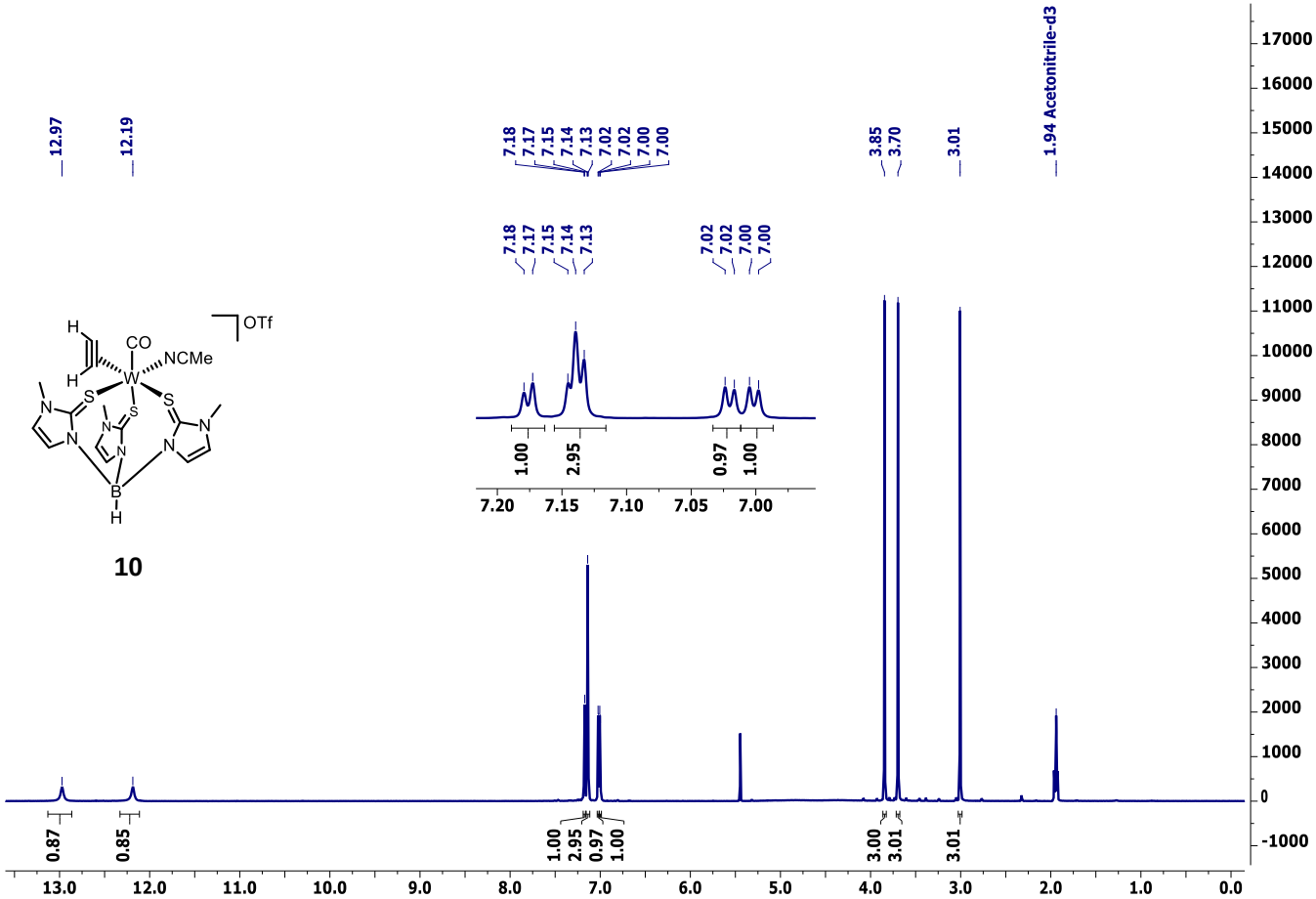

Figure S27: ^{1}H NMR spectrum of [W(CO)(C_2H_2)(MeCN)(Tm^{Me})](OTf) (**10**) in CD_3CN.

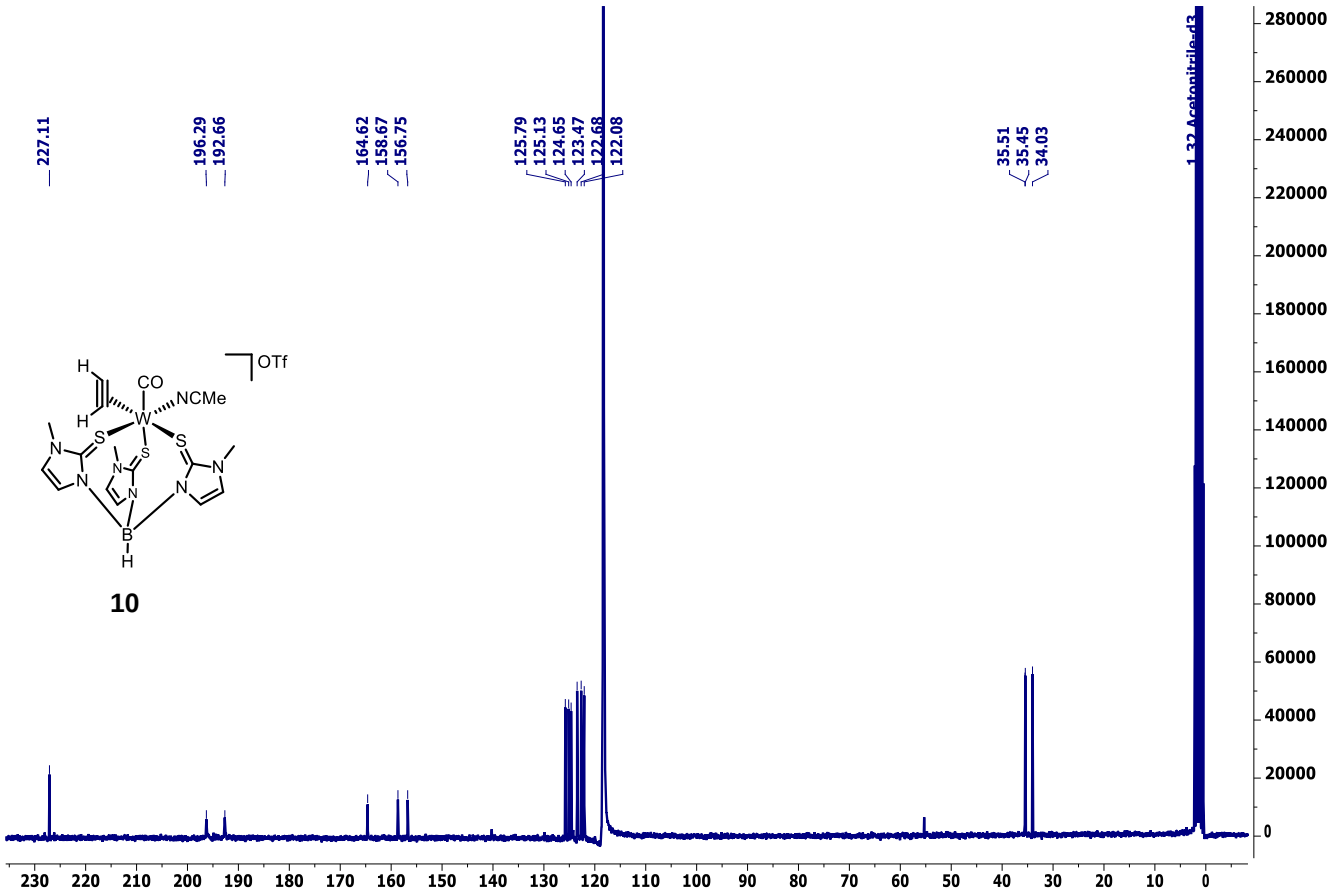

Figure S28: ^{13}C NMR spectrum of [W(CO)(C_2H_2)(MeCN)(Tm^{Me})](OTf) (**10**) in CD_3CN.

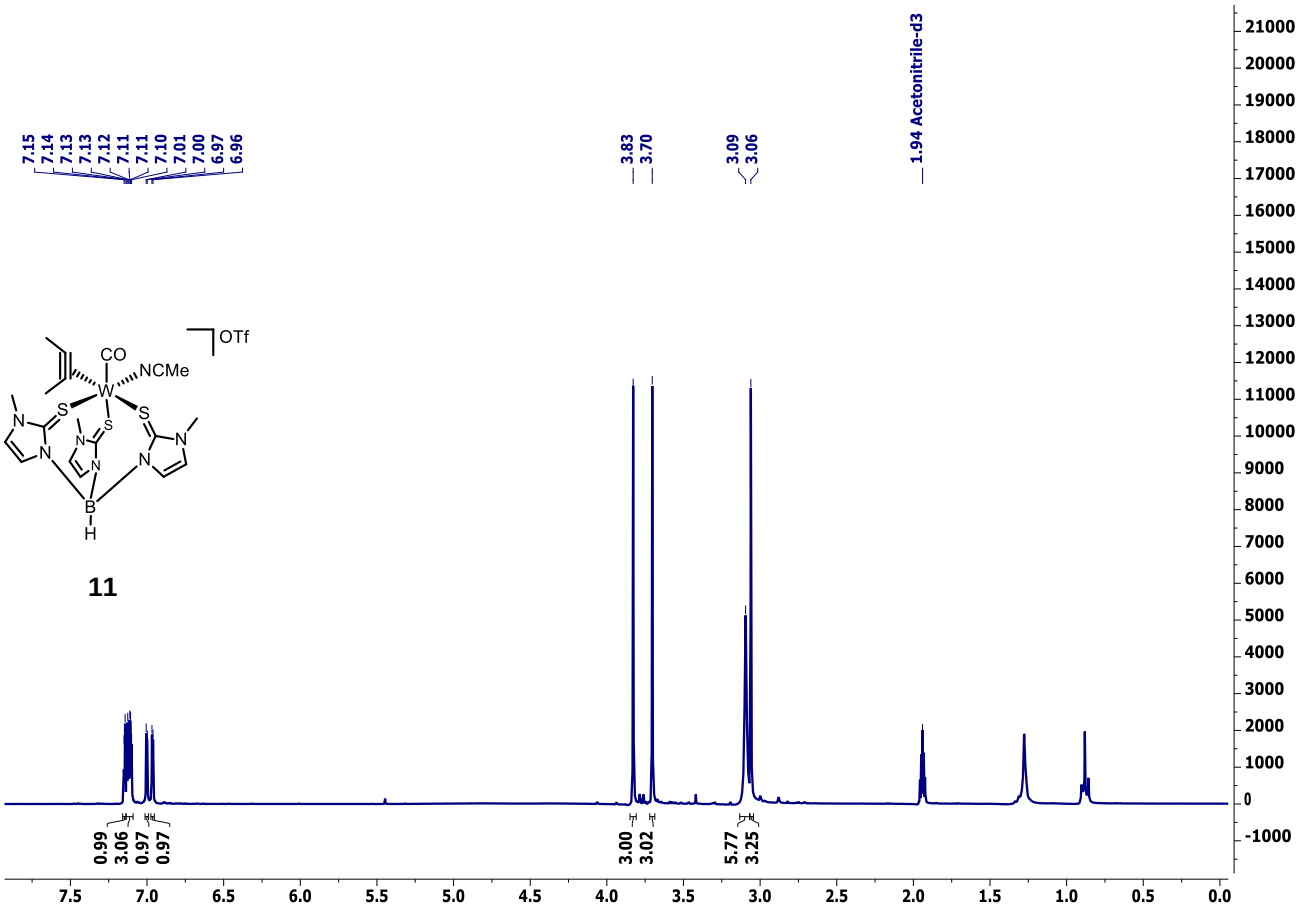

Figure S29: ^{1}H NMR spectrum of [W(CO)(C_2Me_2)(MeCN)(Tm^{Me})](OTf) (**11**) in CD_3CN.

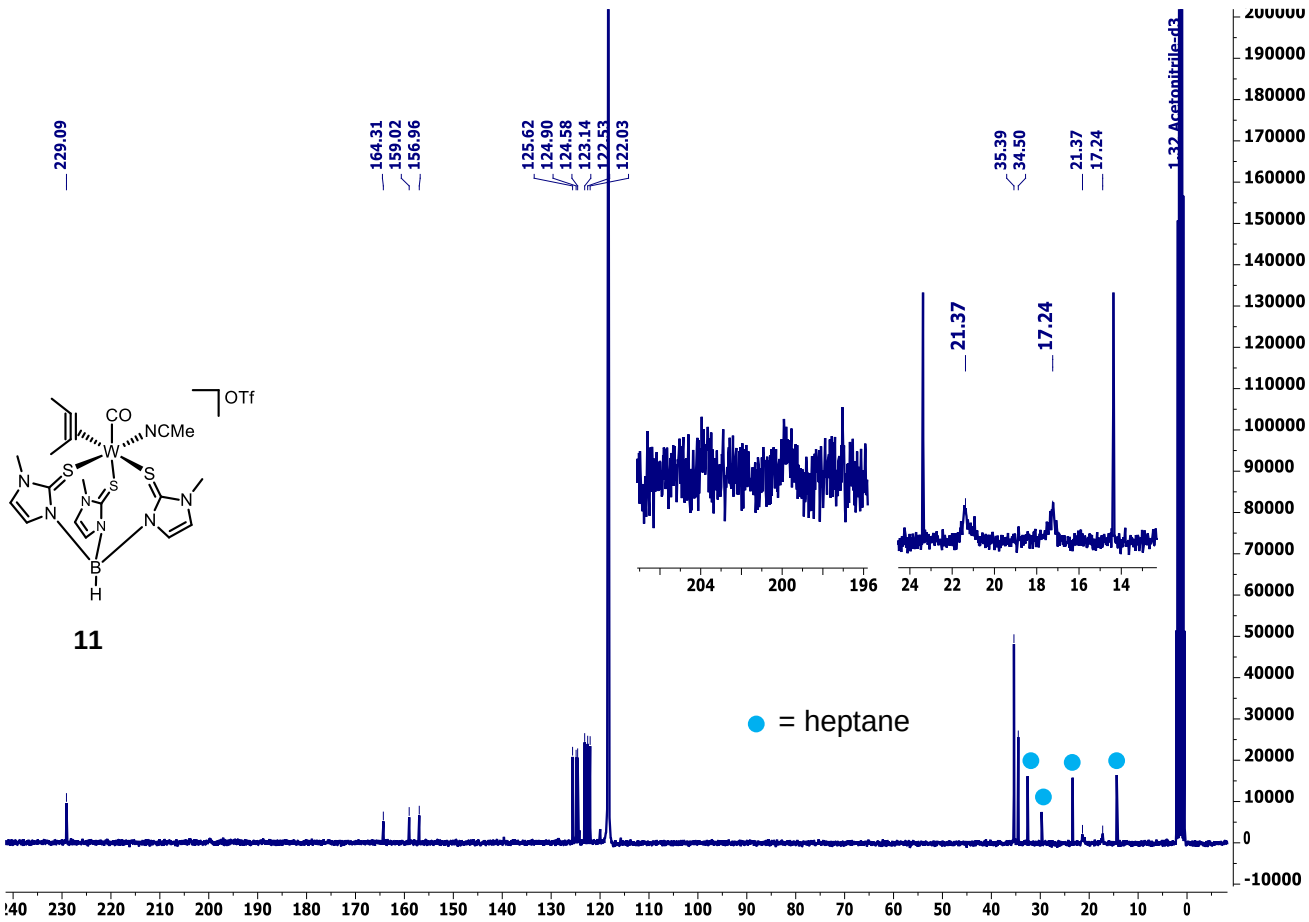

Figure S30: ^{13}C NMR spectrum of [W(CO)(C_2Me_2)(MeCN)(Tm^{Me})](OTf) (**11**) in CD_3CN.

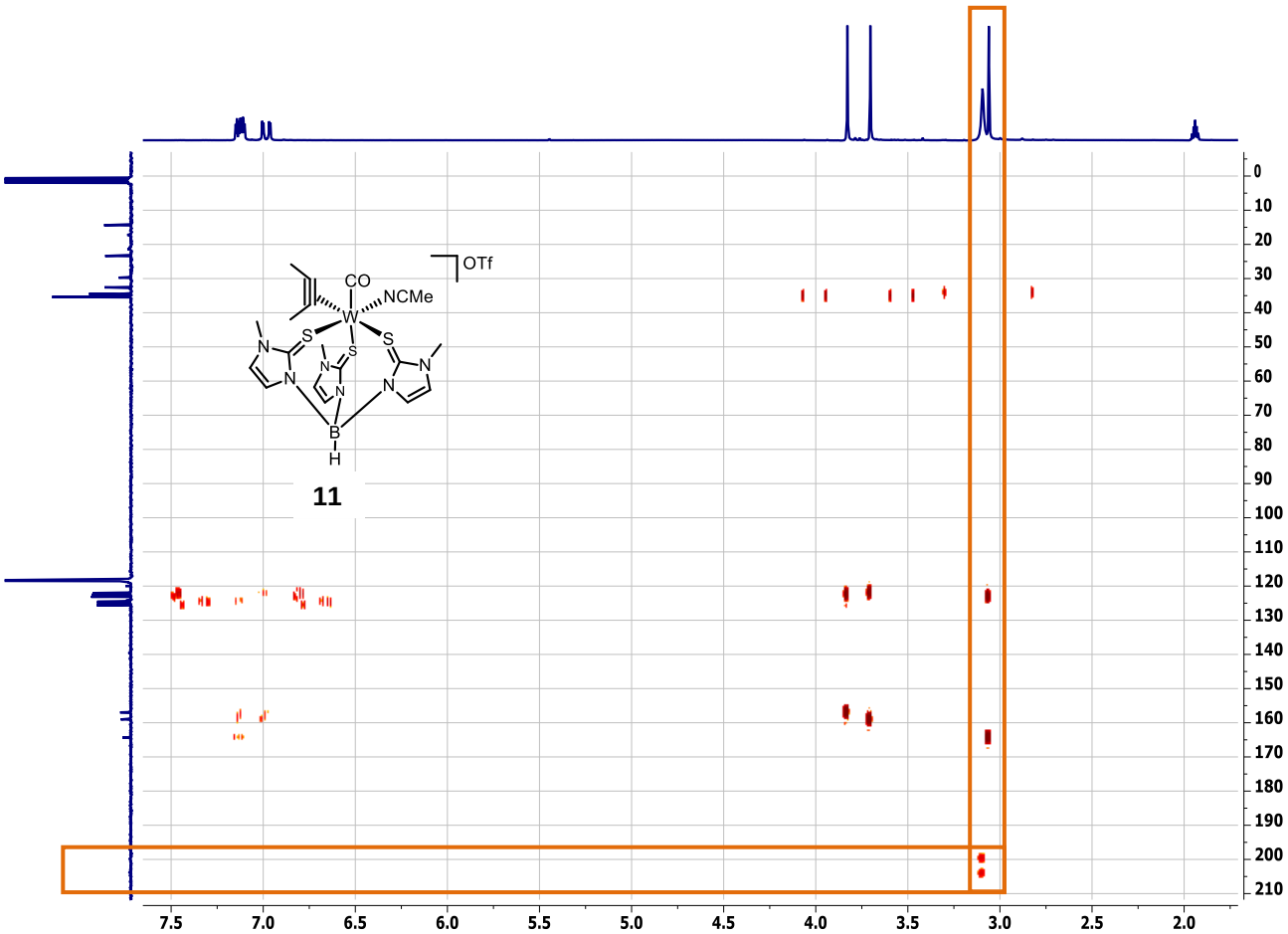

Figure S31: HMBC NMR spectrum of [W(CO)(C_2Me_2)(MeCN)(Tm^{Me})](OTf) (**11**) in CD_3CN.

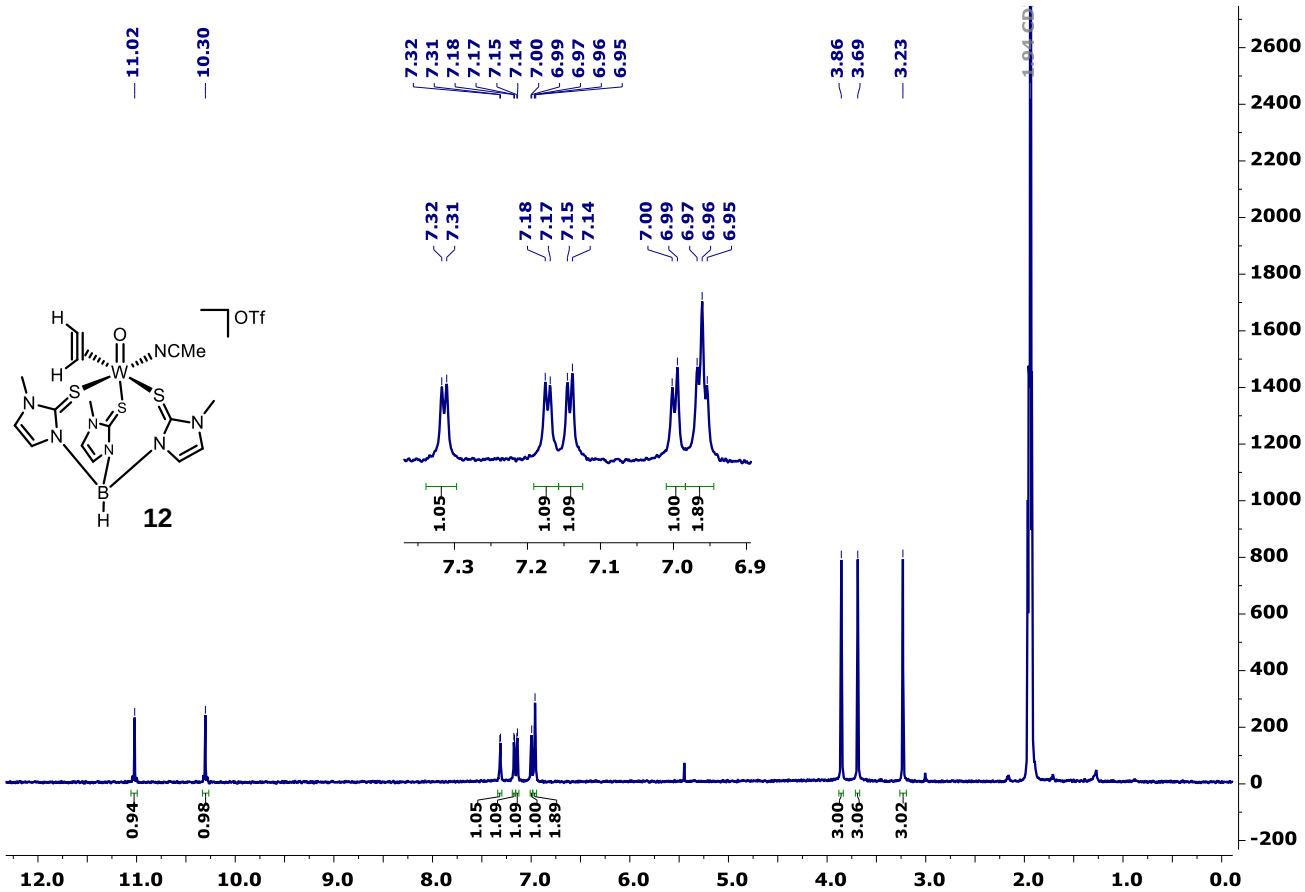

Figure S32: ^1H NMR spectrum of [WO(C_2H_2)(MeCN)(Tm^{Me})](OTf) (**12**) · PyHBr with 2 equiv of TlOTf in CD_3CN.

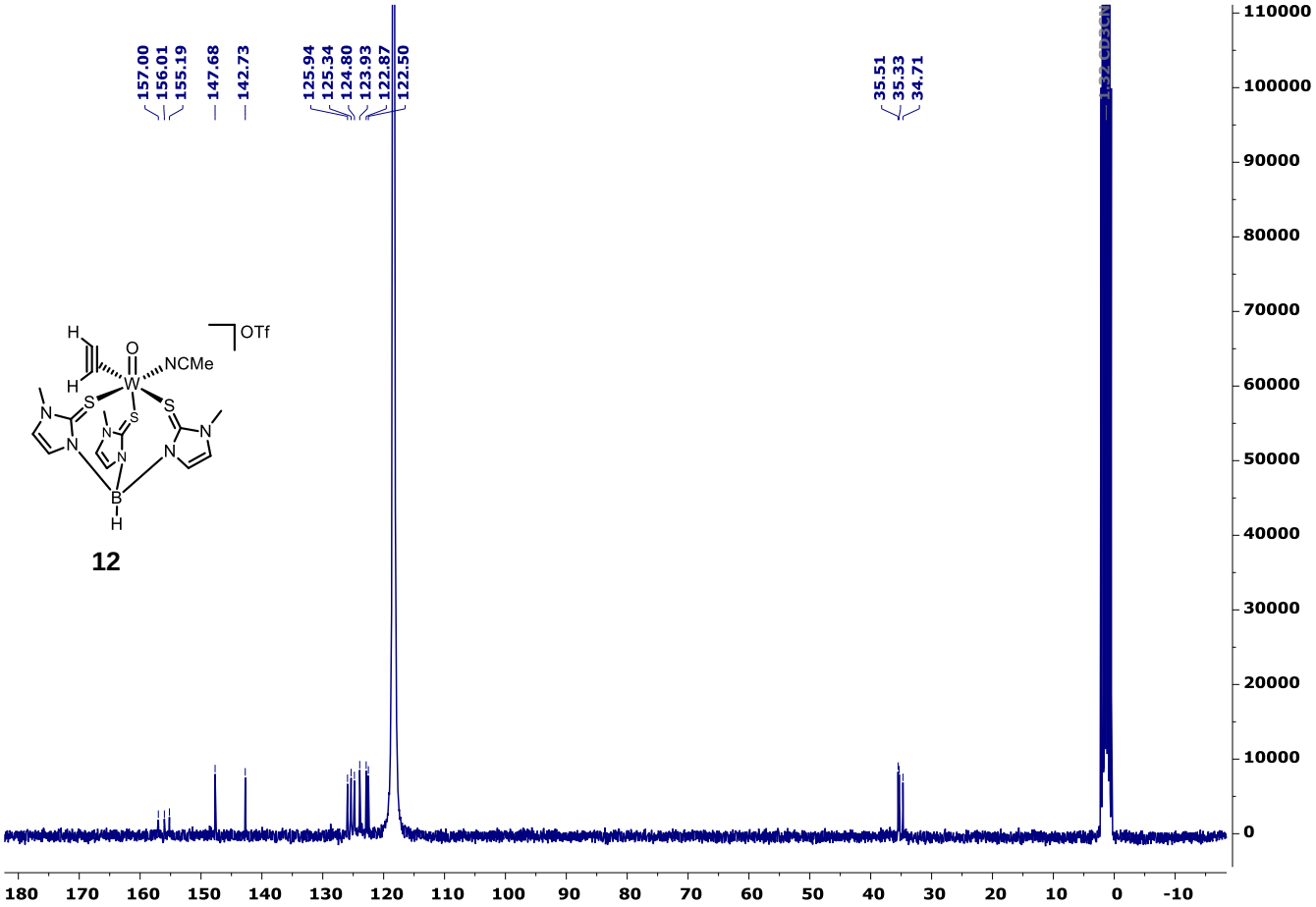

Figure S33: ^{13}C NMR spectrum of [WO(C_2H_2)(MeCN)(Tm^{Me})](OTf) (**12**) in CD_3CN.

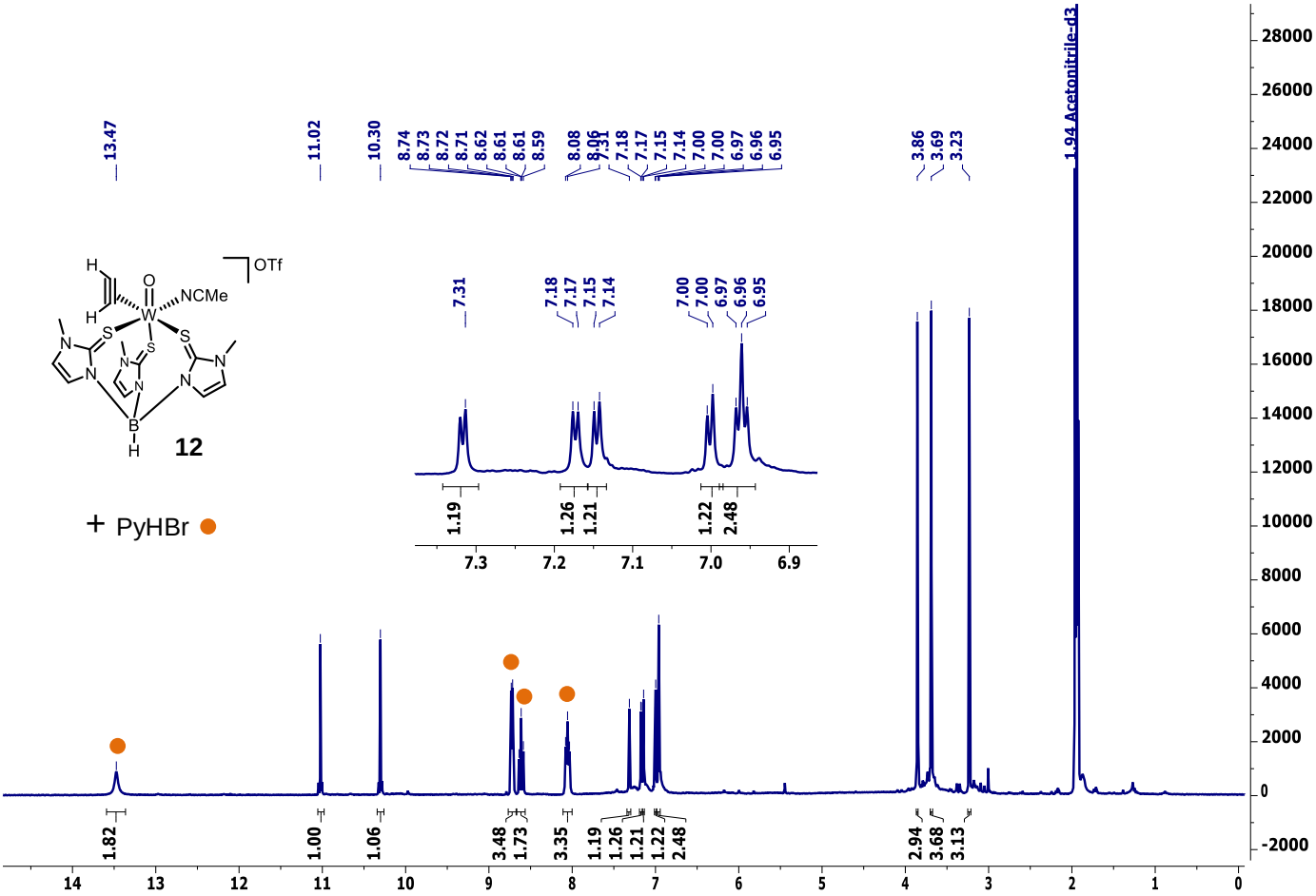

Figure S34: ^{1}H NMR spectrum of [WO(C_2H_2)(MeCN)(Tm^{Me})](OTf) (**12**) · PyHBr with 2 equiv of TlOTf in CD_3CN.

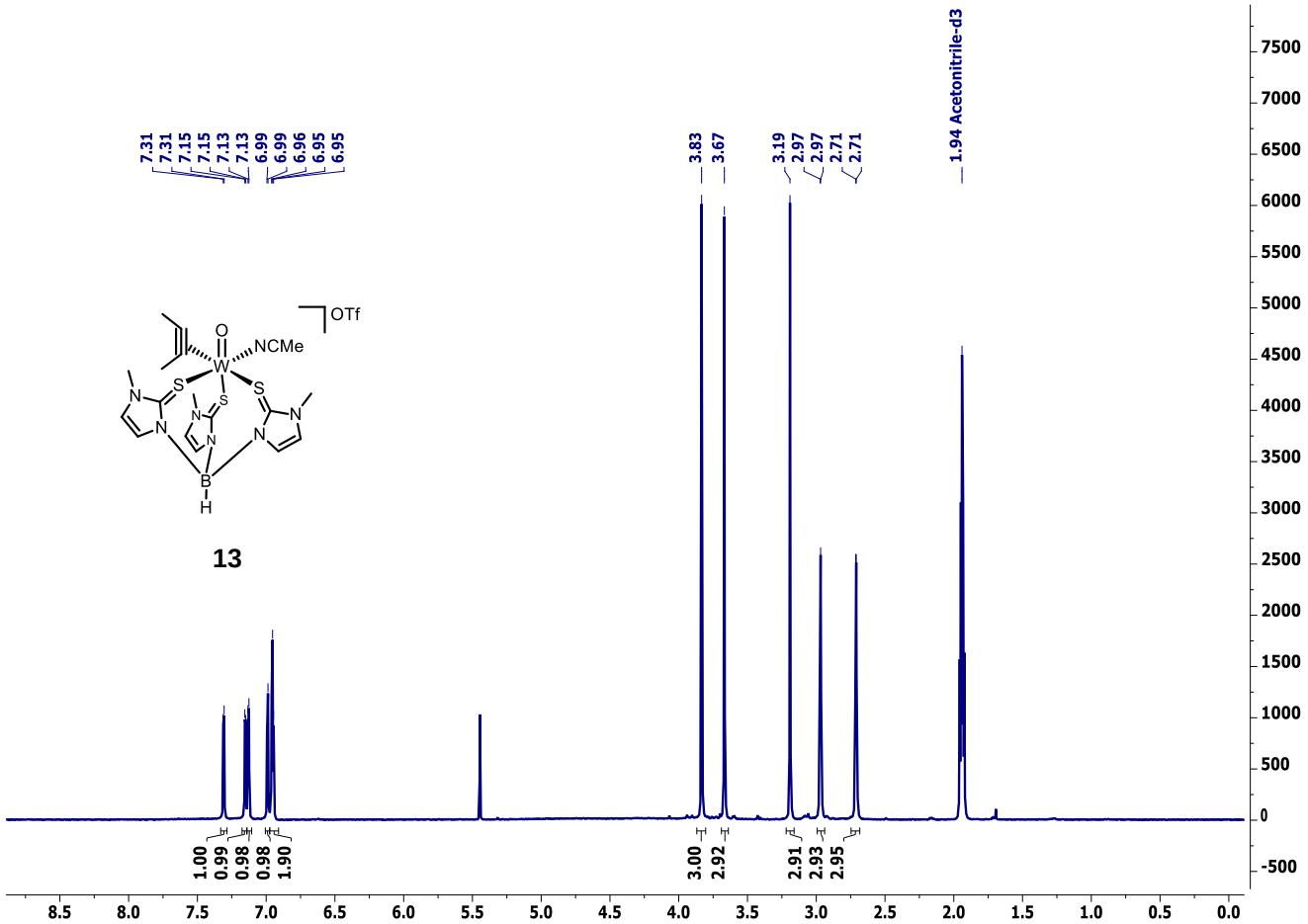

Figure S35: ^{1}H NMR spectrum of [WO(C_2Me_2)(MeCN)(Tm^{Me})](OTf) (**13**) in CD_3CN.

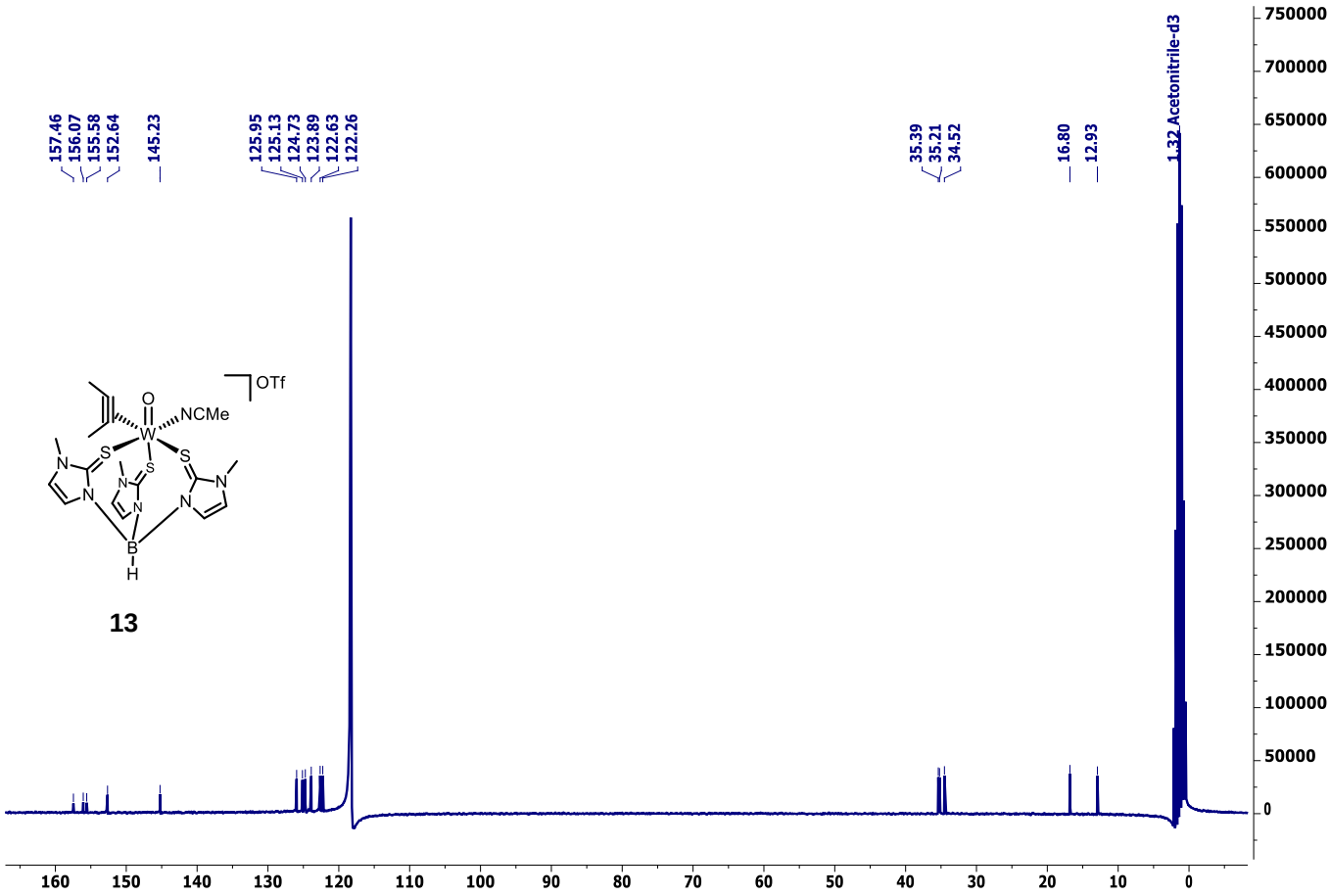

Figure S36: ^{13}C NMR spectrum of [WO(C_2Me_2)(MeCN)(Tm^{Me})](OTf) (**13**) in CD_3CN.

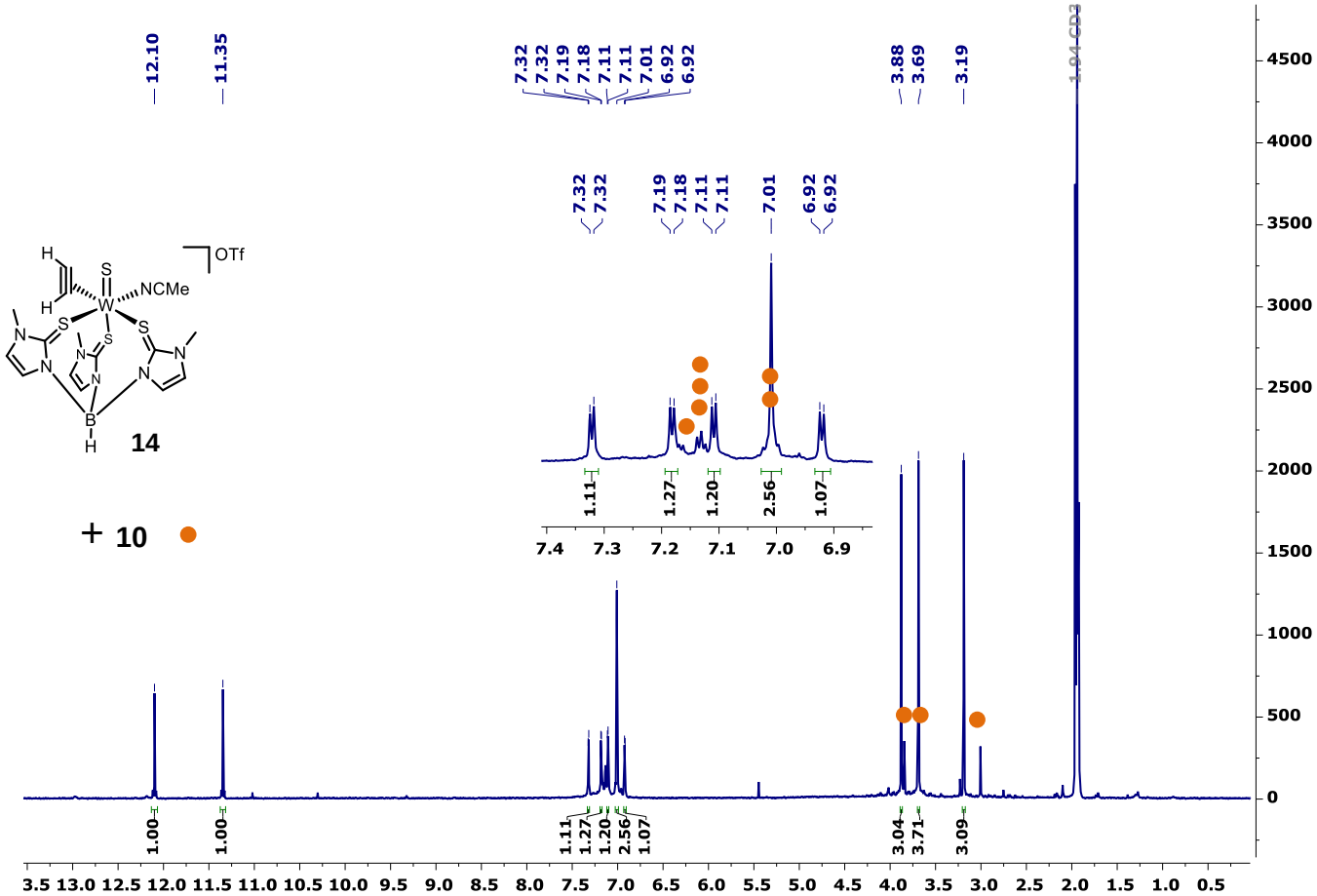

Figure S37: ^{1}H NMR spectrum of [WS(C_2H_2)(MeCN)(Tm^{Me})](OTf) (**14**) in CD_3CN.

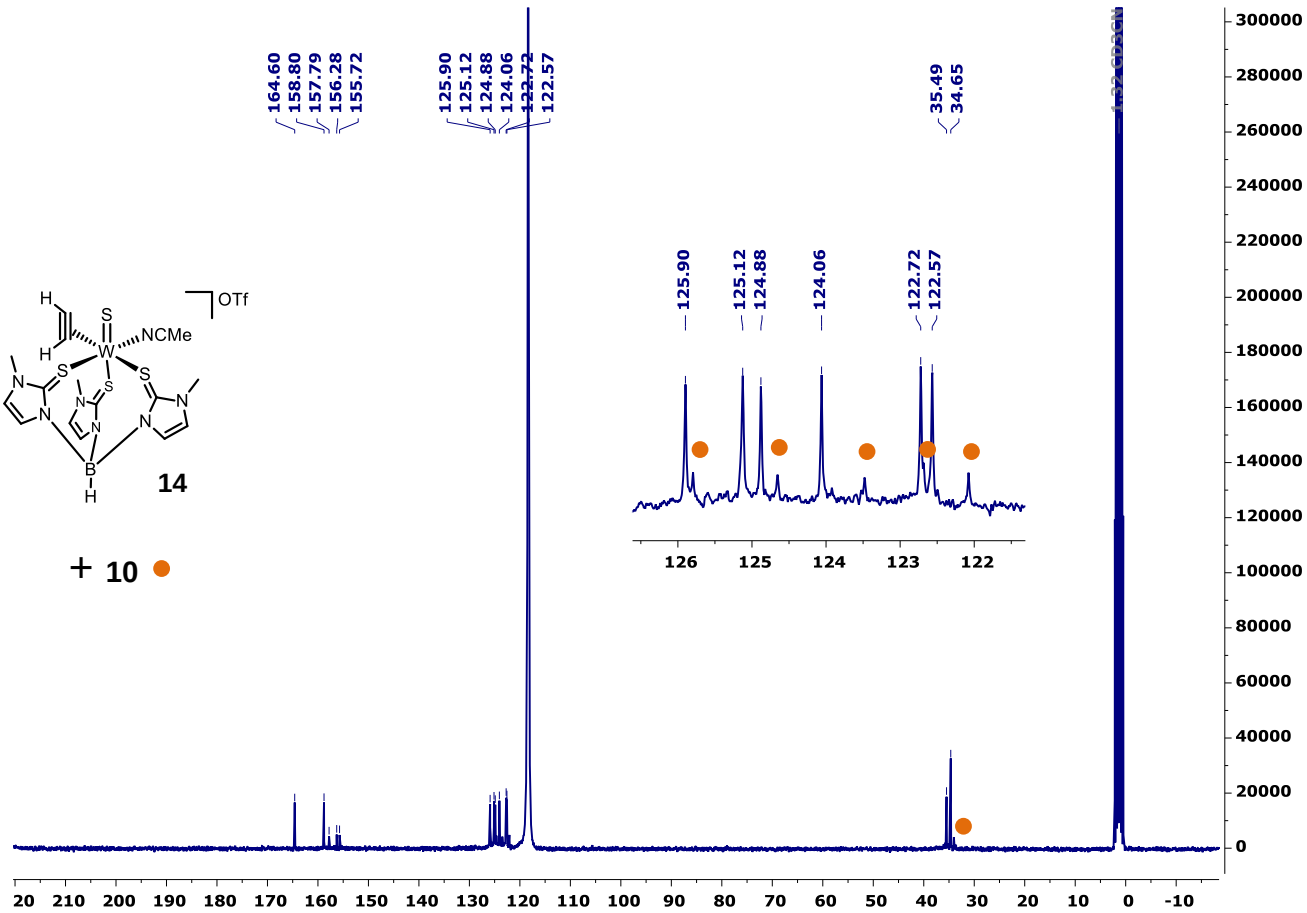

Figure S38: ^{13}C NMR spectrum of [WS(C_2H_2)(MeCN)(Tm^{Me})](OTf) (**14**) in CD_3CN.

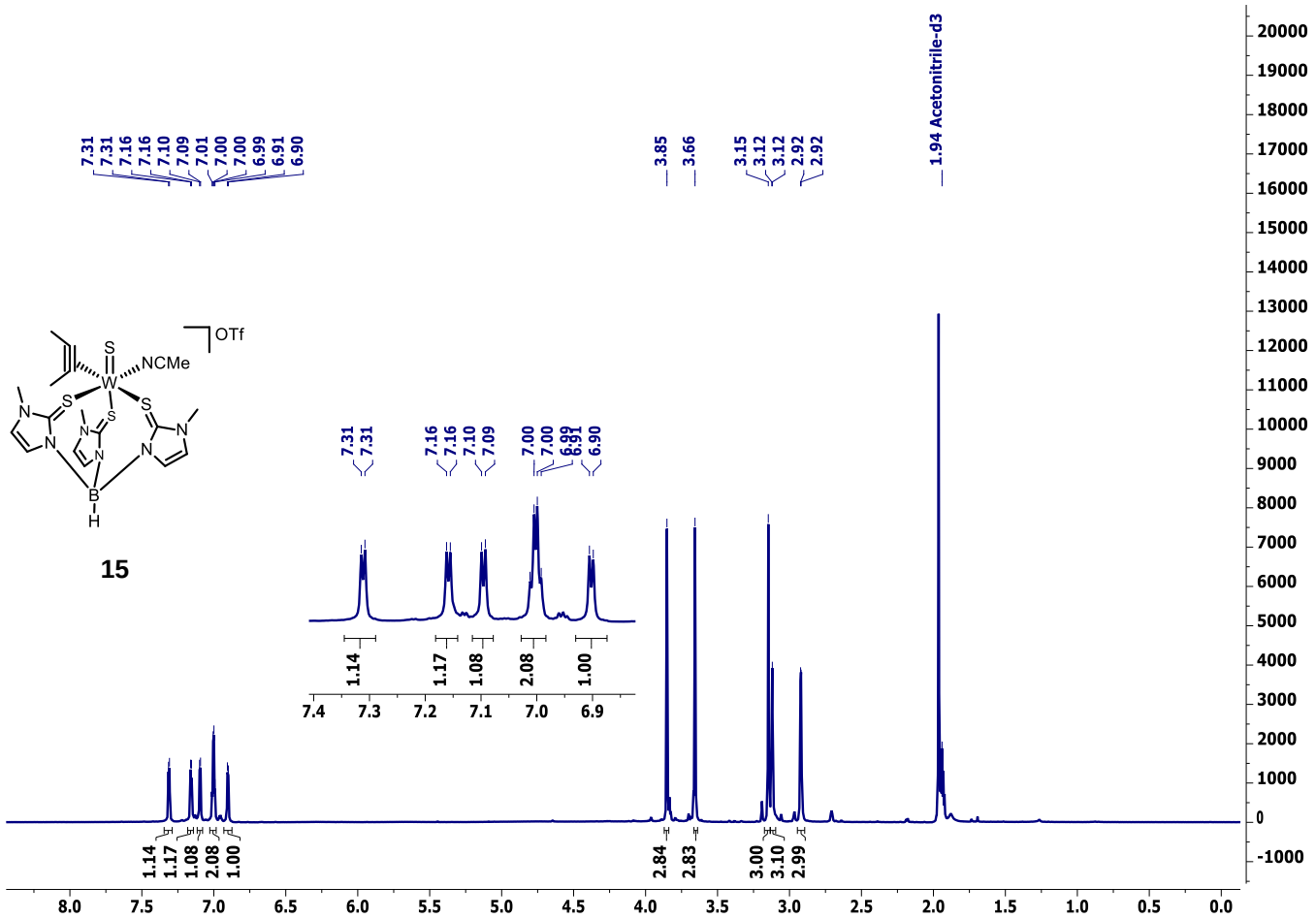

Figure S39: ^{1}H NMR spectrum of [WS(C_2Me_2)(MeCN)(Tm^{Me})](OTf) (**15**) in CD_3CN.

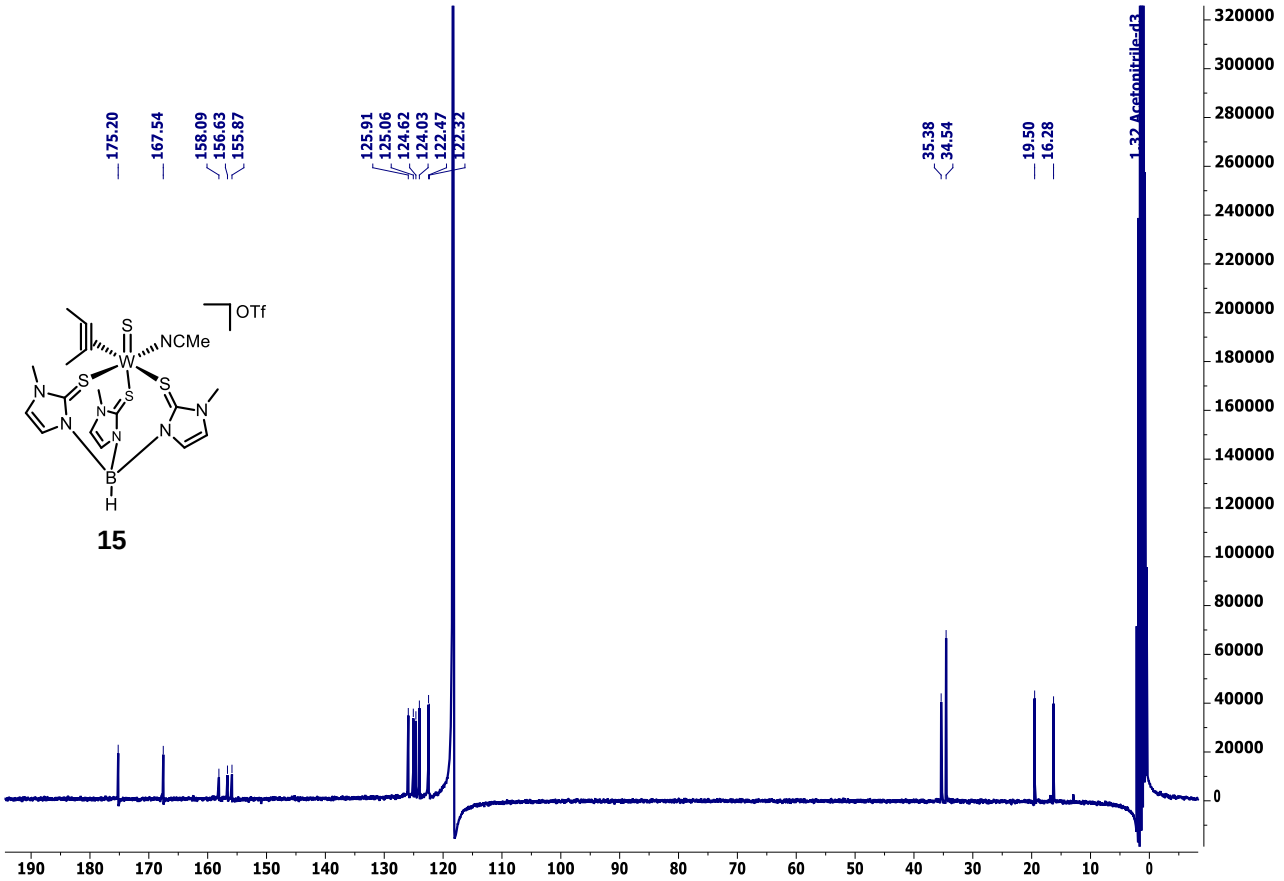

Figure S40: ^{13}C NMR spectrum of [WS(C_2Me_2)(MeCN)(Tm^{Me})](OTf) (**15**) in CD_3CN.

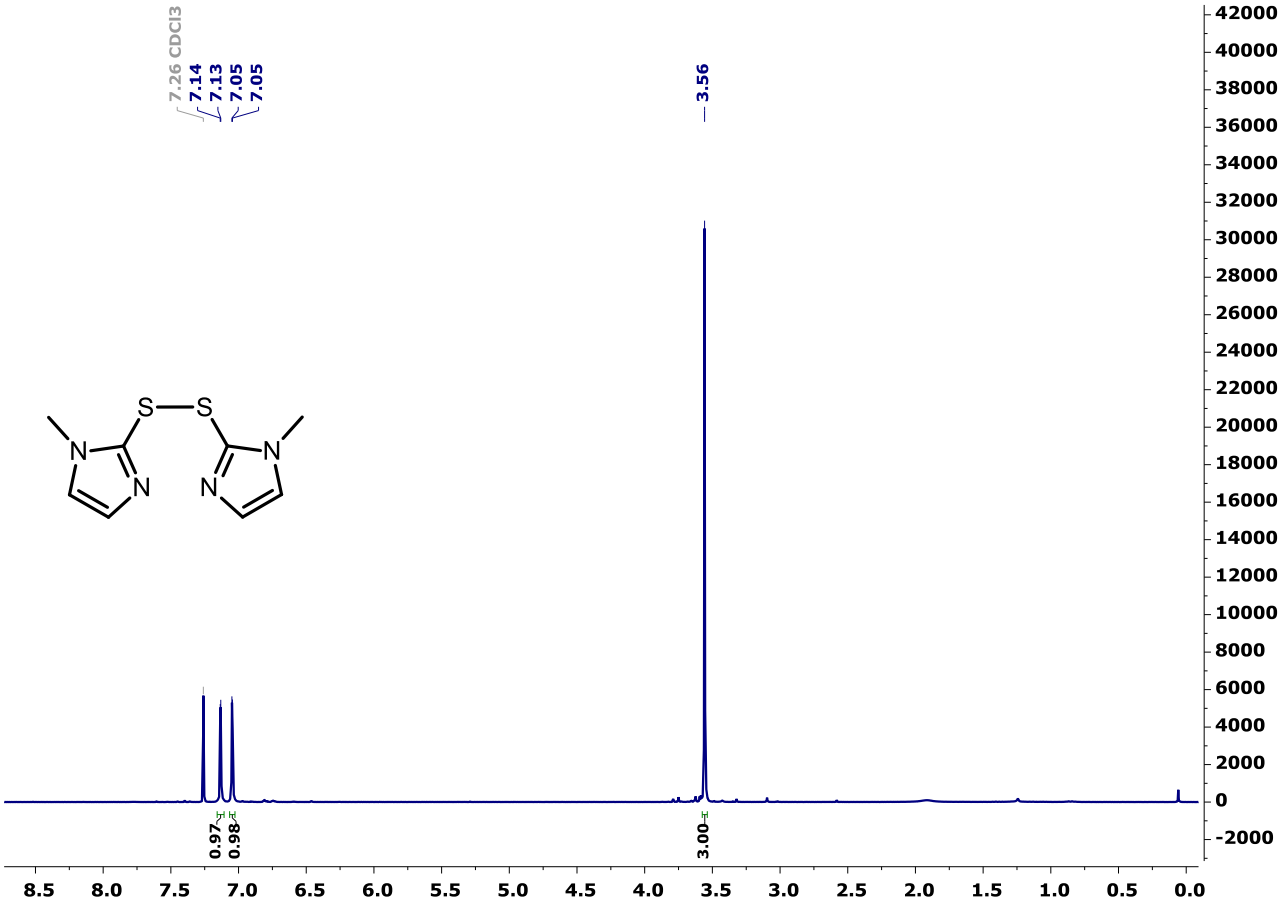

Figure S41: ^{1}H NMR spectrum of mt-S-S-mt in $CDCl_3$.

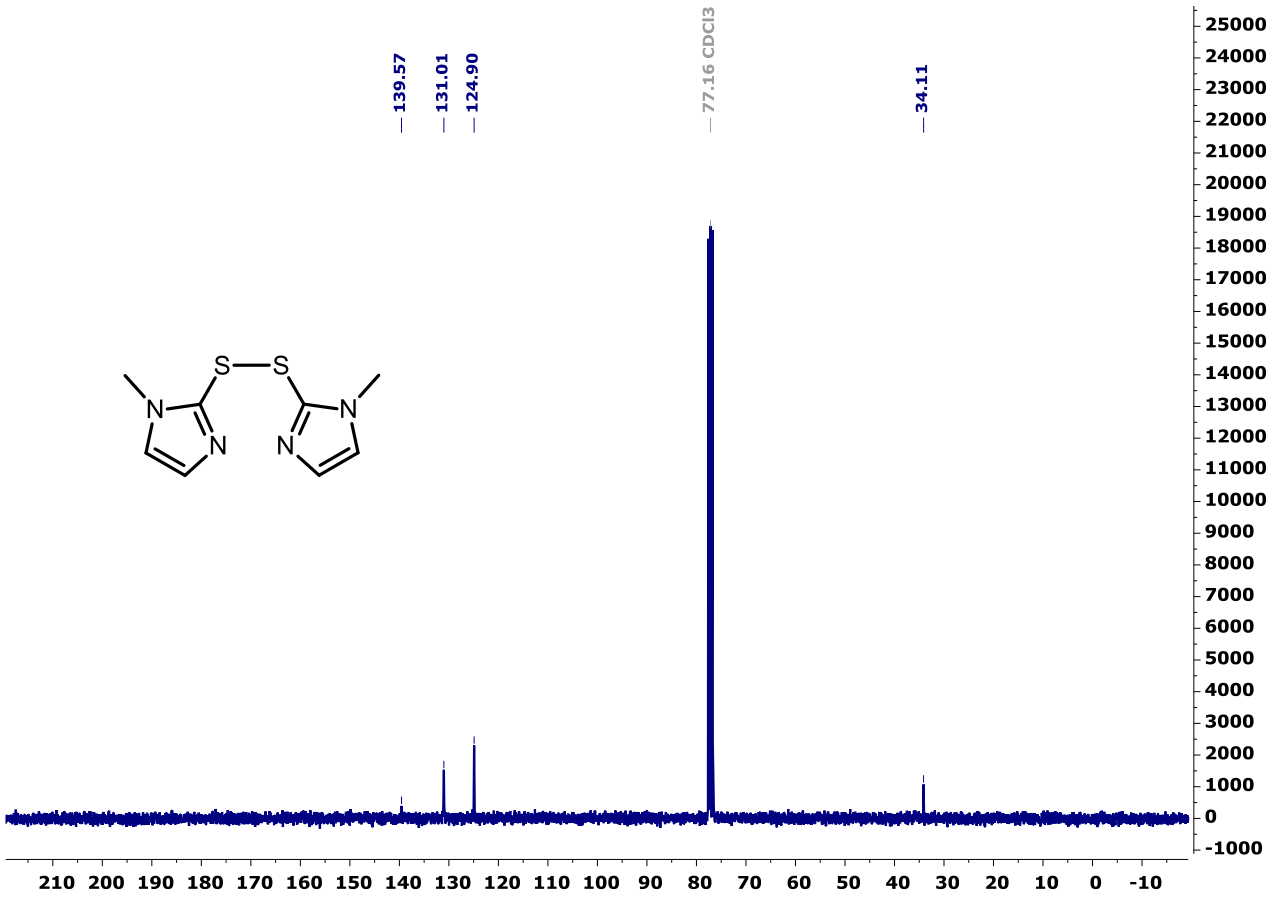

Figure S42: ^{13}C NMR spectrum of mt-S-S-mt in $CDCl_3$.

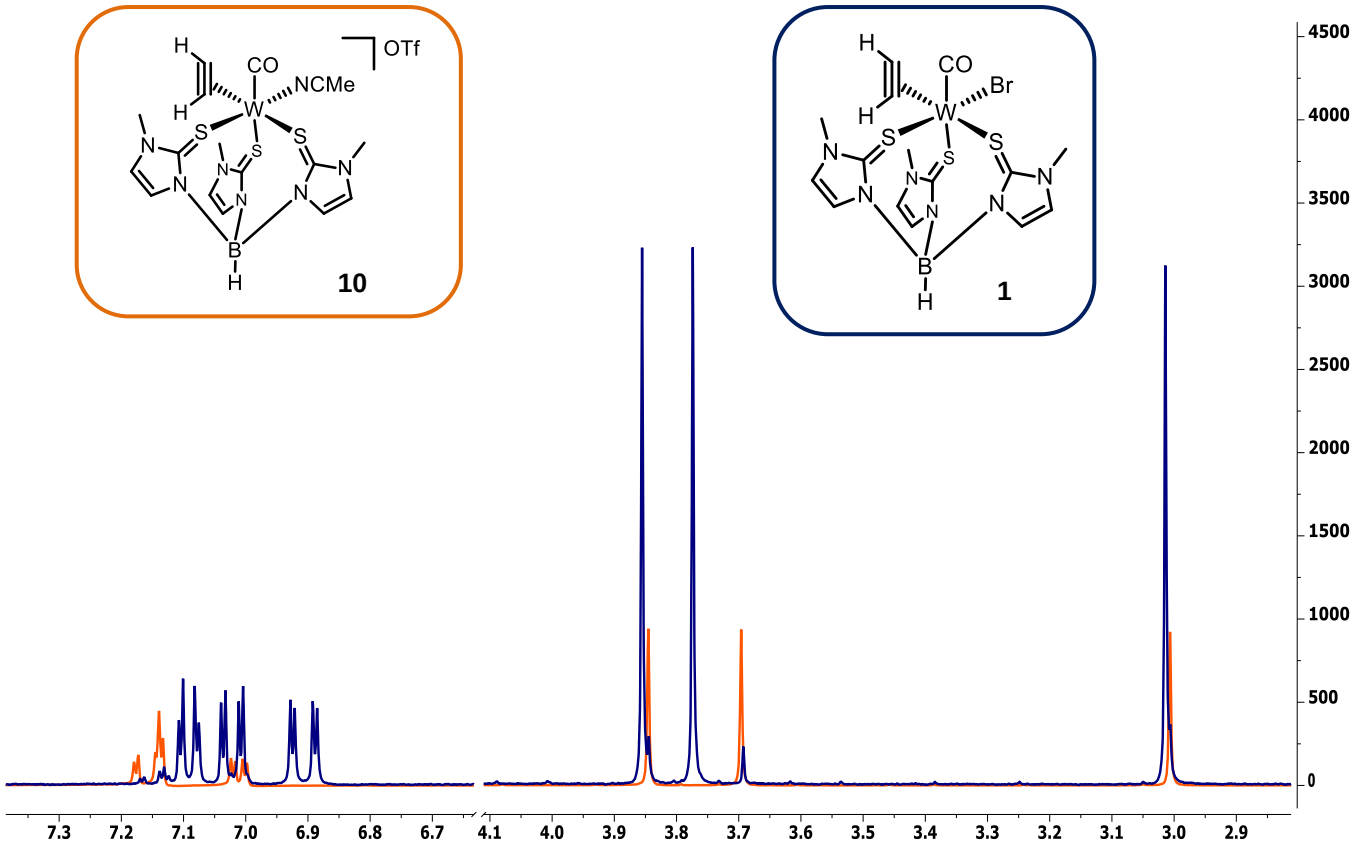

Figure S43: Superimposed spectra of [W(CO)(C_2H_2)(Tm^{Me})Br] (**1**, blue) and [W(CO)(C_2H_2)(MeCN)(Tm^{Me})](OTf) (**10**, orange) in CD_3CN.

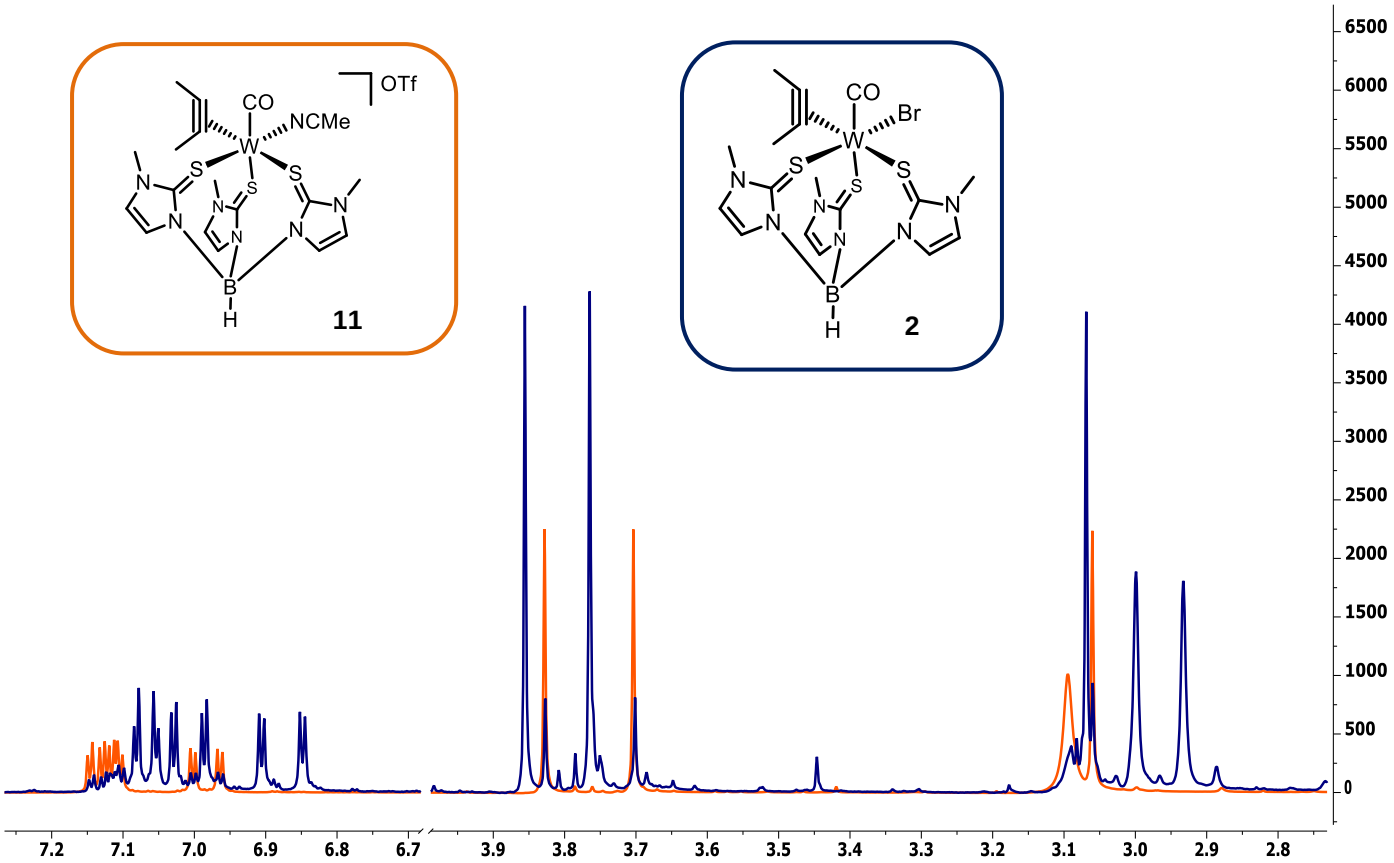

Figure S44: Superimposed spectra of [W(CO)(C_2Me_2)(Tm^{Me})Br] (**2**, blue) and [W(CO)(C_2Me_2)(MeCN)(Tm^{Me})](OTf) (**11**, orange) in CD_3CN.

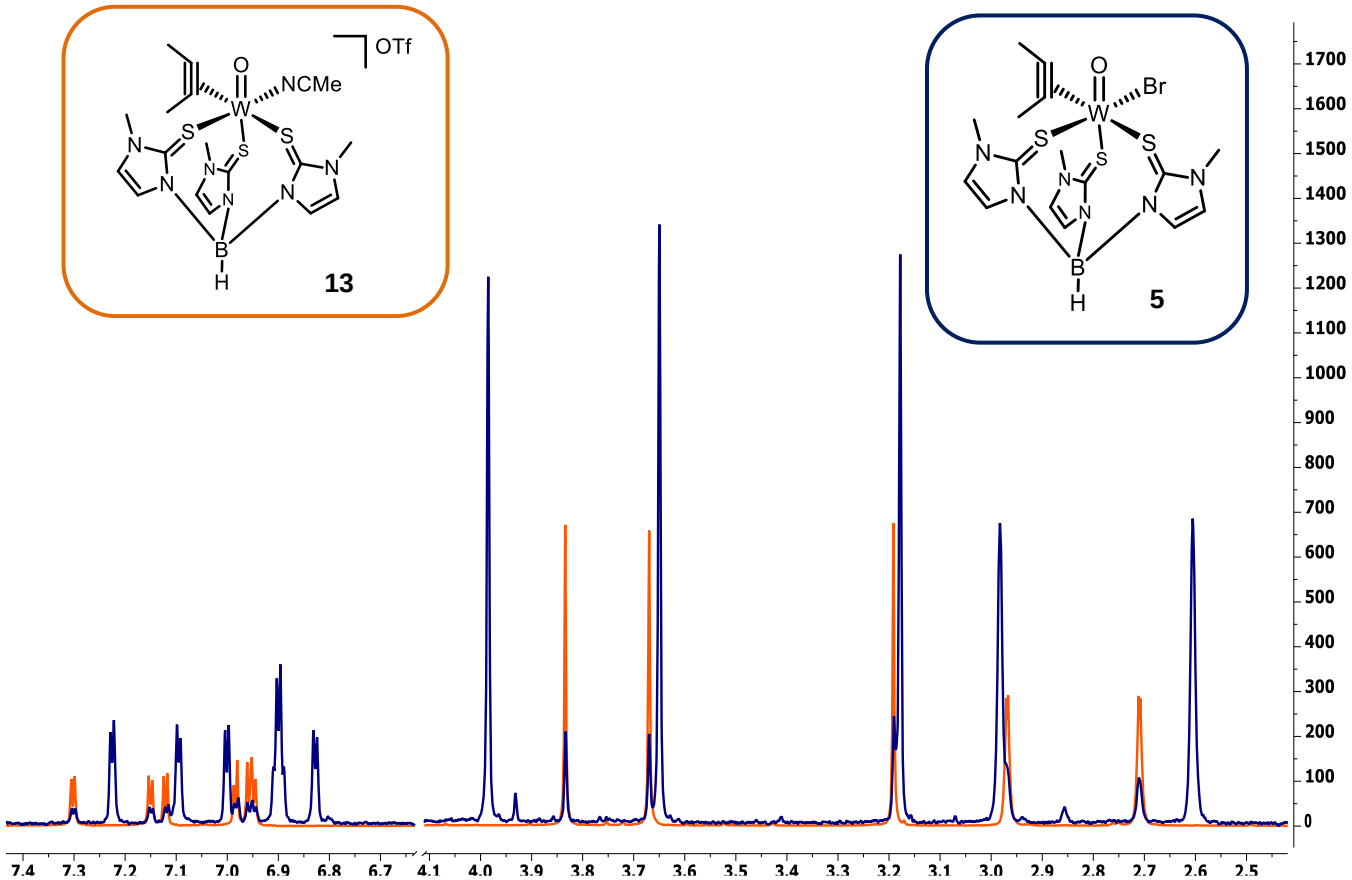

Figure S45: Superimposed spectra of [WO(C_2Me_2)(Tm^{Me})Br] (**5**, blue) and [WO(C_2Me_2)(MeCN)(Tm^{Me})](OTf) (**13**, orange) in CD_3CN.

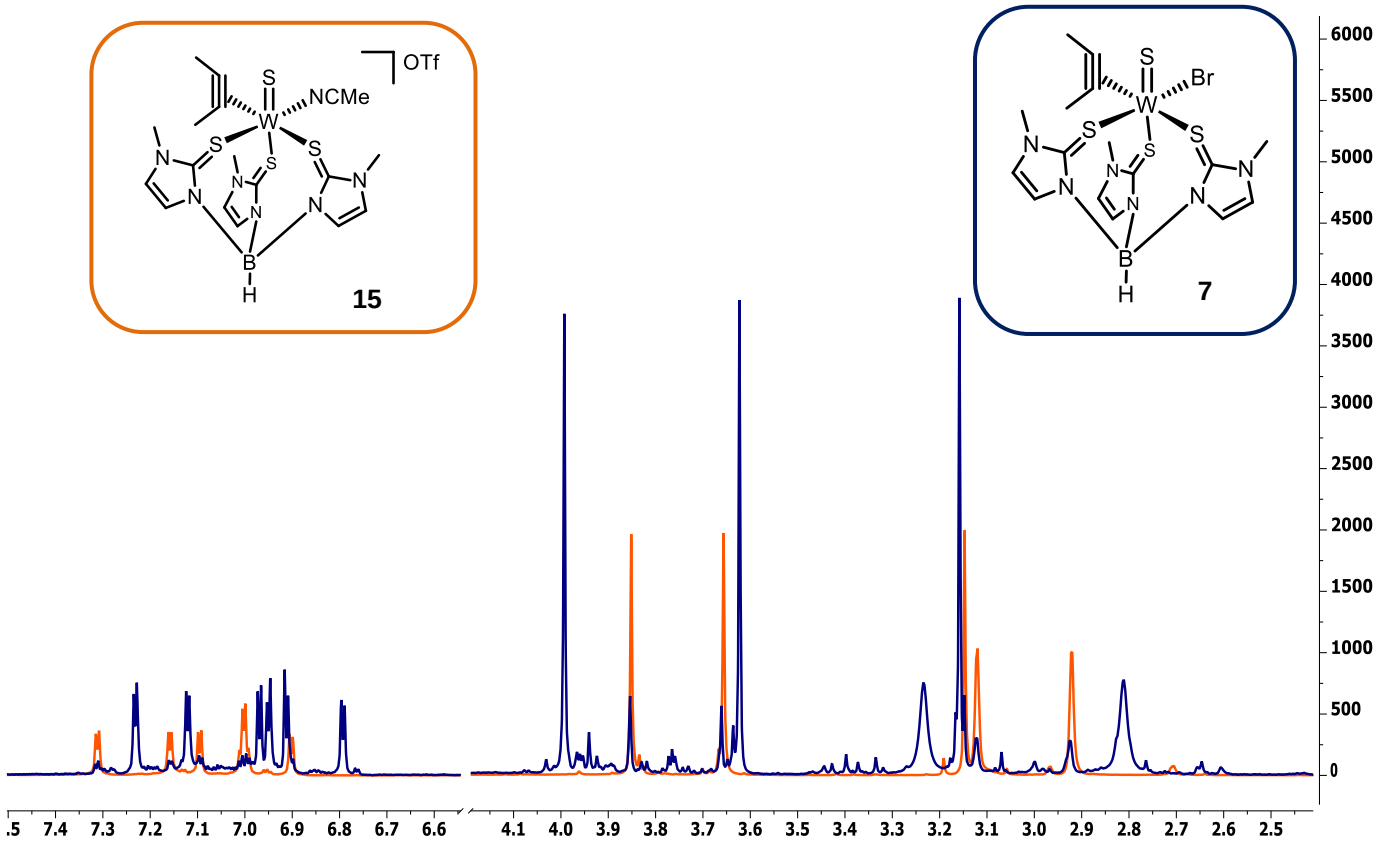

Figure S46: Superimposed spectra of [WS(C_2Me_2)(Tm^{Me})Br] (**7**, blue) and [WS(C_2Me_2)(MeCN)(Tm^{Me})](OTf) (**15**, orange) in CD_3CN.

3 HIGH-RESOLUTION MASS SPECTRA

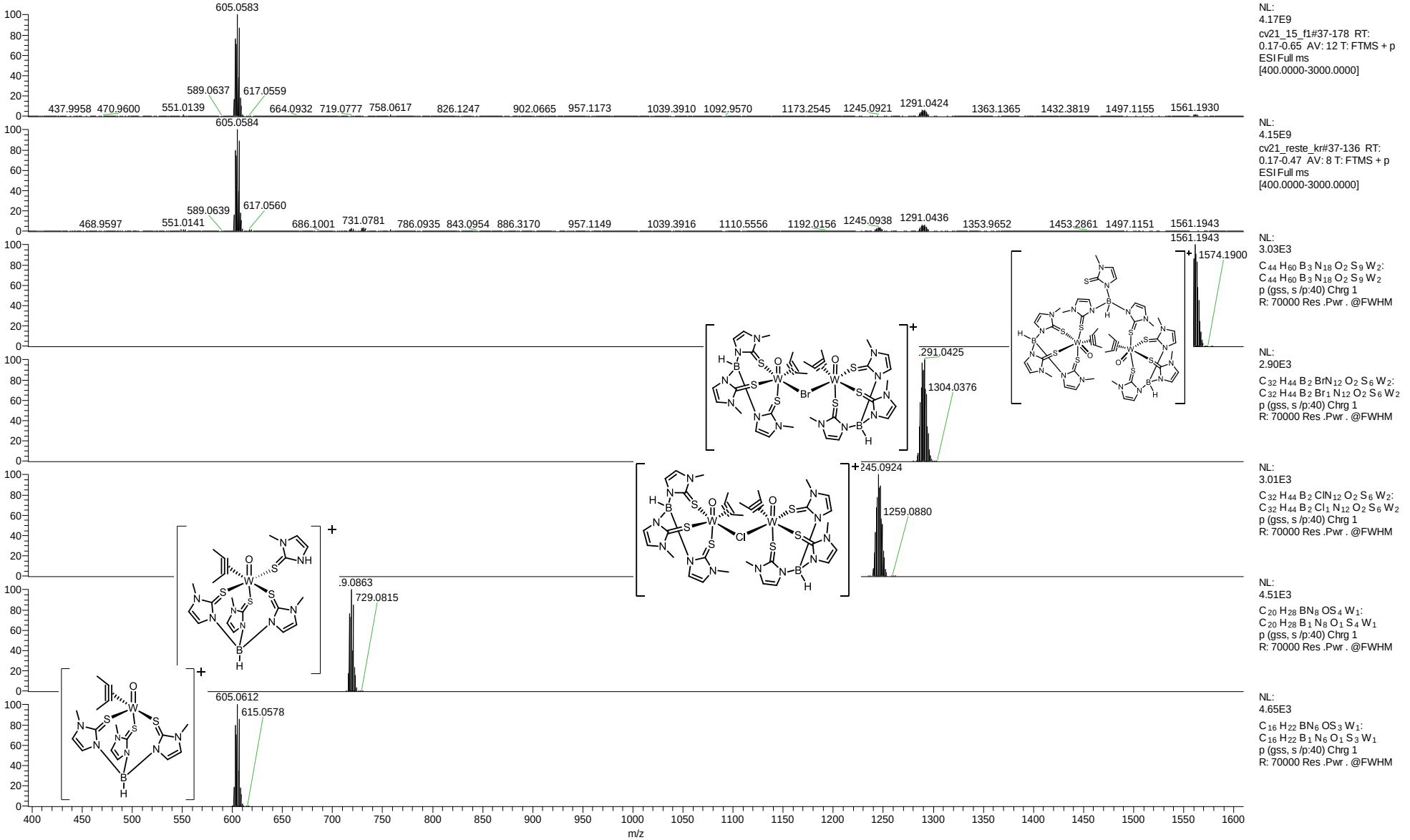

Figure S47: High-resolution mass spectrum of [WO(C_2Me_2)(Tm^{Me})$Br_{0.82}Cl_{0.18}$] (**5**) and the calculated masses of various fragments.

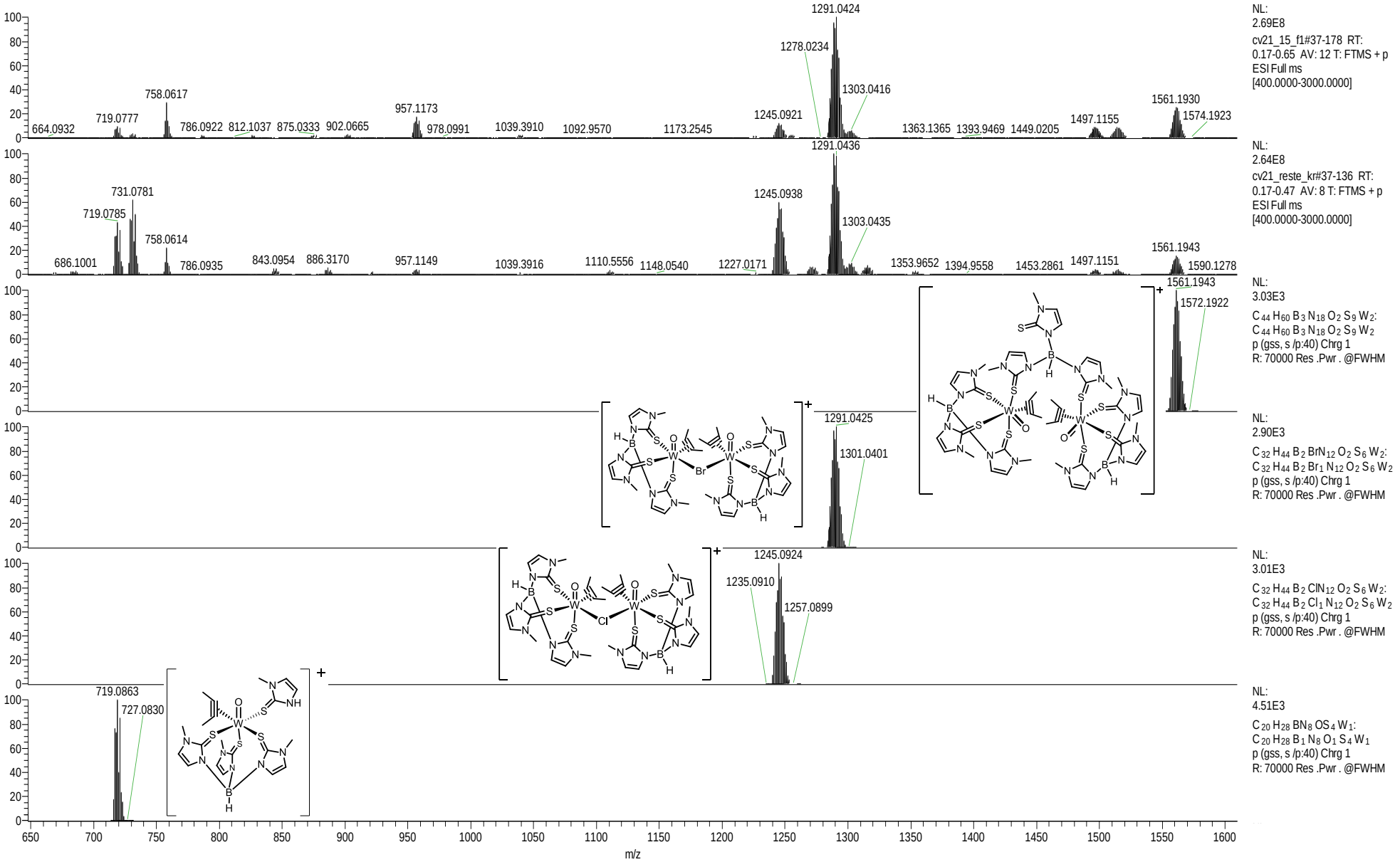

Figure S48: Zoomed in high-resolution mass spectrum of [WO(C_2Me_2)(Tm^{Me})$Br_{0.82}Cl_{0.18}$] (**5**) and the calculated masses of various fragments.

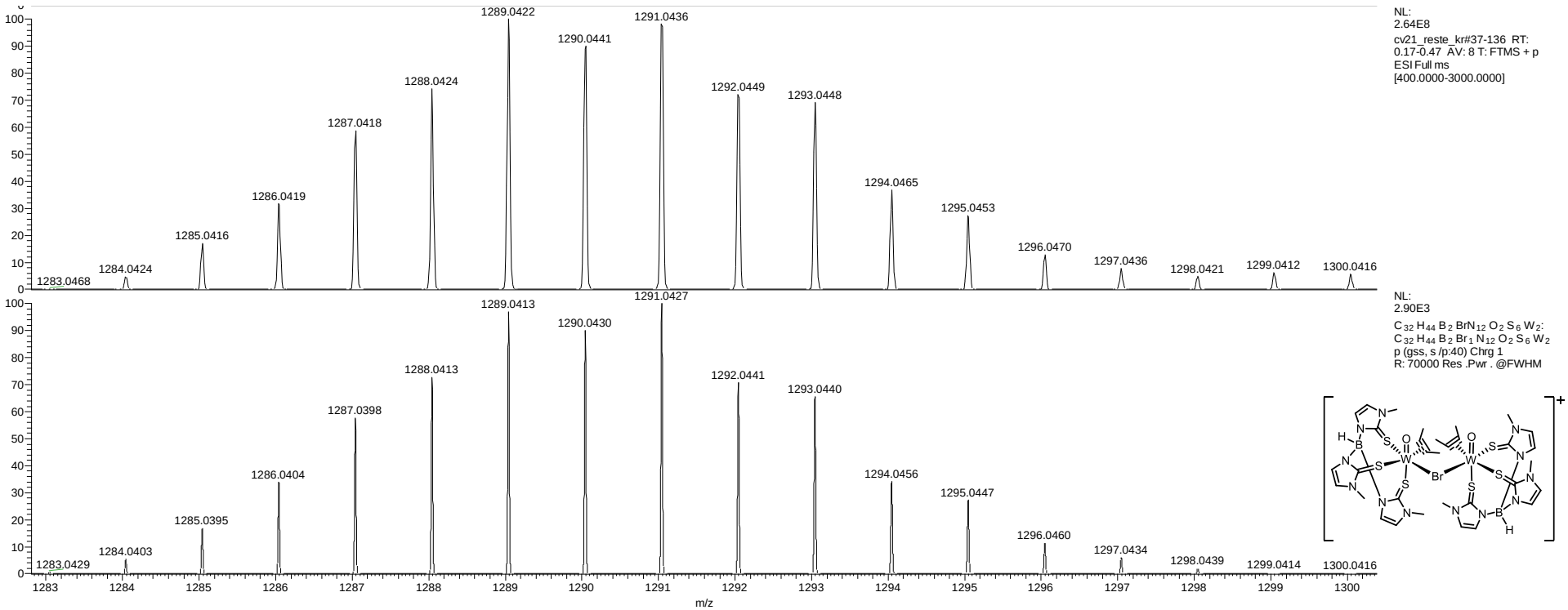

Figure S49: High-resolution mass spectrum of [WO(C_2Me_2)(Tm^{Me})$Br_{0.82}Cl_{0.18}$] (**5**) showing the peak for the [WO(C_2Me_2)(Tm^{Me})(**μ-Br**)(Tm^{Me})(C_2Me_2)OW]$^+$ ion (top) and its calculated mass (bottom).

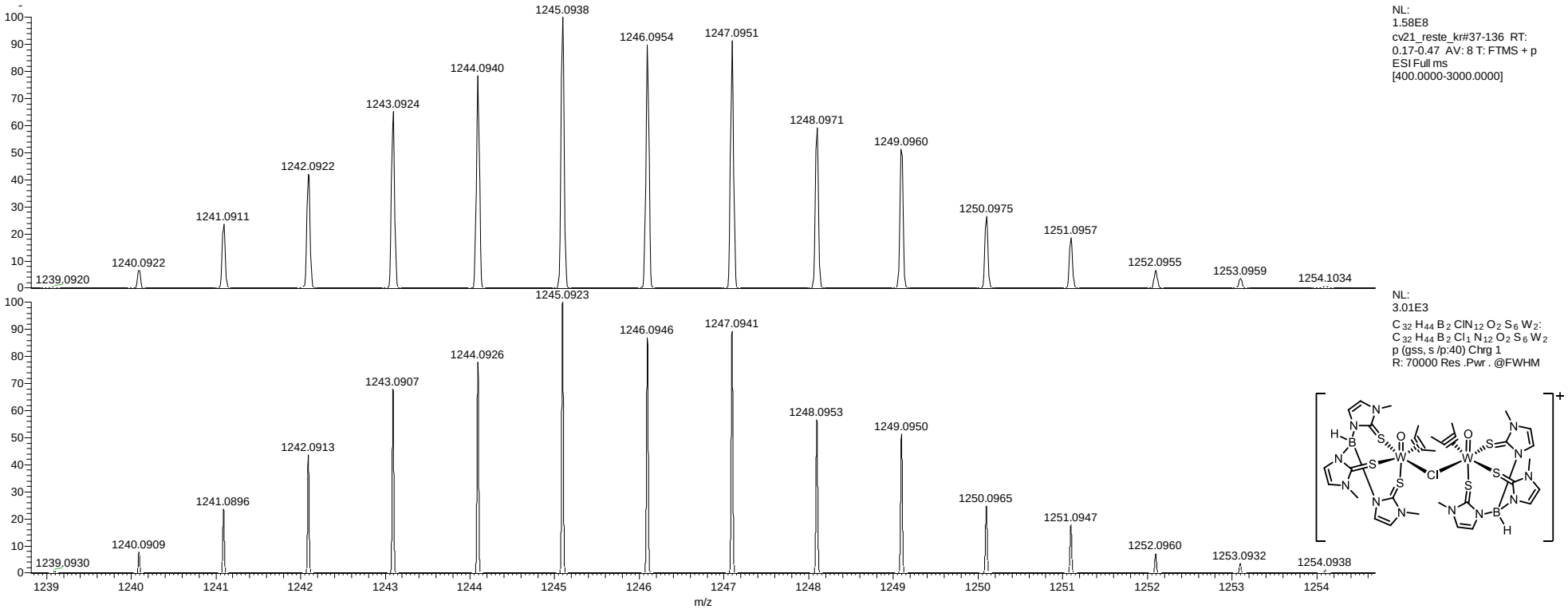

Figure S50: High-resolution mass spectrum of [WO(C_2Me_2)(Tm^{Me})$Br_{0.82}Cl_{0.18}$] (**5**) showing the peak for the [WO(C_2Me_2)(Tm^{Me})(**μ-Cl**)(Tm^{Me})(C_2Me_2)OW]$^+$ ion (top) and its calculated mass (bottom).

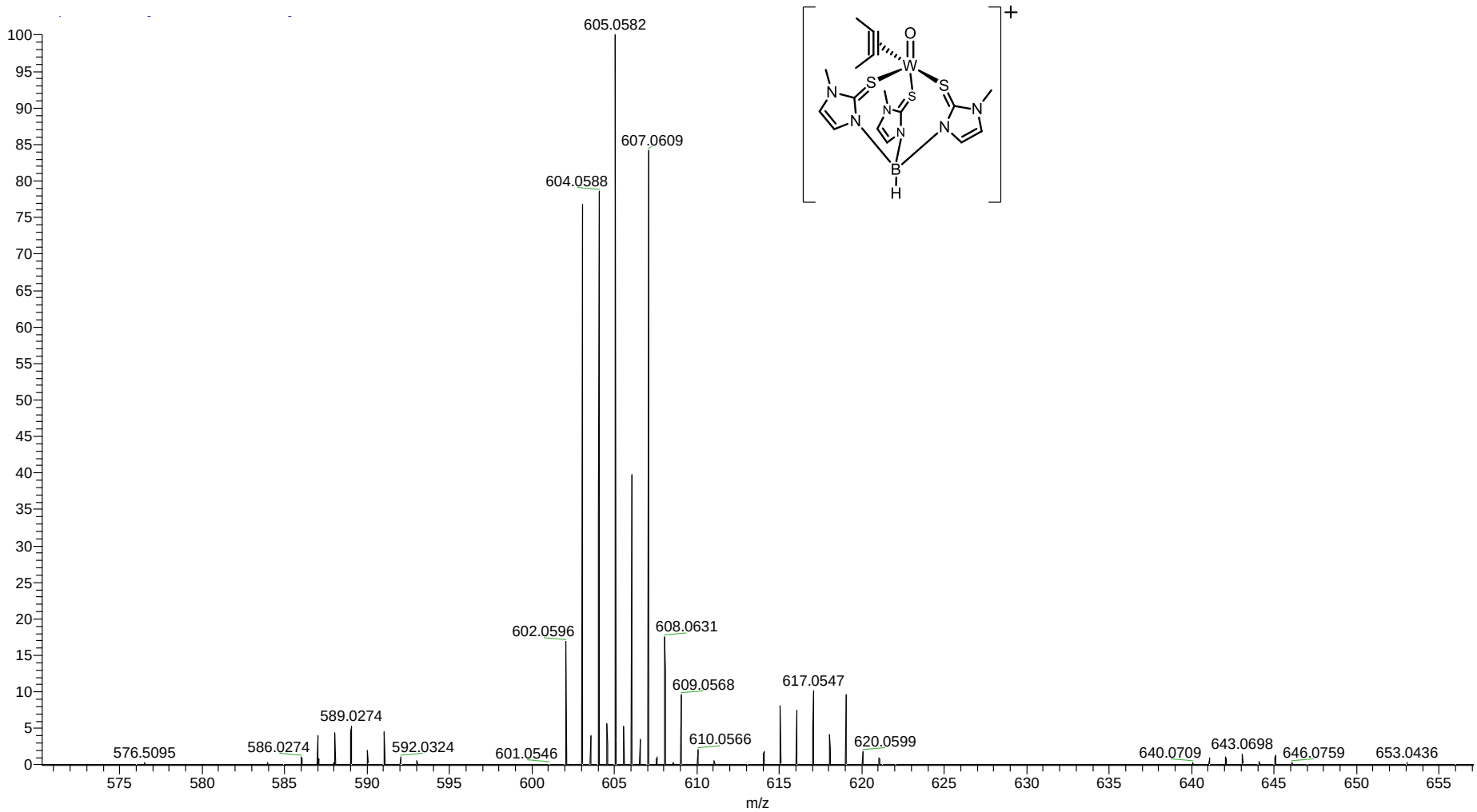

Figure S51: Zoomed in high-resolution mass spectrum of $[W_2O(\mu\text{-}O)_2(C_2Me_2)_2(Tm^{Me})_2](OTf)_2$ (**8**) showing the peak for the $[WO(C_2Me_2)(Tm^{Me})]^+$ fragment. .

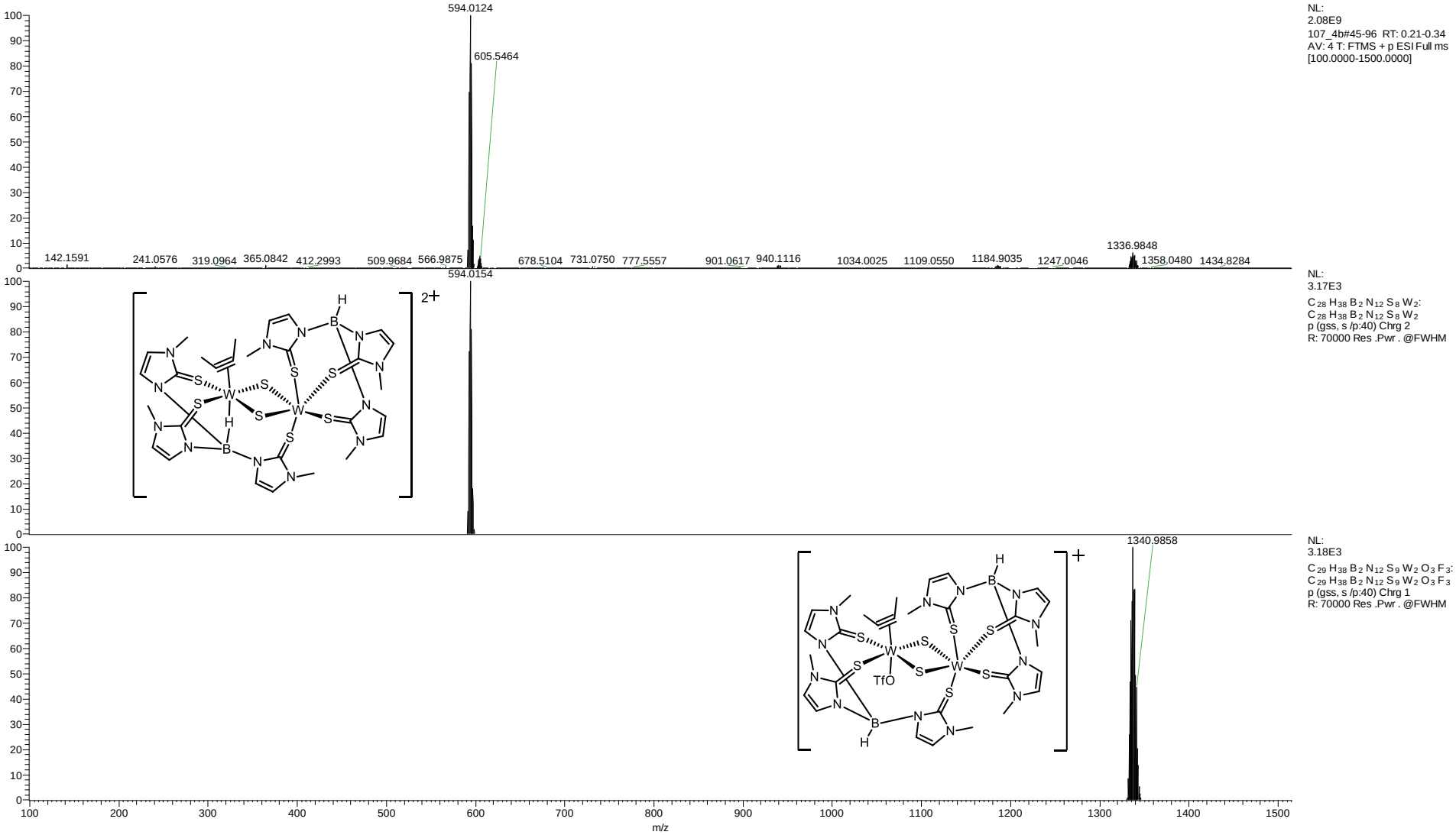

Figure S52: High-resolution mass spectrum of $[W_2(\mu\text{-}S)_2(C_2Me_2)(Tm^{Me})_2](OTf)_2$ (**9**) and the calculated masses of various fragments.

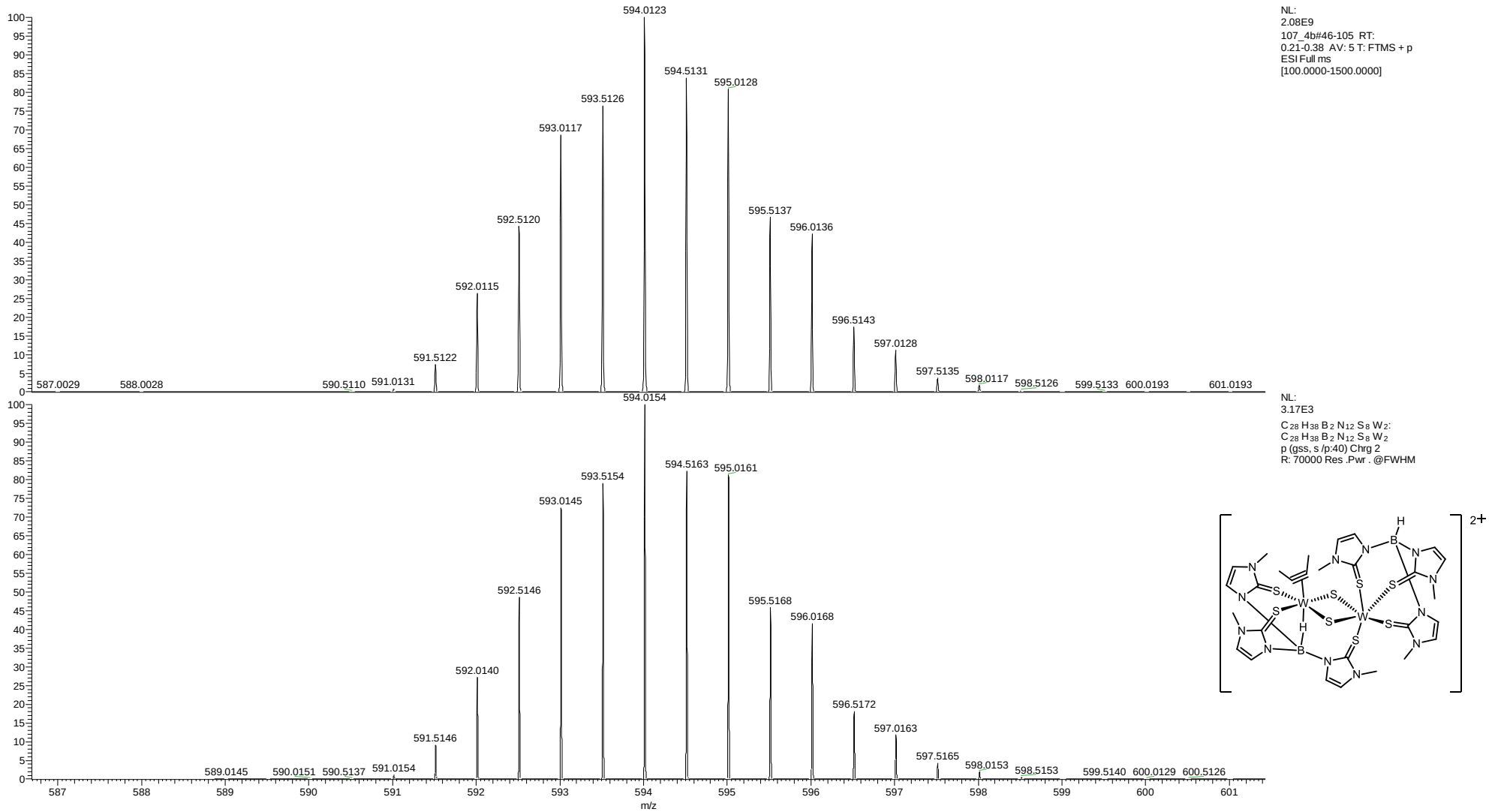

Figure S53: High-resolution mass spectrum of $[W_2(\mu\text{-}S)_2(C_2Me_2)(Tm^{Me})_2](OTf)_2$ (**9**) showing the peak for the $[W_2(\mu\text{-}S)_2(C_2Me_2)(Tm^{Me})_2]^{2+}$ ion (top) and its calculated mass (bottom).

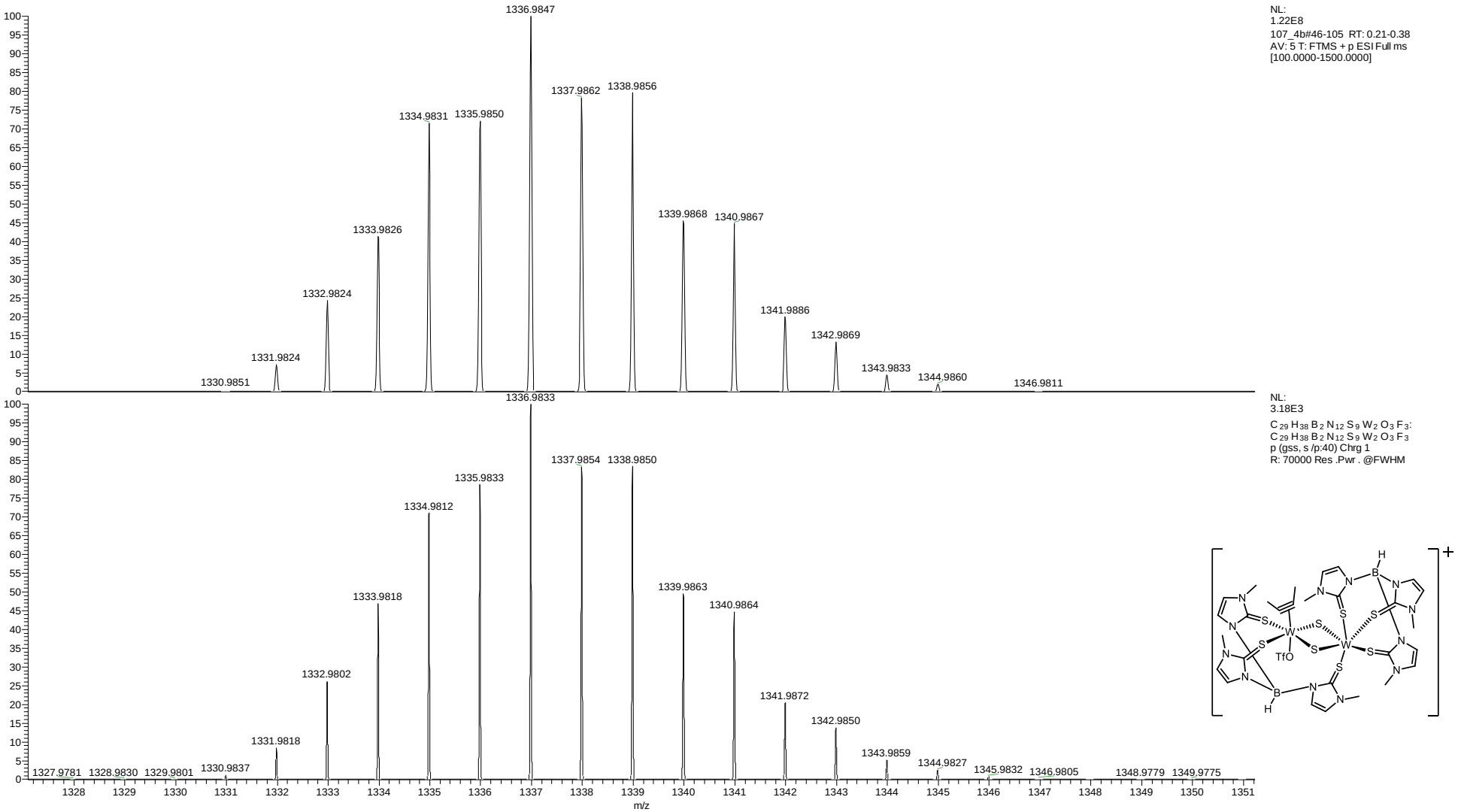

Figure S54: High-resolution mass spectrum of $[W_2(\mu\text{-}S)_2(C_2Me_2)(Tm^{Me})_2](OTf)_2$ (**9**) showing the peak for the $[W_2(\mu\text{-}S)_2(C_2Me_2)(Tm^{Me})_2(OTf)]^+$ ion (top) and its calculated mass (bottom).

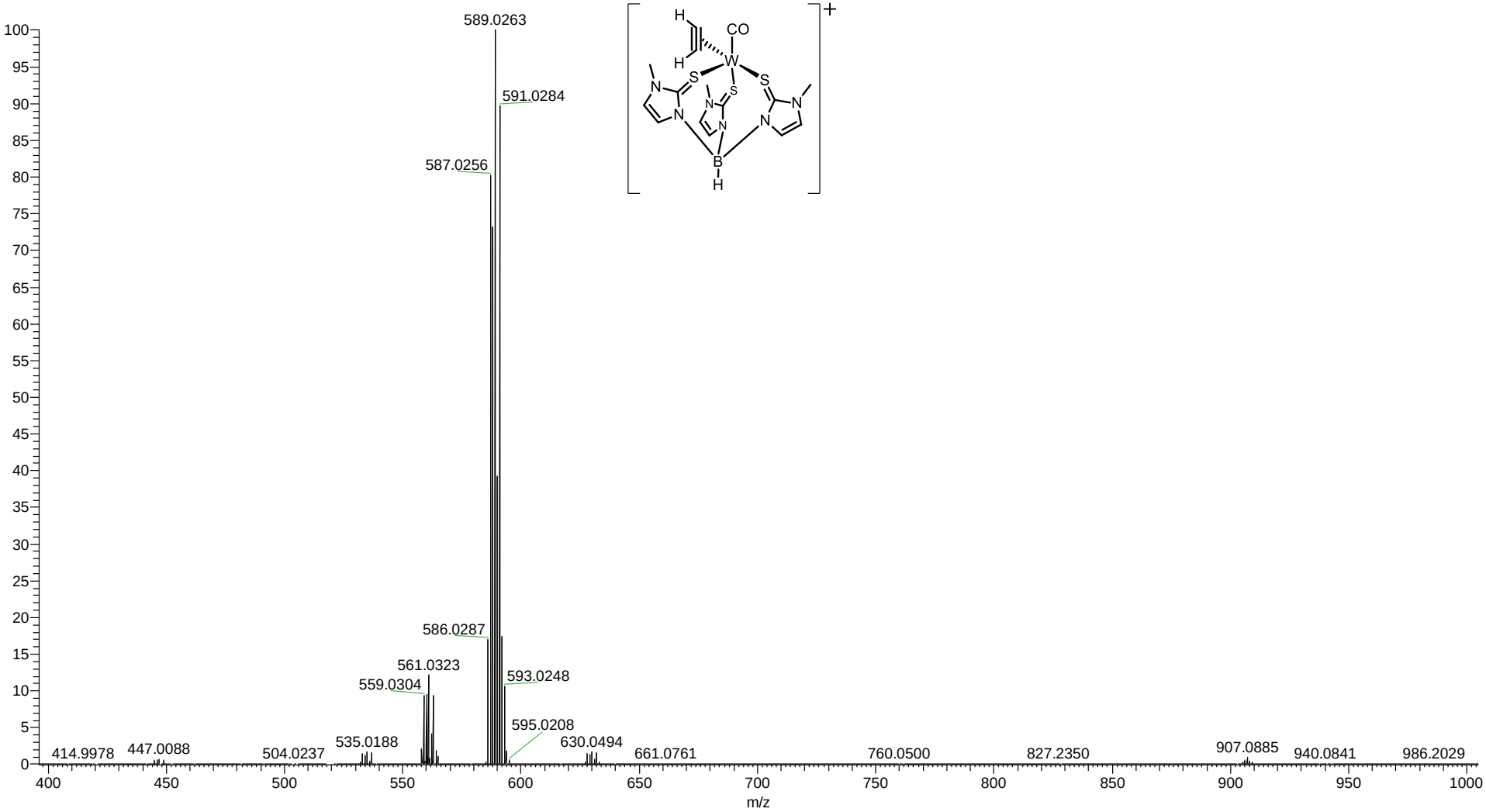

Figure S55: High-resolution mass spectrum of [W(CO)(C_2H_2)(MeCN)(Tm^{Me})](OTf) (**10**).

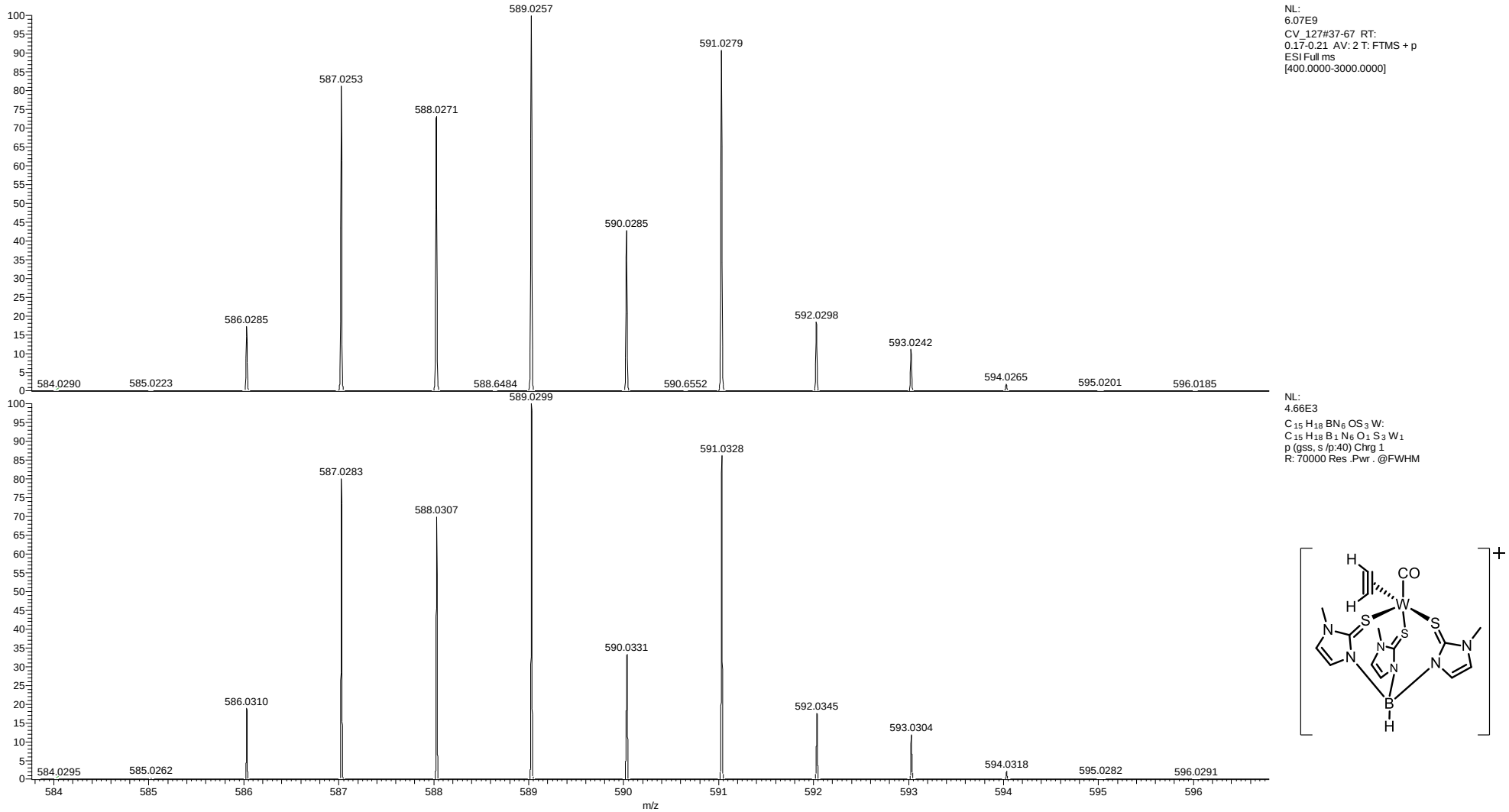

Figure S56: Zoomed in high-resolution mass spectrum of $[W(CO)(C_2H_2)(MeCN)(Tm^{Me})](OTf)$ (**10**) showing the peak for the $[WO(C_2H_2)(Tm^{Me})]^+$ ion (top) and its calculated mass (bottom).

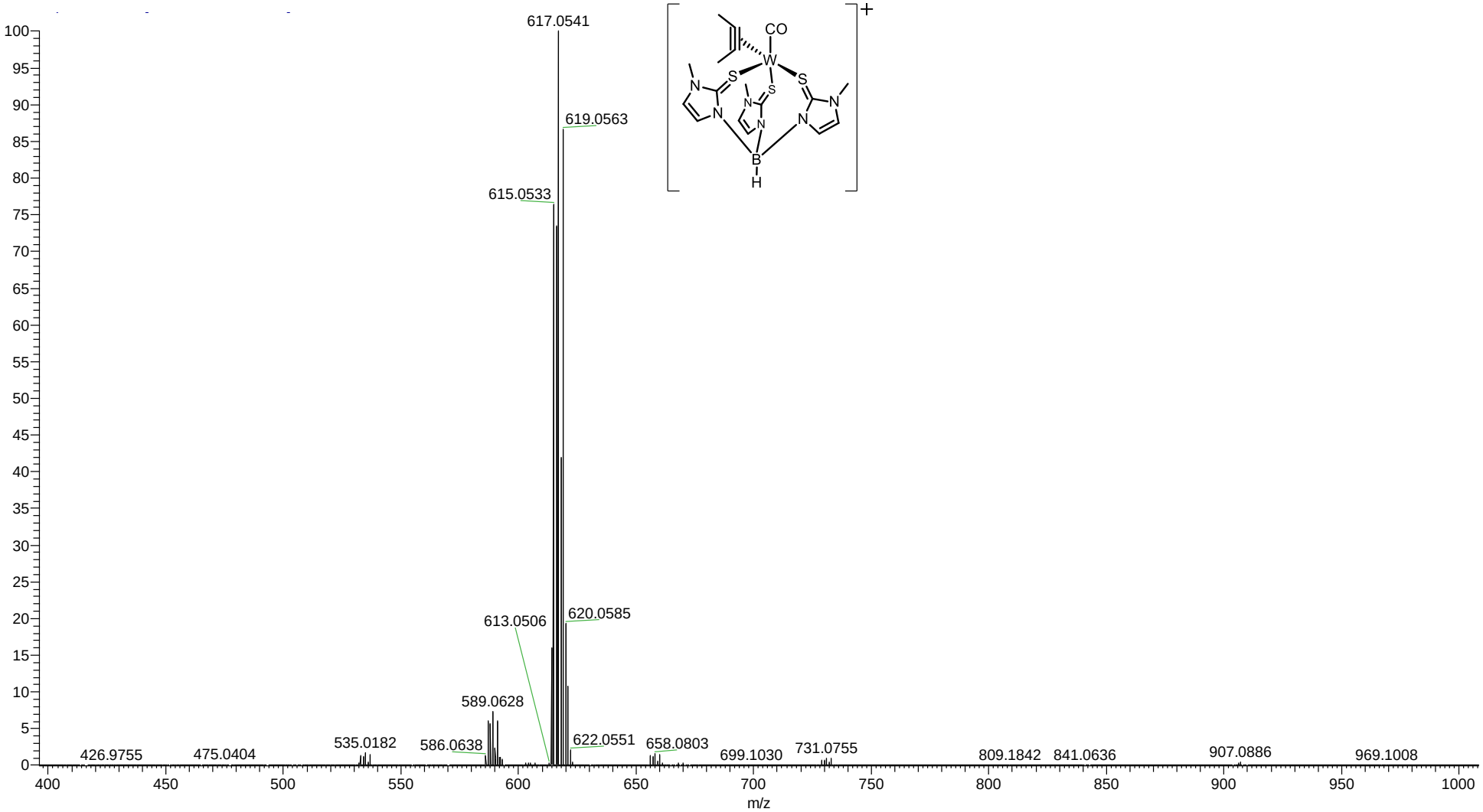

Figure S57: High-resolution mass spectrum of [W(CO)(C_2Me_2)(MeCN)(Tm^{Me})](OTf) (**11**).

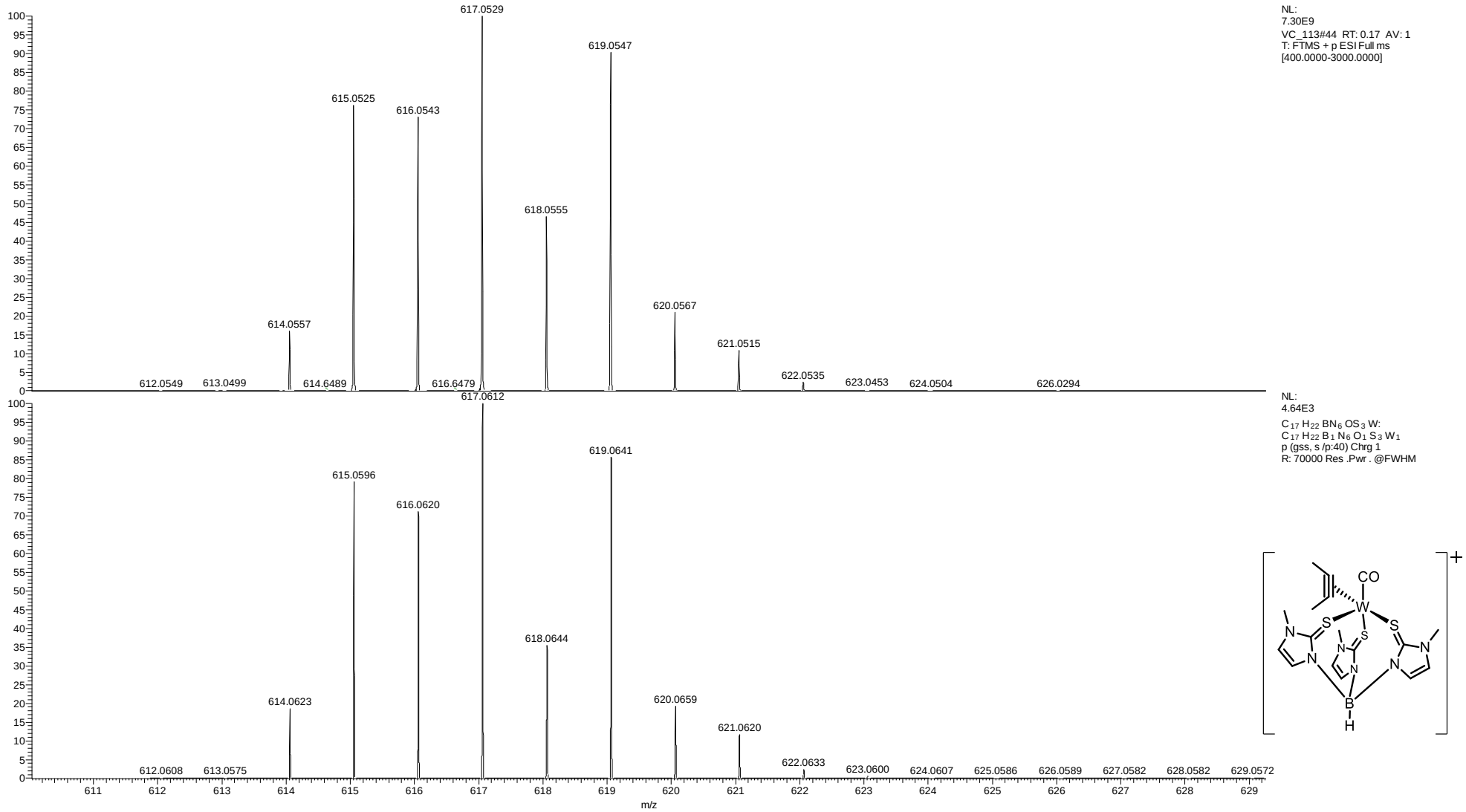

Figure S58: Zoomed in high-resolution mass spectrum of [W(CO)(C_2Me_2)(MeCN)(Tm^{Me})](OTf) (**11**) showing the peak for the [WO(C_2Me_2)(Tm^{Me})]$^+$ ion (top) and its calculated mass (bottom).

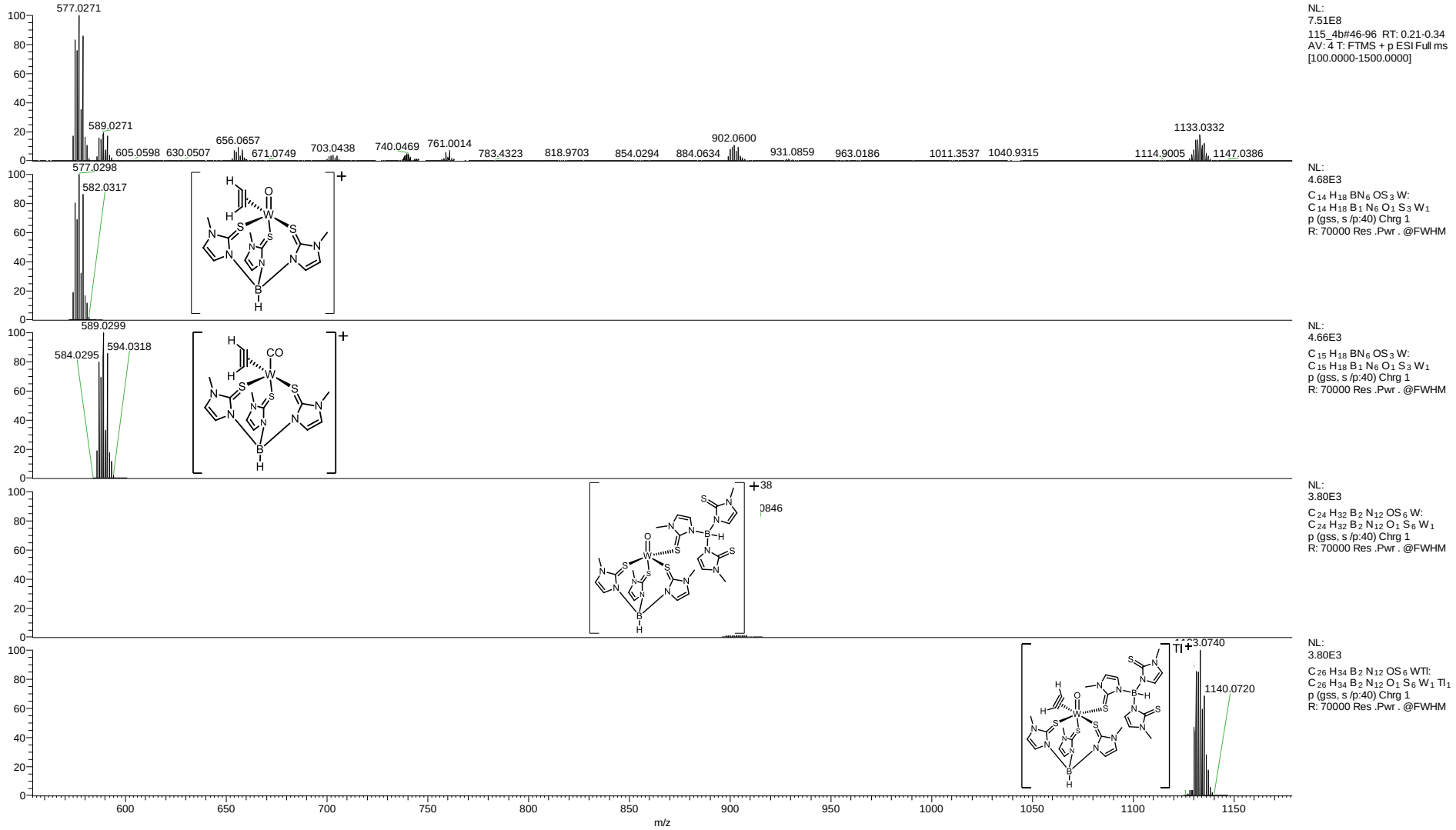

Figure S59: Zoomed in high-resolution mass spectrum of [WO(C_2H_2)(MeCN)(Tm^{Me})](OTf) (**12**) and the calculated masses of various fragments.

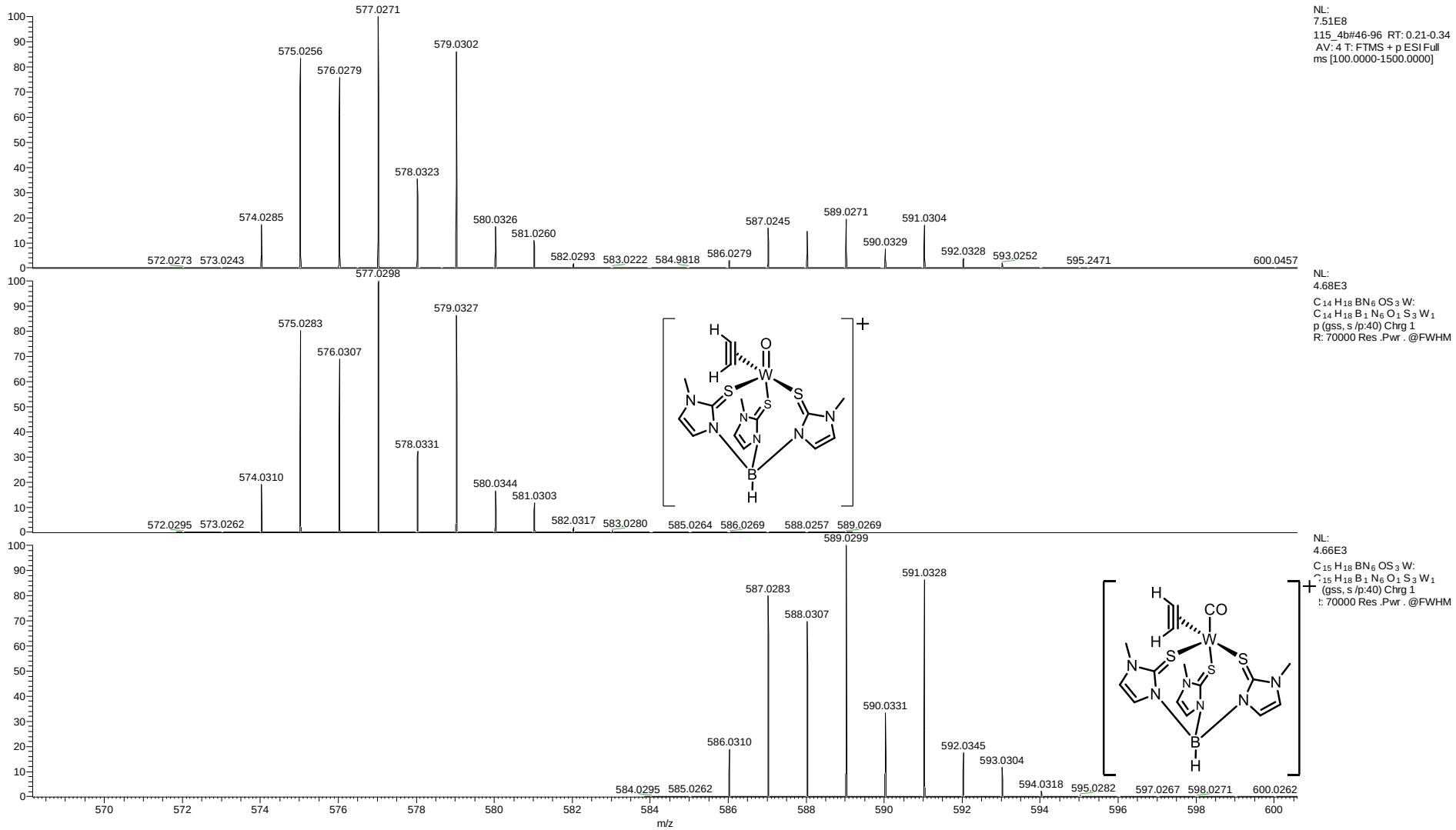

Figure S60: Closer zoom in high-resolution mass spectrum of $[WO(C_2H_2)(MeCN)(Tm^{Me})](OTf)$ (**12**) showing the peak for the $[WO(C_2H_2)(Tm^{Me})]^+$ and $[W(CO)(C_2H_2)(Tm^{Me})]^+$ ion (top) and its calculated masses (middle and bottom).

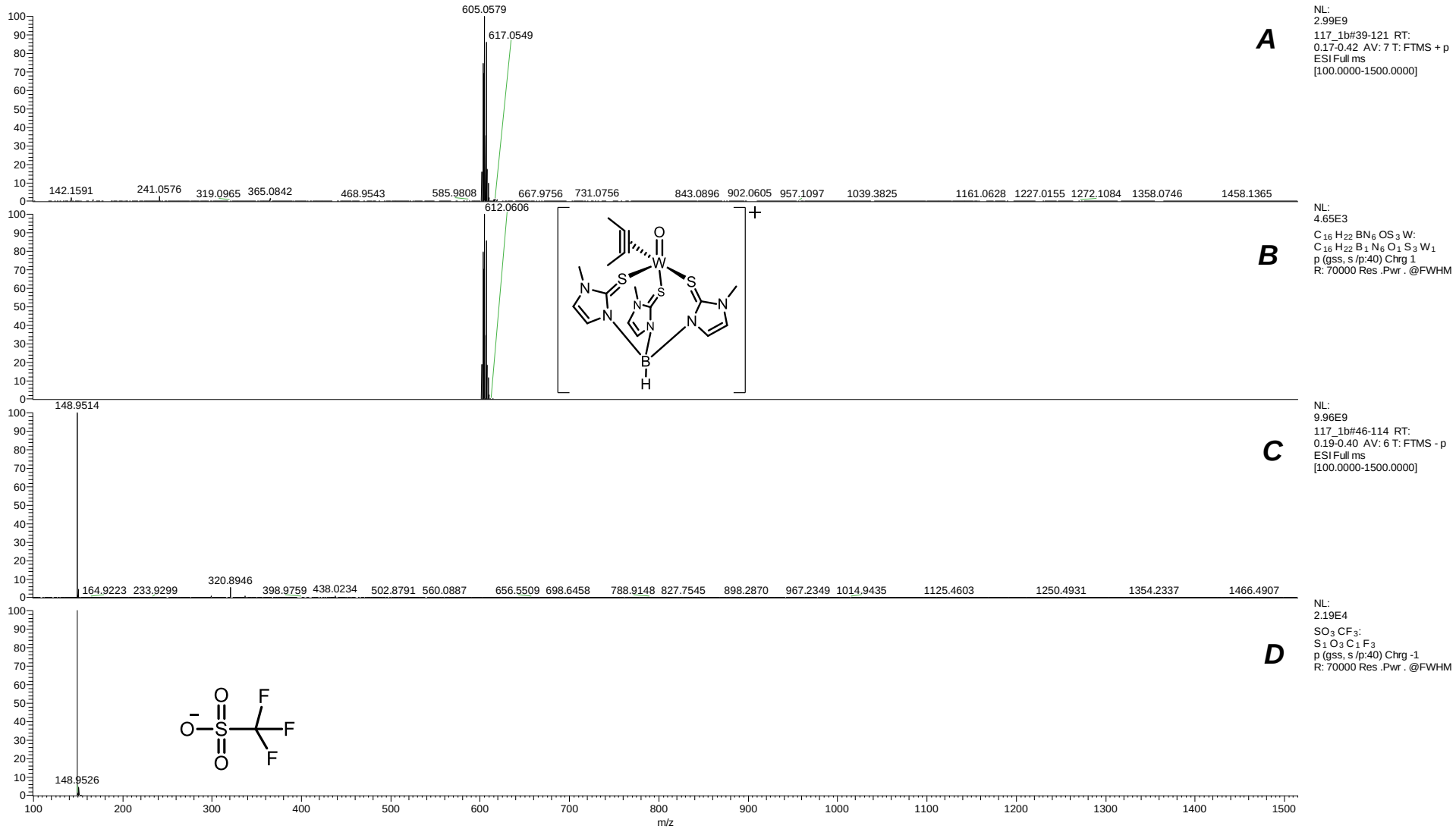

Figure S61: High-resolution mass spectrum of $[WO(C_2Me_2)(MeCN)(Tm^{Me})](OTf)$ (**13**) showing the scan for kations (A) and for anions (B) and the calclated masses for $[WO(C_2Me_2)(Tm^{Me})]^+$ (B) and $(OTf)^-$ ion (D).

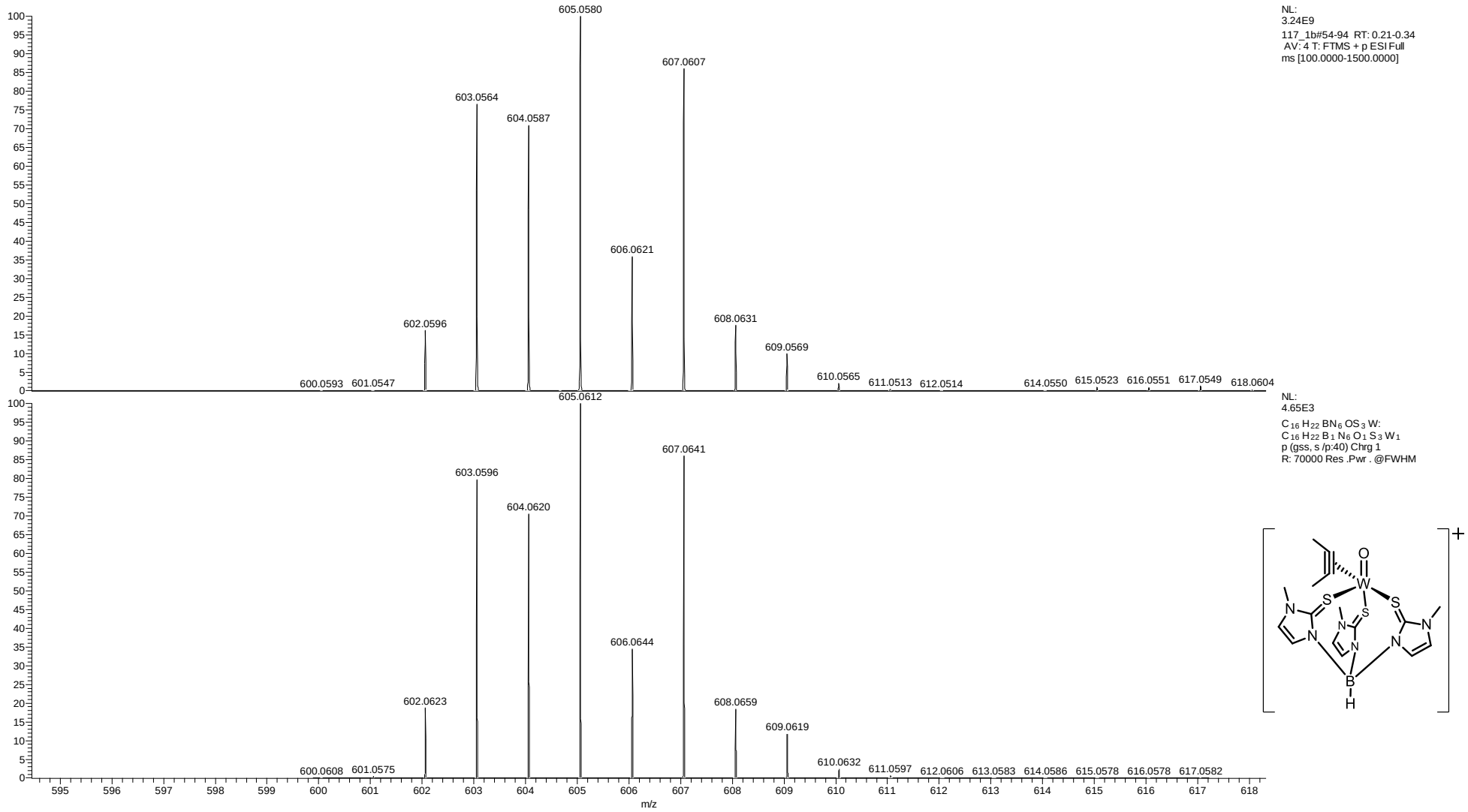

Figure S62: Zoomed in high-resolution mass spectrum of $[WO(C_2Me_2)(MeCN)(Tm^{Me})](OTf)$ (**13**) showing the peak for the $[WO(C_2Me_2)(Tm^{Me})]^+$ ion (top) and its calculated mass (bottom).

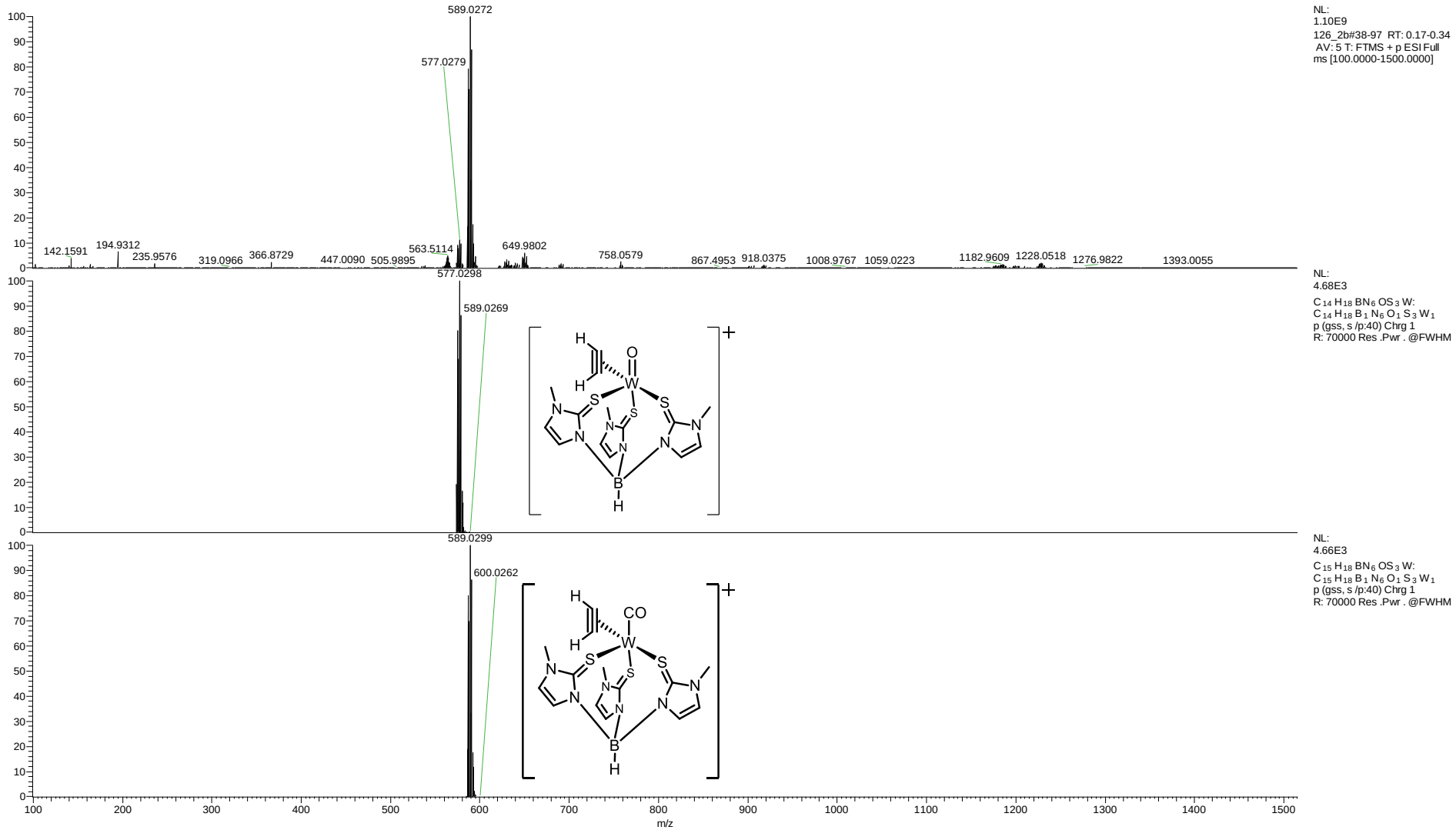

Figure S63: High-resolution mass spectrum of [WS(C_2H_2)(MeCN)(Tm^{Me})](OTf) (**14**) and the calculated masses of various fragments.

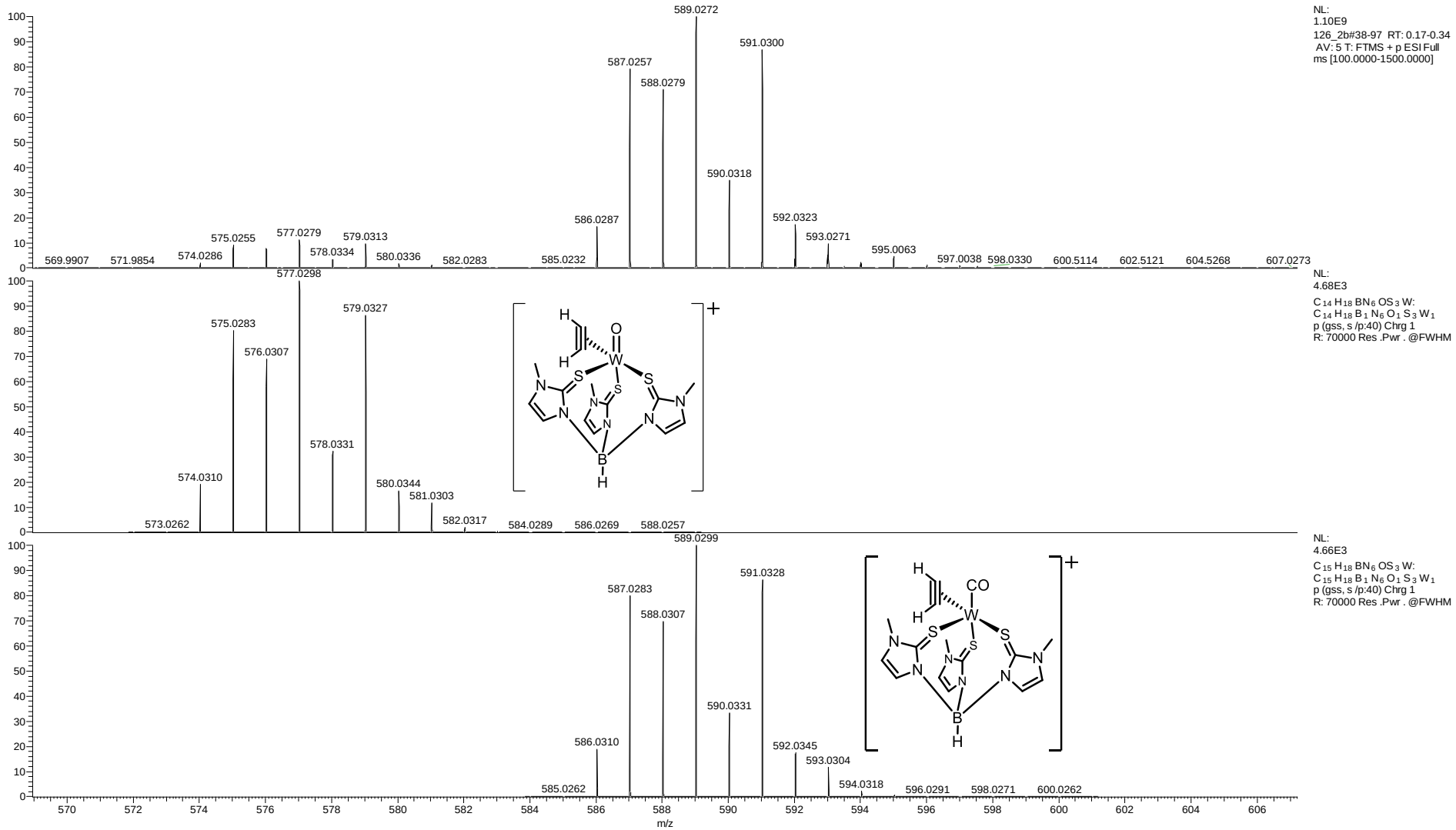

Figure S64: Zoomed in high-resolution mass spectrum of $[WS(C_2H_2)(MeCN)(Tm^{Me})](OTf)$ (**14**) showing the peak for the $[WO(C_2H_2)(Tm^{Me})]^+$ and the $[W(CO)(C_2H_2)(Tm^{Me})]^+$ ion and their calculated mass (middle and bottom).

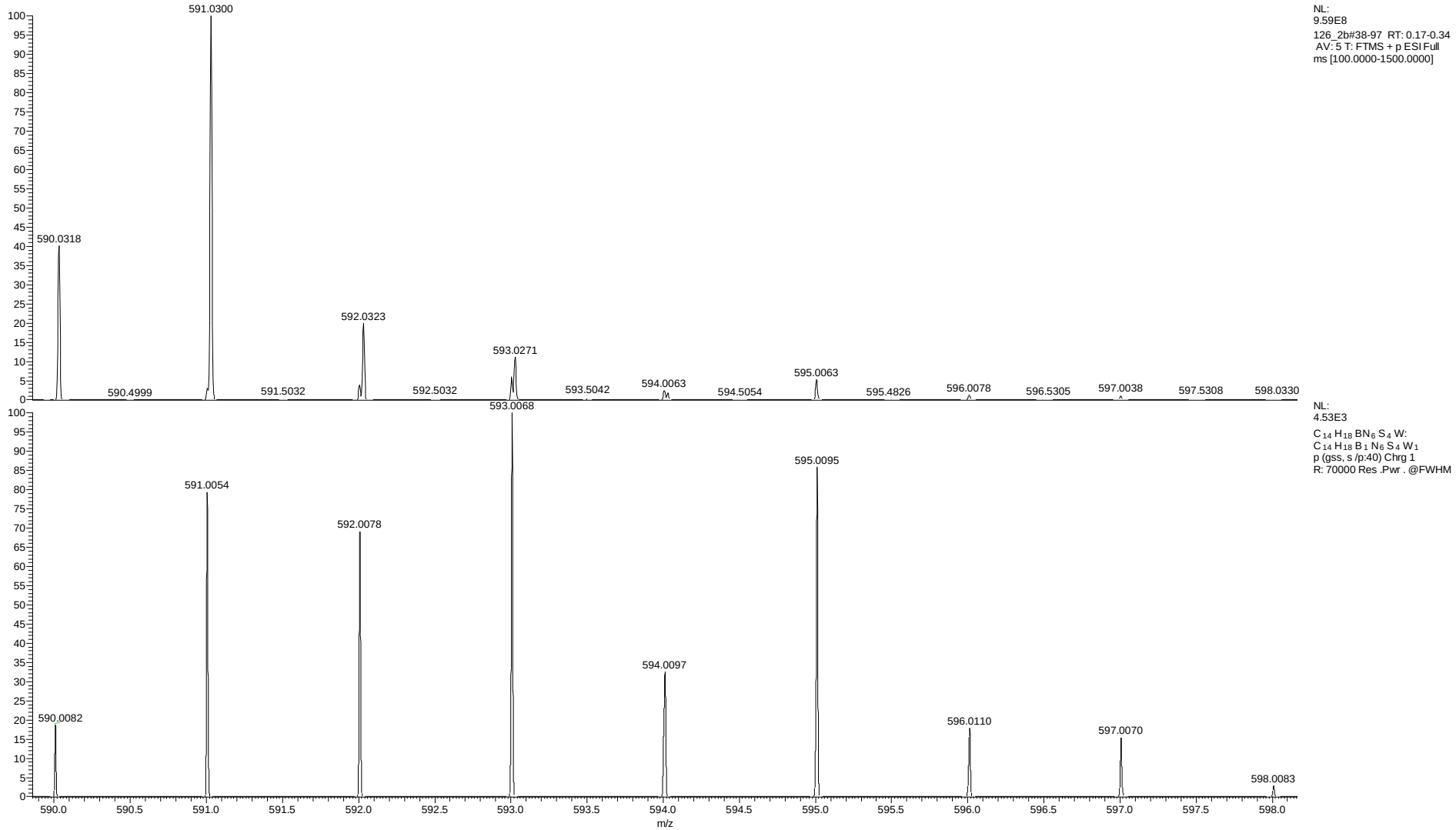

Figure S65: Zoomed in high-resolution mass spectrum of $[WS(C_2H_2)(MeCN)(Tm^{Me})](OTf)$ (**14**) showing the peak for the $[WS(C_2H_2)(Tm^{Me})]^+$ ion overlapping with the $[W(CO)(C_2H_2)(Tm^{Me})]^+$ ion (top) and its calculated mass (bottom).

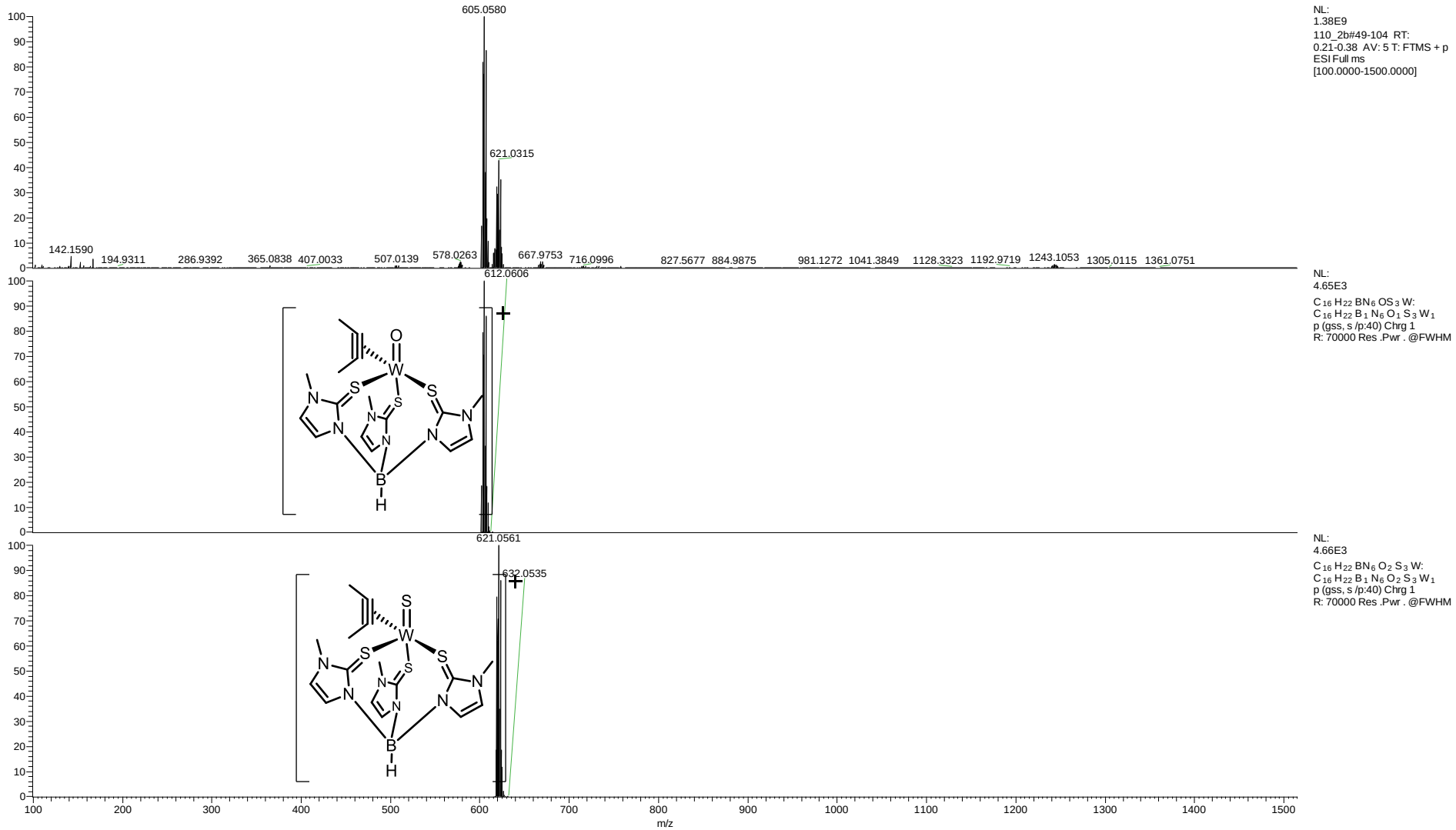

Figure S66: High-resolution mass spectrum of [WS(C_2Me_2)(MeCN)(Tm^{Me})](OTf) (**15**) and the calculated masses of various fragments.

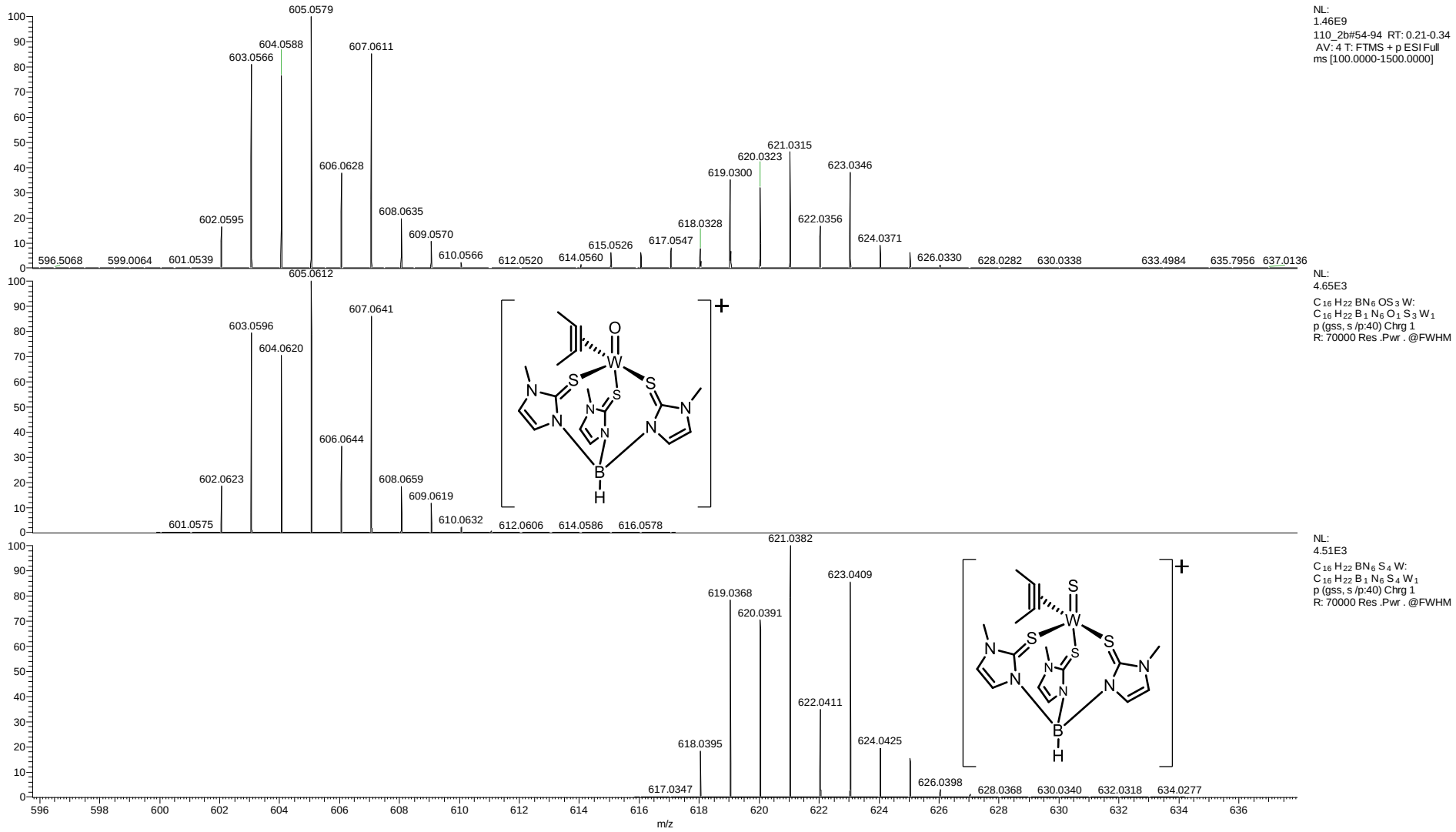

Figure S67: Zoomed in high-resolution mass spectrum of $[WS(C_2Me_2)(MeCN)(Tm^{Me})](OTf)$ (**15**) showing the peak for the $[WO(C_2Me_2)(Tm^{Me})]^+$ and $[WS(C_2Me_2)(Tm^{Me})]^+$ ion (top) and their calculated masses (middle and bottom).

4 Crystal Structure Determinations

General. All the single crystal measurements were performed on a Bruker APEX-II CCD diffractometer at 100 K using Mo K_α radiation with a wavelength of 0.71073 Å from an Incoatec microfocus sealed tube equipped with a multilayer monochromator. Absorption corrections were made semi-empirically from equivalents. The structures were solved by direct methods (SHELXS-97)[4] and refined by full-matrix least-squares techniques against F^2 (SHELXL-2014/6)[5]. A weighting scheme of $w = 1/[\sigma^2(F_o^2)+(aP)^2+bP]$ where $P = (F_o^2+2F_c^2)/3$ was used. The non-hydrogen atoms were refined with anisotropic displacement parameters without any constraints except for some complexes given below or for solvent molecules or triflate anions. The positions of the H atoms bonded to boron as well as those of the acetylene ligands were taken from difference Fourier maps, the C–H distances of the acetylene ligands were fixed to 0.95 Å, and these H atoms were refined with individual isotropic displacement parameters without any constraints to the bond angles. The H atoms of the aromatic rings were put at the external bisectors of the X–C–C angles at C–H distances of 0.95 Å and common isotropic displacement parameters were refined for the H atoms of the same ring. The H atoms of the CH_2 groups were refined with common isotropic displacement parameters for the H atoms of the same group and idealized geometry with approximately tetrahedral angles and C–H distances of 0.99 Å. The H atoms of the methyl groups and *tert*-butyl groups were refined with common isotropic displacement parameters for the H atoms of the same group and idealized geometries with tetrahedral angles, enabling rotation around the C–C bonds, and C–H distances of 0.98 Å. Crystal data, data collection parameters and structure refinement details are given in Tables S2-S7. Further refinement information, structure and bonding parameters, SHELXL .res and .hkl files are given in the deposited CIF file which is available free of charge from The Cambridge Crystallographic Data Centre (CCDC **XXXXXX-XXXXXX**).

Crystal structure determination of 1: The bromido ligand and the carbonyl ligand are disordered over two orientations and were refined with site occupation factors of 0.900(2) and 0.100(2), respectively. The same anisotropic displacement parameters were refined for atoms closer than 1.1 Å in the disordered part, and the equivalent bonds were restrained to have the same lengths.

Crystal structure determination of 3: The borato ligand was disordered over two orientations and refined with site occupation factors of 0.548(6) and 0.452(6), respectively. The equivalent bonds in this disordered ligand were restrained to have the same lengths and the same anisotropic displacement parameters were used for equivalent atoms. The imidazole rings were refined as rigid groups. The equivalent W–S bonds to the disordered ligand were restrained to have the same lengths. One of the phenyl rings was disordered, too. The C atoms of the phenyl ring in the less occupied orientation [0.193(8)] were fitted to a regular hexagon with C–C distances of 1.39 Å. The bonds to the phenyl rings were restrained to have the same lengths.

Crystal structure determination of 6: The bromo, acetylene and sulfido ligands and concomitantly the central W atom were disordered over two orientations which refined to site occupation factors of 0.8488(15) and 0.1512(15), respectively. For these disordered atoms the same anisotropic displacement parameters were used for atoms whose positions are close together and the equivalent bonds were restrained to have the same lengths. The other non-

hydrogen atoms of the metal complex were refined with anisotropic displacement parameters without any constraints. Since the H atoms of the acetylene ligands could not be refined without any constraints due to disorder, they were put at the external bisectors of the C–C–W angles at C–H distances of 0.95 Å and one common isotropic displacement parameter was refined for these H atoms.

Crystal structure determination of 8: For the H atoms bonded to boron which were included at calculated positions with all N–B–H angles equal at B–H distances of 1.17 Å individual isotropic displacement parameters were refined.

Crystal structure determination of [$WCl_3(Tm^{Me})$]: Since racemic twinning was detected, a scale factor between the two components was refined to a value of 0.505(7). Applying the twin matrix (-1 0 0 / 0 -1 0 / 0 0 -1) lowered the R-factor R1 from 0.0480 to 0.0320 by only one additional parameter. The absolute structure was arbitrarily assigned to one of the chiral molecules of the racemate.

Crystal structure determinations of [$WCl_3(Tm^{Me})$] · 3 $CDCl_3$ and [$W(CO)(C_2Ph_2)_2(MeCN)Br_2$]: The absolute configuration was established by anomalous dispersion effects in the diffraction measurements on the crystal.

Crystal structure determination [$W(CO)(C_2Ph_2)_2(MeCN)Br_2$]': The non-hydrogen atoms were refined with anisotropic displacement parameters. Due to the pseudo-symmetry between the two molecules of the asymmetric unit the same anisotropic displacement parameters were used for the atoms of the CO ligands and for those of the acetonitrile ligands as well as for some atoms of the acetylene ligands.

Table S2: Crystallographic data and structure refinement details of **1**–**2**.

Crystal data	**[W(CO)(C_2H_2)(Tm^{Me})Br] (1)**	**[W(CO)(C_2H_2)(Tm^{Me})Br] (1')**	**[W(CO)(C_2Me_2)(Tm^{Me})Br] (2)**
CIF data code	**CV42B**	**CV42N**	**CV201**
Empirical formula	$C_{15}H_{18}BBrN_6OS_3W \cdot 2CH_2Cl_2$	$C_{15}H_{18}BBrN_6OS_3W \cdot 2C_2H_3N$	$8C_{17}H_{22}BBrN_6OS_3W \cdot 16CH_2Cl_2 \cdot 3C_7H_{16}$
Formula weight	838.95	751.21	7236.64
Crystal description	needle, green	block, blue	plate, blue
Crystal size	0.23 x 0.12 x 0.05mm	0.24 x 0.11 x 0.10mm	0.28 x 0.27 x 0.13mm
Crystal system	monoclinic	triclinic	tetragonal
Space group	P 2_1/c	P -1	P 4/n
a	9.6972(11)Å	10.3862(4)Å	24.8216(6)Å
b	16.0343(13)Å	11.7353(5)Å	
c	17.7938(7)Å	12.4831(5)Å	10.9795(3)Å
α		96.2205(19)°	
β	93.325(3)°	108.4188(16)°	
γ		109.6561(17)°	
Volume	2762.1(4)Å^3	1319.63(9)Å^3	6764.6(4)Å^3
Z	4	2	1
Calc. density	2.018Mg/m^3	1.891Mg/m^3	1.776Mg/m^3
F(000)	1616	728	3534
Linear absorption coefficient μ	6.267mm^{-1}	6.157mm^{-1}	5.125mm^{-1}
Max. and min. transmission	1.000 and 0.610	1.000 and 0.772	1.000 and 0.561
Unit cell determination	2.46° < Θ < 25.65°	2.66° < Θ < 40.76°	2.48° < Θ < 30.60°
Reflections used at 100K	6986	9967	9817
Data collection			
Θ range for data collection	2.46 to 25.70°	2.25 to 35.00°	2.48 to 30.00°
Reflections collected/ unique	17989 / 5238	30792 / 11605	65451 / 9861
Significant unique reflections	4253 with I > 2σ(I)	10628 with I > 2σ(I)	6396 with I > 2σ(I)
R(int), R(sigma)	0.0569, 0.0536	0.0311, 0.0375	0.0665, 0.0781
Completeness to Θ_{max}	99.8%	99.9%	99.9%
Refinement			
Data/ parameters/ restraints	5238 / 328 / 7	11605 / 331 / 3	9861 / 402 / 23
Goodness-of-fit on F^2	1.087	1.093	1.031
Final R indices [I > 2σ(I)]	R1 = 0.0416, wR2 = 0.1085	R1 = 0.0228, wR2 = 0.0508	R1 = 0.0421, wR2 = 0.0968
R indices (all data)	R1 = 0.0550, wR2 = 0.1126	R1 = 0.0277, wR2 = 0.0523	R1 = 0.0861, wR2 = 0.1118
Weighting scheme param. a, b	0.0636, 1.4275	0.0047, 1.5758	0.0440, 0.7237
Largest Δ/σ in last cycle	0.002	0.002	0.003
Largest diff. peak and hole	2.048 and -1.313e/Å^3	1.564 and -1.200e/Å^3	2.201 and -1.692e/Å^3
CCDC no.	**1987770**	**1987771**	**1987772**

Table S3: Crystallographic data and structure refinement details of **3–5.**

Crystal data	**[W(CO)(C_2Ph_2)(Tm^{Me})Br] (3)**	**[WO(C_2H_2)(Tm^{Me})Br] (4)**	**[WO(C_2Me_2)(Tm^{Me})Br] (5)**
CIF data code	**CV5**	**CV16**	**CV21**
Empirical formula	$C_{27}H_{26}BBrN_6OS_3W$	$C_{14}H_{18}BBrN_6OS_3W \cdot 1.25CH_2Cl_2$	$C_{16}H_{22}BBrN_6OS_3W \cdot 2CH_2Cl_2$
Formula weight	821.29	763.25	855.00
Crystal description	block, blue	plate, yellow	plate, yellow
Crystal size	0.20 x 0.17 x 0.13mm	0.27 x 0.25 x 0.07mm	0.25 x 0.20 x 0.07mm
Crystal system	monoclinic	triclinic	monoclinic
Space group	P 2_1/c	P -1	C 2/c
a	18.3284(4)Å	13.0139(5)Å	31.2959(15)Å
b	9.8286(2)Å	13.7281(6)Å	11.7023(7)Å
c	19.4451(4)Å	15.8785(7)Å	18.1517(9)Å
α		71.467(2)°	
β	99.9363(12)°	77.5417(18)°	113.829(2)°
γ		89.064(2)°	
Volume	3450.35(13)$Å^3$	2622.16(19)$Å^3$	6081.1(6)$Å^3$
Z	4	4	8
Calc. density	1.581Mg/m^3	1.933Mg/m^3	1.868Mg/m^3
F(000)	1600	1466	3312
Linear absorption coefficient μ	4.716mm^{-1}	6.443mm^{-1}	5.695mm^{-1}
Max. and min. transmission	0.746 and 0.490	1.000 and 0.382	1.000 and 0.673
Unit cell determination	2.67° < Θ < 30.63°	2.40° < Θ < 35.80°	2.45° < Θ < 28.49°
Reflections used at 100K	9951	9869	8302
Data collection			
Θ range for data collection	2.33 to 26.00°	2.18 to 30.00°	1.88 to 28.00°
Reflections collected/ unique	26479 / 6758	42943 / 15292	26989 / 7342
Significant unique reflections	5457 with I > 2σ(I)	10492 with I > 2σ(I)	5380 with I > 2σ(I)
R(int), R(sigma)	0.0416, 0.0536	0.0618, 0.1137	0.0447, 0.0606
Completeness to Θ_{max}	99.9%	99.9%	99.9%
Refinement			
Data/ parameters/ restraints	6758 / 400 / 69	15292 / 600 / 4	7342 / 354 / 8
Goodness-of-fit on F^2	1.082	1.034	1.036
Final R indices [I > 2σ(I)]	R1 = 0.0381, wR2 = 0.1065	R1 = 0.0584, wR2 = 0.1434	R1 = 0.0407, wR2 = 0.0923
R indices (all data)	R1 = 0.0499, wR2 = 0.1118	R1 = 0.0931, wR2 = 0.1594	R1 = 0.0653, wR2 = 0.1002
Weighting scheme param. a, b	0.0603, 3.7977	0.0653, 0.5461	0.0487, 1.5403
Largest Δ/σ in last cycle	0.001	0.001	0.001
Largest diff. peak and hole	1.953 and -2.445e/$Å^3$	1.898 and -2.104e/$Å^3$	2.408 and -1.572e/$Å^3$
CCDC no.	**1987773**	**1987774**	**1987775**

Table S4: Crystallographic data and structure refinement details of **6–8.**

Crystal data	**[WS(C_2H_2)(Tm^{Me})Br] (6)**	**[WS(C_2Me_2)(Tm^{Me})Br] (7)**	**[WO(μ-O)(C_2Me_2)$_2$(Tm^{Me})]$_2$(OTf)$_2$ (8)**
CIF data code	**CV45B**	**CV27C**	**CV114**
Empirical formula	$C_{14}H_{18}BBrN_6S_4W$ · 1.604C_4H_8O · 0.396CH_2Cl_2	$C_{16}H_{22}BBrN_6S_4W$ · 2CH_2Cl_2	$C_{32}H_{44}B_2N_{12}O_2S_6W_2$ · 2CF_3O_3S · 2CH_2Cl_2
Formula weight	822.41	871.06	1678.46
Crystal description	block, yellow	plate, orange	plate, yellow
Crystal size	0.26 x 0.14 x 0.13mm	0.07 x 0.07 x 0.02mm	0.18 x 0.13 x 0.03mm
Crystal system	monoclinic	monoclinic	triclinic
Space group	P 2_1/n	P 2_1/c	P -1
a	9.4289(4)Å	16.298(3)Å	13.188(5)Å
b	17.4562(8)Å	14.323(3)Å	15.003(6)Å
c	17.5522(8)Å	13.118(2)Å	16.238(6)Å
α			83.664(4)°
β	94.9845(19)°	104.151(9)°	87.934(3)°
γ			68.163(3)°
Volume	2878.0(2)Å^3	2969.3(10)Å^3	2963.9(19)Å^3
Z	4	4	2
Calc. density	1.898Mg/m^3	1.949Mg/m^3	1.881Mg/m^3
F(000)	1611.2	1688	1640
Linear absorption coefficient μ	5.796mm^{-1}	5.899mm^{-1}	4.415mm^{-1}
Max. and min. transmission	1.000 and 0.555	1.000 and 0.662	1.000 and 0.433
Unit cell determination	2.33° < Θ < 30.69°	2.58° < Θ < 20.19°	2.52° < Θ < 27.39°
Reflections used at 100K	9962	9260	9979
Data collection			
Θ range for data collection	2.33 to 30.00°	1.92 to 26.00°	1.76 to 27.00°
Reflections collected/ unique	28792 / 8384	17760 / 5829	34360 / 12924
Significant unique reflections	6601 with I > 2σ(I)	4460 with I > 2σ(I)	9403 with I > 2σ(I)
R(int), R(sigma)	0.0431, 0.0560	0.0384, 0.0660	0.0810, 0.1018
Completeness to Θ_{max}	100.0%	100.0%	99.9%
Refinement			
Data/ parameters/ restraints	8384 / 374 / 43	5829 / 335 / 1	12924 / 732 / 13
Goodness-of-fit on F^2	1.037	1.066	1.087
Final R indices [I > 2σ(I)]	R1 = 0.0370, wR2 = 0.0869	R1 = 0.0461, wR2 = 0.0988	R1 = 0.0627, wR2 = 0.1553
R indices (all data)	R1 = 0.0542, wR2 = 0.0931	R1 = 0.0642, wR2 = 0.1046	R1 = 0.0918, wR2 = 0.1728
Weighting scheme param. a, b	0.0389, 3.7582	0.0462, 2.1055	0.0860, 1.6840
Largest Δ/σ in last cycle	0.001	0.002	0.001
Largest diff. peak and hole	2.015 and -1.947e/Å^3	1.311 and -0.919e/Å^3	2.018 and -1.939e/Å^3
CCDC no.	**1987776**	**1987777**	**1987778**

Table S5: Crystallographic data and structure refinement details of **9**, **[W(CO)(C_2Me_2)$_2$(MeCN)Br_2]** and **[W(CO)(C_2Me_2)$_2$(MeCN)(Br)$_2$]'.**

Crystal data	**[W_2(μ-S)$_2$(C_2Me_2)(Tm^{Me})$_2$](OTf)$_2$ (9)**	**[W(CO)(C_2Me_2)$_2$(MeCN)Br_2]**	**[W(CO)(C_2Me_2)$_2$(MeCN)Br_2]'**
CIF data code	**CV107**	**CV19**	**LPVK3**
Empirical formula	$C_{28}H_{38}B_2N_{12}S_8W_2 \cdot 2CF_3O_3S \cdot 2CH_2Cl_2$	$C_{11}H_{15}Br_2NOW$	$2C_{11}H_{15}Br_2NOW \cdot CH_2Cl_2$
Formula weight	1656.49	520.91	1126.74
Crystal description	plate, violet	block, green	block, colourless
Crystal size	0.28 x 0.15 x 0.05mm	0.24 x 0.24 x 0.17mm	0.31 x 0.25 x 0.16mm
Crystal system	trigonal	orthorhombic	triclinic
Space group	R -3	P b c a	P -1
a	38.265(3)Å	10.7043(4)Å	10.5632(6)Å
b		11.7559(5)Å	10.7543(6)Å
c	19.5669(17)Å	23.3674(10)Å	14.7207(9)Å
α			78.5003(15)°
β			76.7560(13)°
γ			87.6914(14)°
Volume	24812(4)Å^3	2940.5(2)Å^3	1595.09(16)Å^3
Z	18	8	2
Calc. density	1.995Mg/m^3	2.353Mg/m^3	2.346Mg/m^3
F(000)	14508	1920	1044
Linear absorption coefficient μ	4.815mm^{-1}	13.273mm^{-1}	12.406mm^{-1}
Max. and min. transmission	1.000 and 0.528	0.746 and 0.255	0.746 and 0.279
Unit cell determination	2.45° < Θ < 25.73°	2.58° < Θ < 30.73°	2.72° < Θ < 30.32°
Reflections used at 100K	9898	9963	9970
Data collection			
Θ range for data collection	1.93 to 25.00°	2.58 to 30.00°	2.63 to 30.00°
Reflections collected/ unique	50028 / 9712	23563 / 4295	39859 / 9277
Significant unique reflections	7454 with I > 2σ(I)	3872 with I > 2σ(I)	6791 with I > 2σ(I)
R(int), R(sigma)	0.1289, 0.0742	0.0355, 0.0332	0.0778, 0.0616
Completeness to Θ_{max}	99.9%	100.0%	99.9%
Refinement			
Data/ parameters/ restraints	9712 / 710 / 6	4295 / 155 / 0	9277 / 337 / 0
Goodness-of-fit on F^2	1.025	1.070	1.041
Final R indices [I > 2σ(I)]	R1 = 0.0674, wR2 = 0.1641	R1 = 0.0253, wR2 = 0.0564	R1 = 0.0354, wR2 = 0.0877
R indices (all data)	R1 = 0.0828, wR2 = 0.1741	R1 = 0.0303, wR2 = 0.0580	R1 = 0.0551, wR2 = 0.0965
Weighting scheme param. a, b	0.0973, 0.0000	0.0245, 3.3615	0.0301, 0.2860
Largest Δ/σ in last cycle	0.001	0.002	0.002
Largest diff. peak and hole	2.090 and -1.264e/Å^3	2.361 and -2.237e/Å^3	2.275 and -2.340e/Å^3
CCDC no.	**1987779**	**1987780**	**1987781**

Table S6: Crystallographic data and structure refinement details of **[W(CO)(C_2Ph_2)$_2$(MeCN)Br_2]**, **[W(CO)(C_2Ph_2)$_2$(MeCN)Br_2]'** and **[WCl_3Tm^{Me}].**

Crystal data	**[W(CO)(C_2Ph_2)$_2$(MeCN)Br_2]**	**[W(CO)(C_2Ph_2)$_2$(MeCN)Br_2]'**	**[$WCl_3(Tm^{Me})$]**
CIF data code	**LP271G**	**LP138**	**CVMB3**
Empirical formula	$C_{31}H_{23}Br_2NOW$	$C_{31}H_{23}Br_2NOW \cdot CH_2Cl_2$	$C_{12}H_{16}BCl_3N_6S_3W \cdot 2CHCl_3$
Formula weight	769.17	854.10	880.23
Crystal description	block, yellow	block, yellow	needle, red
Crystal size	0.26 x 0.26 x 0.24mm	0.26 x 0.24 x 0.21mm	0.27 x 0.12 x 0.10mm
Crystal system	orthorhombic	monoclinic	orthorhombic
Space group	F d d 2	P 2_1/n	P 2_1 2_1 2_1
a	31.6962(9)Å	10.0599(16)Å	9.5645(7)Å
b	34.4906(11)Å	30.994(5)Å	17.1003(12)Å
c	10.0123(3)Å	19.878(3)Å	17.6083(14)Å
α			
β		91.882(2)°	
γ			
Volume	10945.7(6)Å^3	6194.5(17)Å^3	2879.9(4)Å^3
Z	16	8	4
Calc. density	1.867Mg/m^3	1.832Mg/m^3	2.030Mg/m^3
F(000)	5888	3280	1696
Linear absorption coefficient μ	7.166mm^{-1}	6.508mm^{-1}	5.083mm^{-1}
Max. and min. transmission	1.000 and 0.623	0.745 and 0.568	1.000 and 0.655
Unit cell determination	2.69° < Θ < 35.58°	2.41° < Θ < 26.38°	2.31° < Θ < 30.07°
Reflections used at 100K	9993	9900	9693
Data collection			
Θ range for data collection	2.36 to 35.00°	2.39 to 25.00°	1.66 to 30.00°
Reflections collected/ unique	29760 / 9364	21524 / 10823	70979 / 8397
Significant unique reflections	9180 with I > 2σ(I)	7283 with I > 2σ(I)	7815 with I > 2σ(I)
R(int), R(sigma)	0.0241, 0.0358	0.0344, 0.1164	0.0579, 0.0423
Completeness to Θ_{max}	99.9%	99.2%	100.0%
Refinement			
Data/ parameters/ restraints	9364 / 331 / 1	10823 / 619 / 0	8397 / 333 / 16
Goodness-of-fit on F^2	1.088	1.042	1.024
Final R indices [I > 2σ(I)]	R1 = 0.0221, wR2 = 0.0529	R1 = 0.0485, wR2 = 0.0941	R1 = 0.0320, wR2 = 0.0855
R indices (all data)	R1 = 0.0227, wR2 = 0.0531	R1 = 0.0799, wR2 = 0.0979	R1 = 0.0358, wR2 = 0.0875
Weighting scheme param. a, b	0.0257, 0.6004	0.0000, 3.9636	0.0497, 2.9248
Largest Δ/σ in last cycle	0.002	0.001	0.001
Largest diff. peak and hole	2.894 and -1.243e/Å^3	1.762 and -1.800e/Å^3	1.824 and -1.273e/Å^3
CCDC no.	**1987782**	**1987783**	**1987784**

Table S7: Crystallographic data and structure refinement details of **$[WCl_3(Tm^{Me})] \cdot CDCl_3$, mt-S-S-mt** and **$[WO(C_2H_2)(S_2CNEt_2)_2]$.**

Crystal data	**$[WCl_3(Tm^{Me})] \cdot CDCl_3$**	**mt-S-S-mt**	**$[WO(C_2H_2)(S_2CNEt_2)_2]$**
CIF data code	**CV16B**	**CV11**	**AH13**
Empirical formula	$C_{12}H_{16}BCl_3N_6S_3W \cdot 3CHCl_3$	$C_8H_{10}N_4S_2$	$C_{12}H_{22}N_2OS_4W$
Formula weight	999.60	226.32	522.40
Crystal description	block, yellow	block, yellow	needle, yellow
Crystal size	0.22 x 0.19 x 0.12mm	0.35 x 0.18 x 0.15mm	0.22 x 0.12 x 0.10mm
Crystal system	trigonal	monoclinic	monoclinic
Space group	R 3 c	C 2/c	P 2_1/n
a	14.8478(15)Å	12.2450(6)Å	9.3486(17)Å
b		7.3769(4)Å	15.236(3)Å
c	26.430(3)Å	11.2441(5)Å	13.272(3)Å
α			
β		98.6227(15)°	103.312(3)°
γ			
Volume	5046.1(14)Å^3	1004.20(9)Å^3	1839.6(6)Å^3
Z	6	4	4
Calc. density	1.974Mg/m^3	1.497Mg/m^3	1.886Mg/m^3
F(000)	2892	472	1016
Linear absorption coefficient μ	4.595mm^{-1}	0.494mm^{-1}	6.730mm^{-1}
Max. and min. transmission	1.000 and 0.570	1.000 and 0.620	1.000 and 0.807
Unit cell determination	2.21° < Θ < 27.58°	3.23° < Θ < 40.84°	2.61° < Θ < 35.54°
Reflections used at 100K	6869	9881	9915
Data collection			
Θ range for data collection	2.21 to 28.00°	3.23 to 34.99°	2.07 to 35.00°
Reflections collected/ unique	19539 / 2593	12388 / 2213	47472 / 8099
Significant unique reflections	1473 with I > 2σ(I)	2022 with I > 2σ(I)	6560 with I > 2σ(I)
R(int), R(sigma)	0.0430, 0.0845	0.0461, 0.0304	0.0495, 0.0339
Completeness to Θ_{max}	100.0%	100.0%	100.0%
Refinement			
Data/ parameters/ restraints	2593 / 121 / 2	2213 / 67 / 0	8099 / 200 / 2
Goodness-of-fit on F^2	1.039	1.075	1.037
Final R indices [I > 2σ(I)]	R1 = 0.0483, wR2 = 0.0942	R1 = 0.0346, wR2 = 0.0924	R1 = 0.0238, wR2 = 0.0474
R indices (all data)	R1 = 0.0918, wR2 = 0.1049	R1 = 0.0378, wR2 = 0.0953	R1 = 0.0368, wR2 = 0.0514
Weighting scheme param. a, b	0.0171, 2.2476	0.0517, 0.7947	0.0145, 1.4190
Largest Δ/σ in last cycle	0.001	0.001	0.002
Largest diff. peak and hole	1.203 and -1.079e/Å^3	0.783 and -0.504e/Å^3	1.700 and -1.410e/Å^3
CCDC no.	**1987785**	**1987786**	**1987787**

4.1 Stereoscopic ORTEP plots

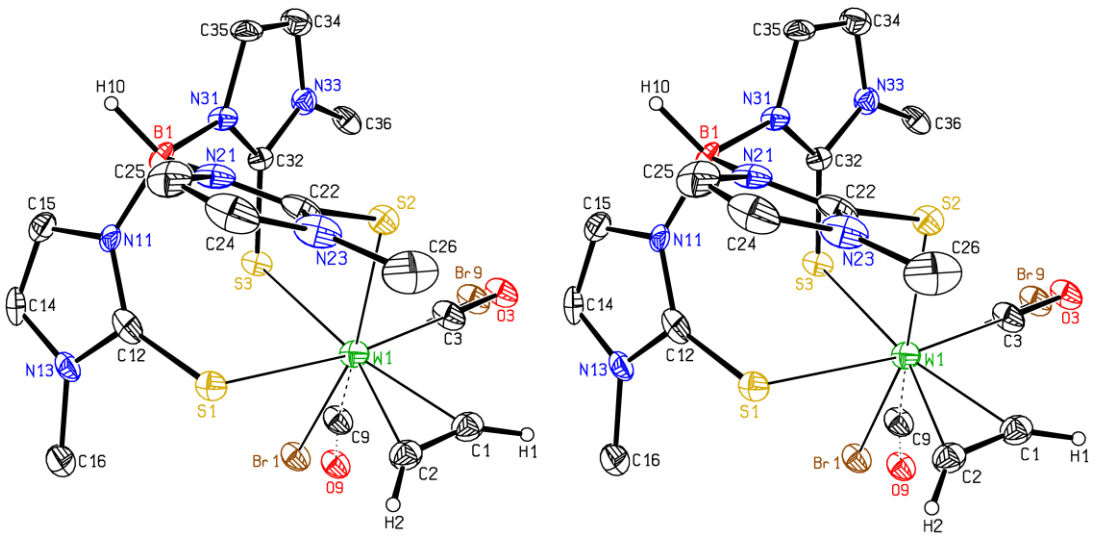

Figure S68: Stereoscopic ORTEP[9] plot of **[W(CO)(C_2H_2)(Tm^{Me})Br] (1)** showing the atomic numbering scheme. The probability ellipsoids are drawn at the 50% probability level. The H atoms of the B–H group and of the acetylene ligand were drawn with arbitrary radii, the other H atoms as well as the solvent molecules were omitted for clarity reasons. The bonds to the atoms of the disordered parts of the complex (e.g. Br9, C9, O9) in the orientations with low site occupation factors of 0.100(2) were plotted with dashed lines.

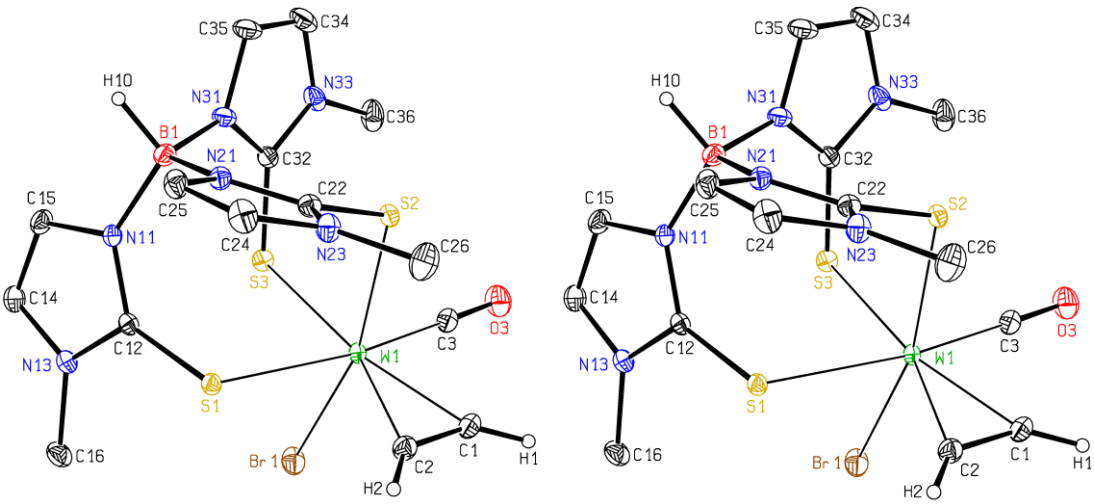

Figure S69: Stereoscopic ORTEP[9] plot of **[W(CO)(C_2H_2)(Tm^{Me})Br] (1)'** showing the atomic numbering scheme. The probability ellipsoids are drawn at the 50% probability level. The H atoms of the acetylene ligand and the hydrido atom were drawn with arbitrary radii, the other H atoms as well as the solvent molecules were omitted for clarity.

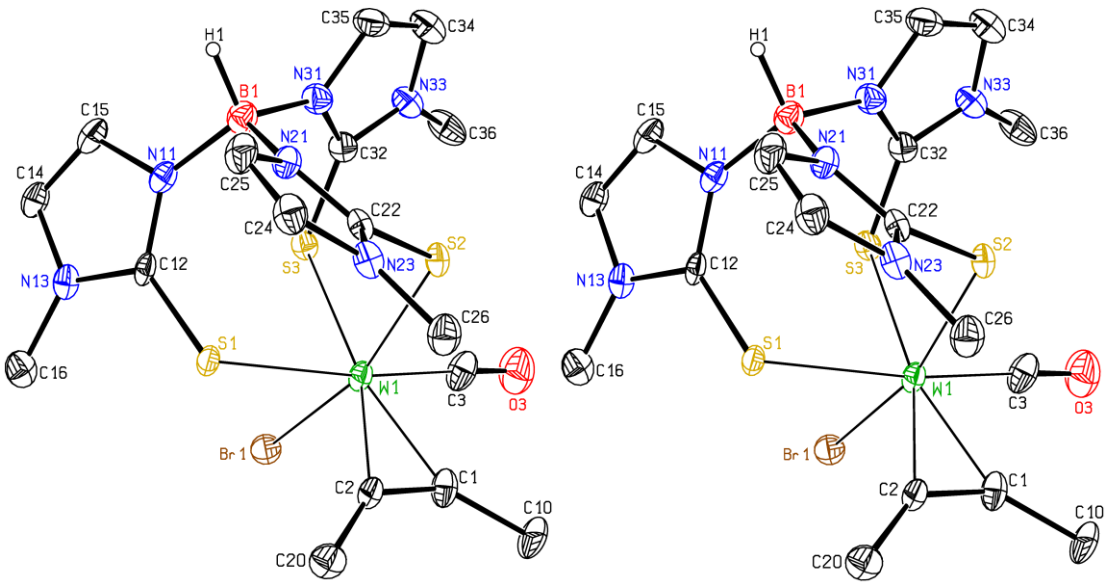

Figure S70: Stereoscopic ORTEP[9] plot of **[W(CO)(C_2Me_2)(Tm^{Me})Br] (2)** showing the atomic numbering scheme. The probability ellipsoids are drawn at the 50% probability level. The H atom H1 is drawn with an arbitrary radius, the other H atoms as well as the solvent molecules were omitted for clarity reasons.

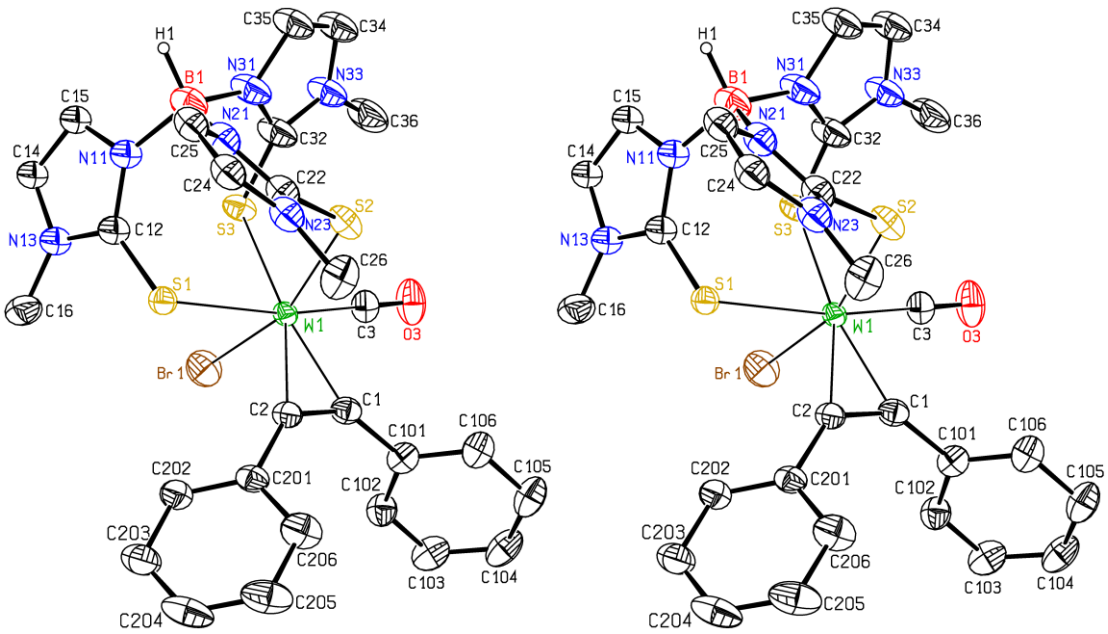

Figure S71: Stereoscopic ORTEP[8] plot of **[W(CO)(C_2Ph_2)(Tm^{Me})Br] (3)** showing the atomic numbering scheme. The probability ellipsoids are drawn at the 50% probability level. The H atom H1 is drawn with an arbitrary radius, the other H atoms as well as the less occupied disordered parts were omitted for clarity reasons.

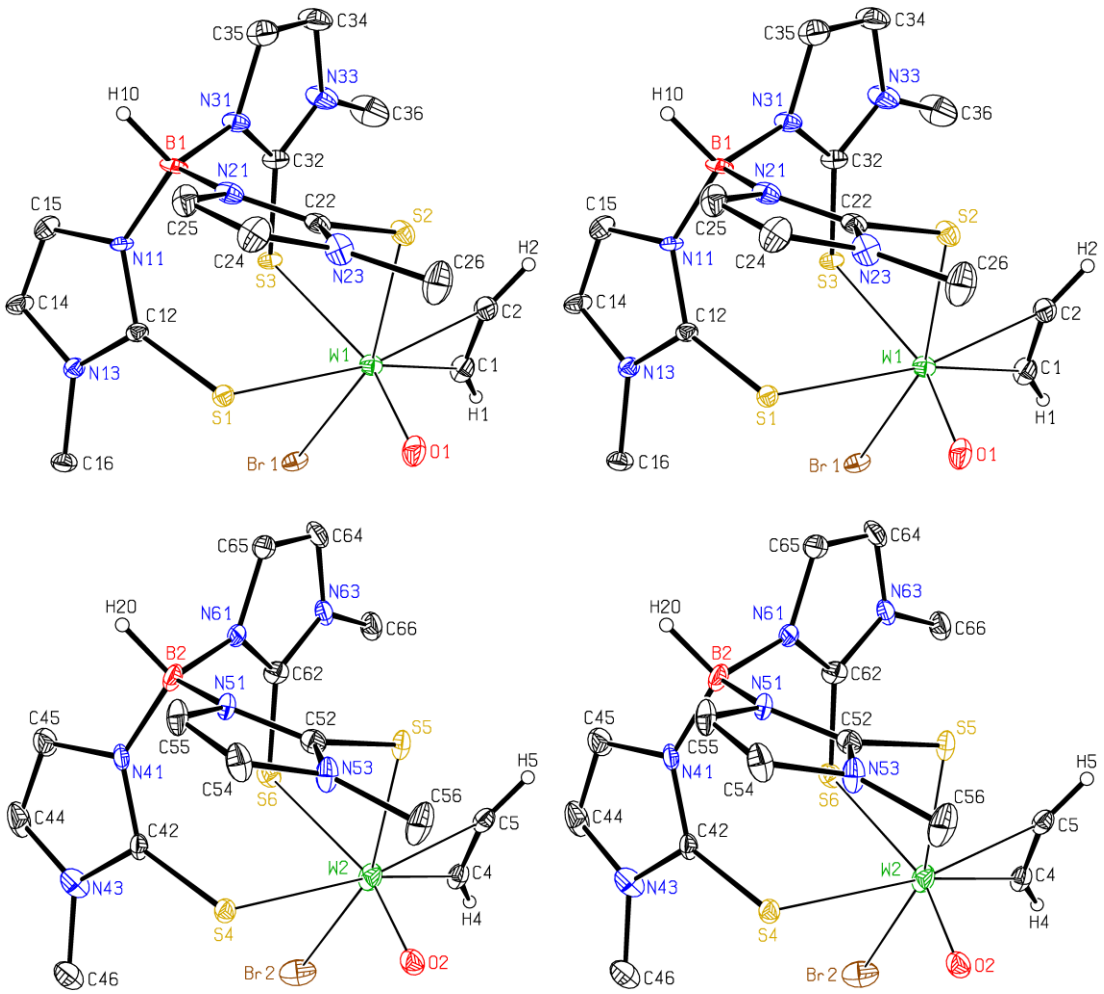

Figure S72: Stereoscopic ORTEP[9] plots of the molecules **A** (above) and **B** (below) of **[WO(C_2H_2)(Tm^{Me})Br] (4)** showing the atomic numbering schemes. The probability ellipsoids are drawn at the 30% probability level. The hydrido atom and the H atoms of the acetylene ligand are drawn with arbitrary radii, the other H atoms were omitted for clarity.

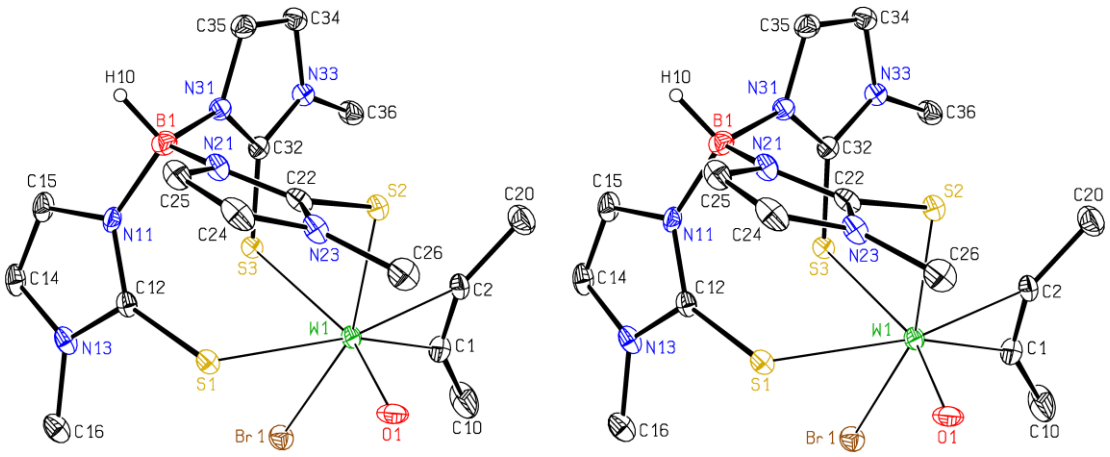

Figure S73: Stereoscopic ORTEP[9] plot of **[WO(C_2Me_2)(Tm^{Me})Br] (5)** showing the atomic numbering scheme. The probability ellipsoids are drawn at the 30% probability level. The hydrido atom is drawn with an arbitrary radius, the other H atoms and the disordered solvent molecules were omitted for clarity.

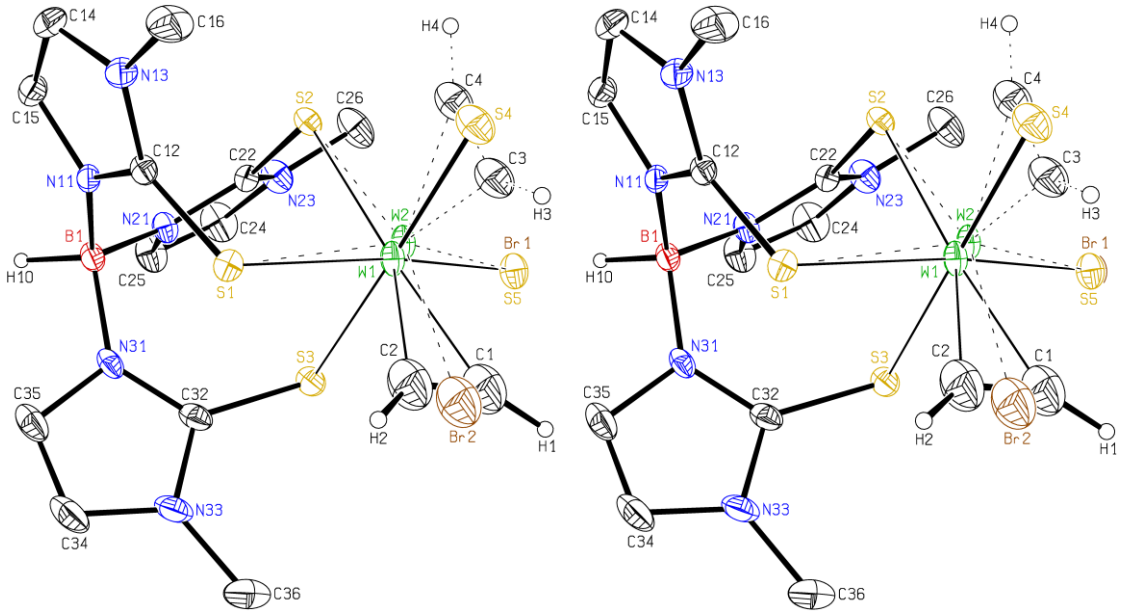

Figure S74: ORTEP[9] plot of the metal complex of **[WS(C₂H₂)(Tm^{Me})Br] (6)** showing the atomic numbering scheme. The probability ellipsoids are drawn at the 50% probability level. The H atoms of the imidazole rings and those of the methyl groups were omitted for clarity, the other H atoms are drawn with arbitrary radii. The bonds of the less prominent occupied orientation of the $WBrSC_2H_2$ fragment [15.12(15)%] are plotted with dashed lines.

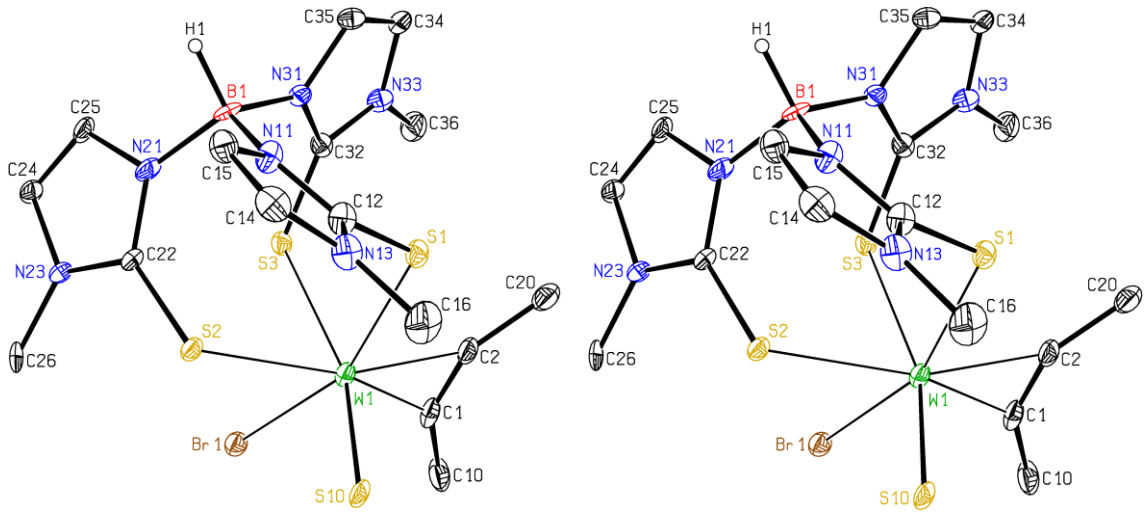

Figure S75: Stereoscopic ORTEP[9] plot of **[WS(C₂Me₂)(Tm^{Me})Br] (7)** showing the atomic numbering scheme. The probability ellipsoids are drawn at the 30% probability level. The H atom H1 is drawn with an arbitrary radius, the other H atoms as well as the solvent molecules were omitted for clarity.

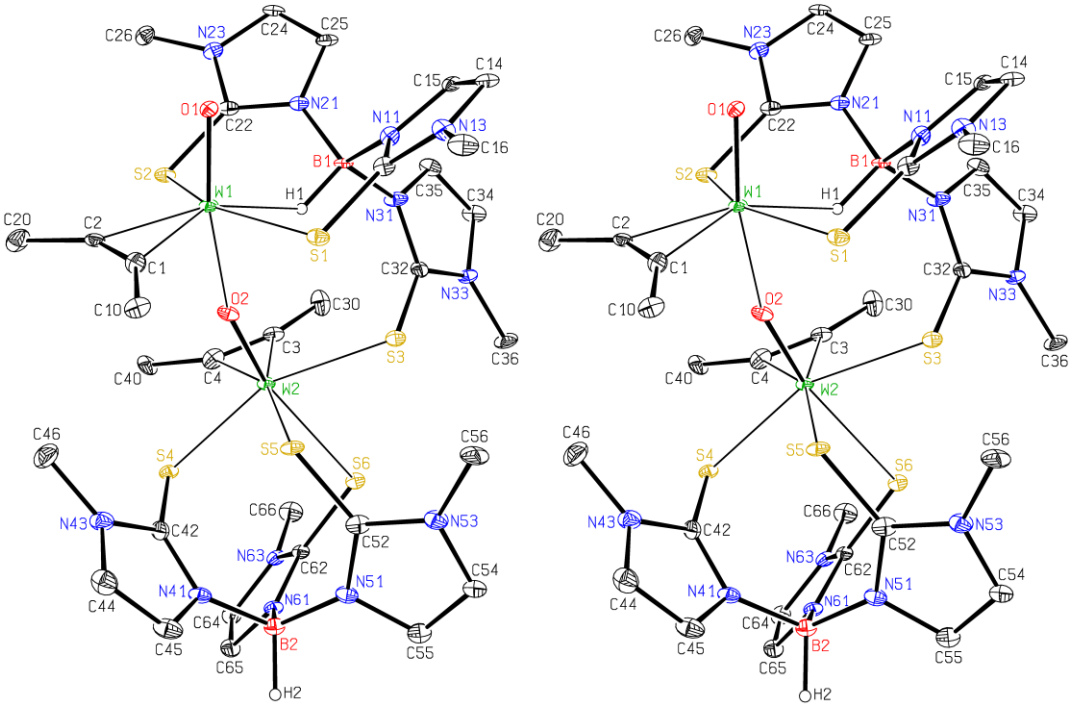

Figure S76: Stereoscopic ORTEP[9] plot of the cationic metal complex of **[WO(μ-O)(C₂Me₂)₂(Tm^{Me})₂](OTf)₂** (**8**) showing the atomic numbering scheme. The probability ellipsoids are drawn at the 30% probability level. The H atoms bonded to boron are drawn with arbitrary radii, the other H atoms were omitted for clarity.

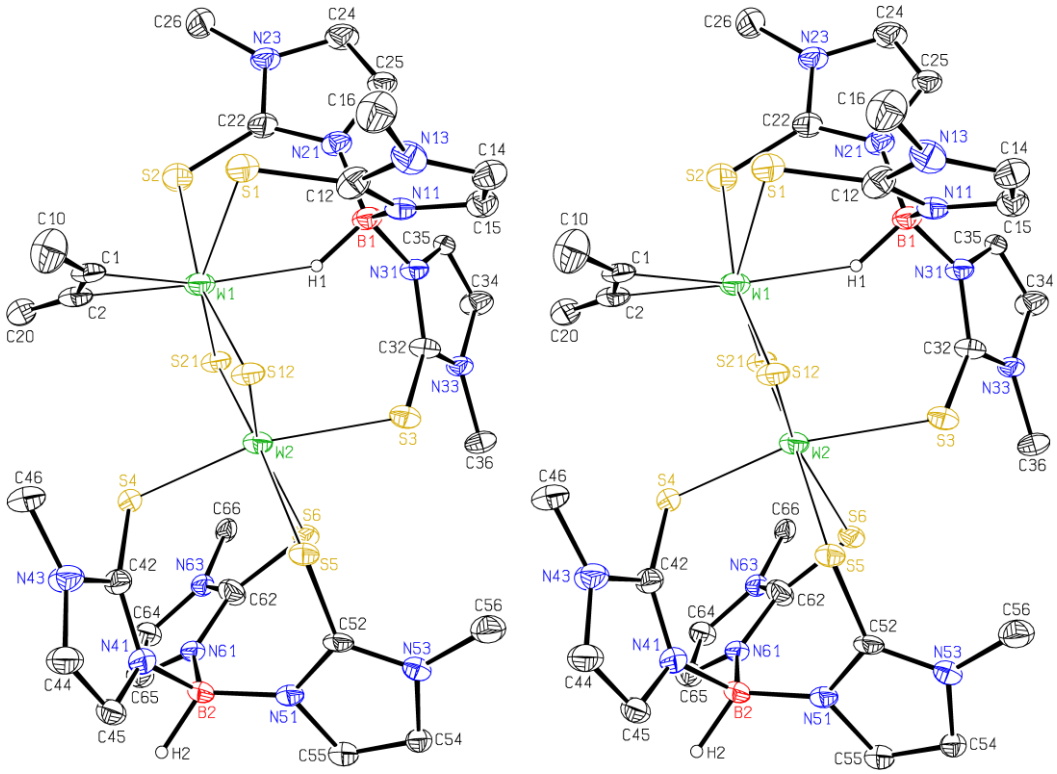

Figure S77: Stereoscopic ORTEP[9] plot of the cationic metal complex of **[W₂(μ-S)₂(C₂Me₂)(Tm^{Me})₂](OTf)₂** (**9**) showing the atomic numbering scheme. The probability ellipsoids are drawn at the 20% probability level. The H atoms bonded to boron are drawn with arbitrary radii, the other H atoms were omitted for clarity.

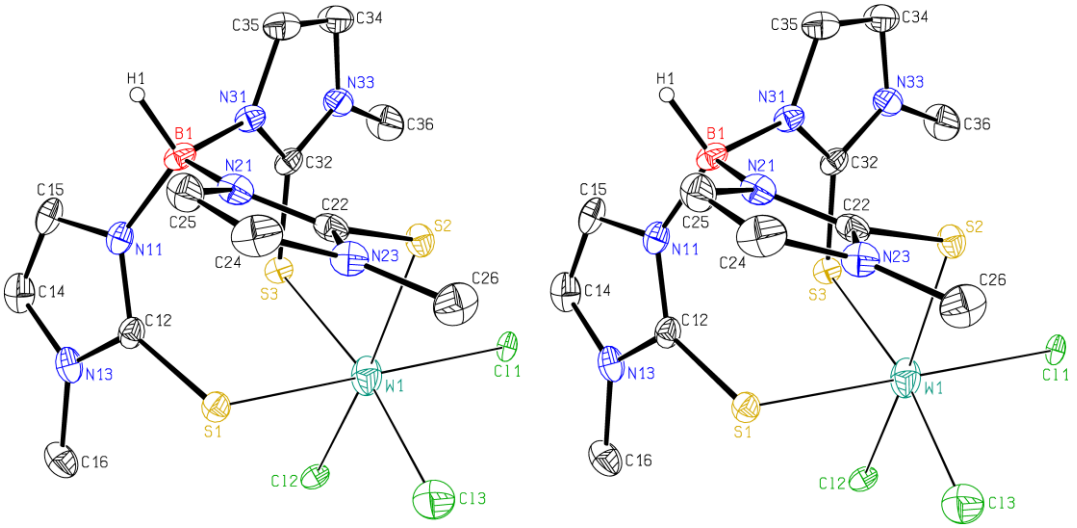

Figure S78: Stereoscopic ORTEP[9] plot of **[WCl₃(Tm^{Me})]** showing the atomic numbering scheme. The probability ellipsoids are drawn at the 50% probability level. The H atom H1 is drawn with an arbitrary radius, the other H atoms as well as the solvent molecules were omitted for clarity.

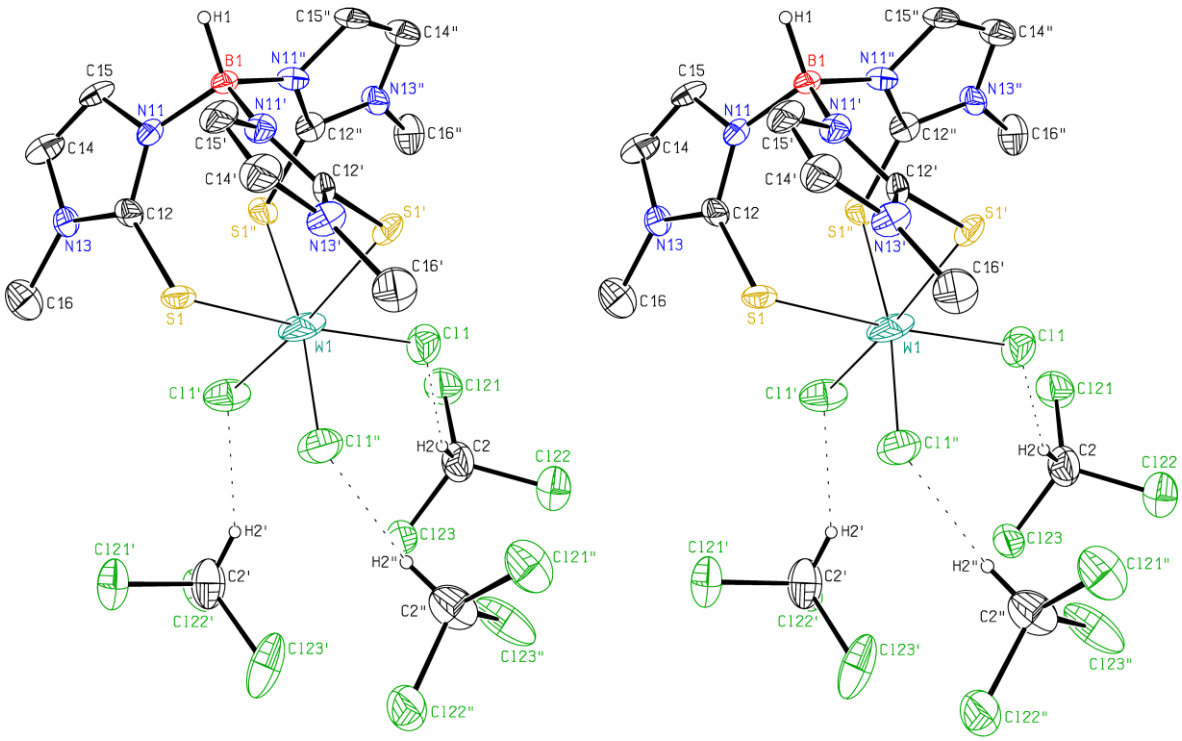

Figure S79: Stereoscopic ORTEP[9] plot of **[WCl₃(Tm^{Me})] · 3 CDCl₃** showing the atomic numbering scheme. The probability ellipsoids are drawn at the 30% probability level. The H1 and the H atoms of the coordinating chloroform molecules are drawn with arbitrary radii, the other H atoms were omitted for clarity.

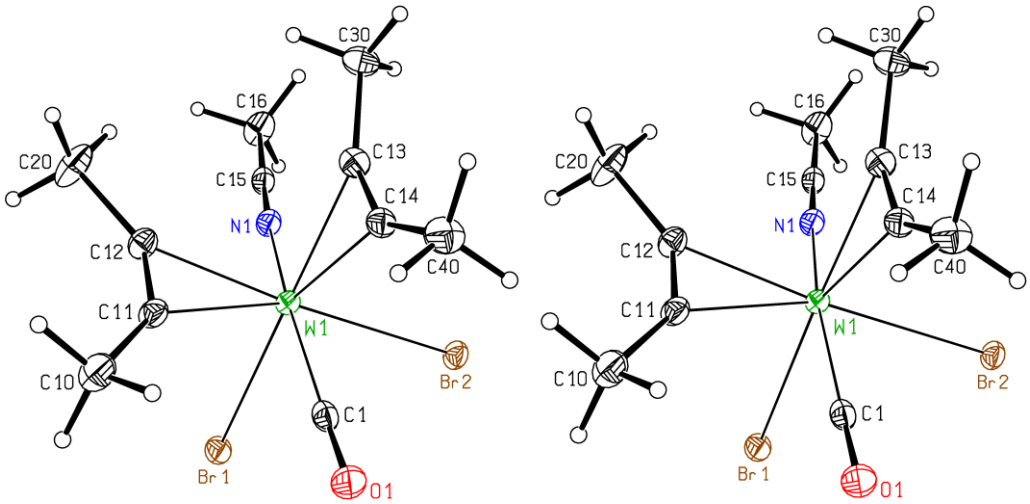

Figure S80: Stereoscopic ORTEP[9] plot of **[W(CO)(C₂Me₂)₂(MeCN)Br₂]** showing the atomic numbering scheme. The probability ellipsoids are drawn at the 50% probability level. The H atoms are drawn with arbitrary radii.

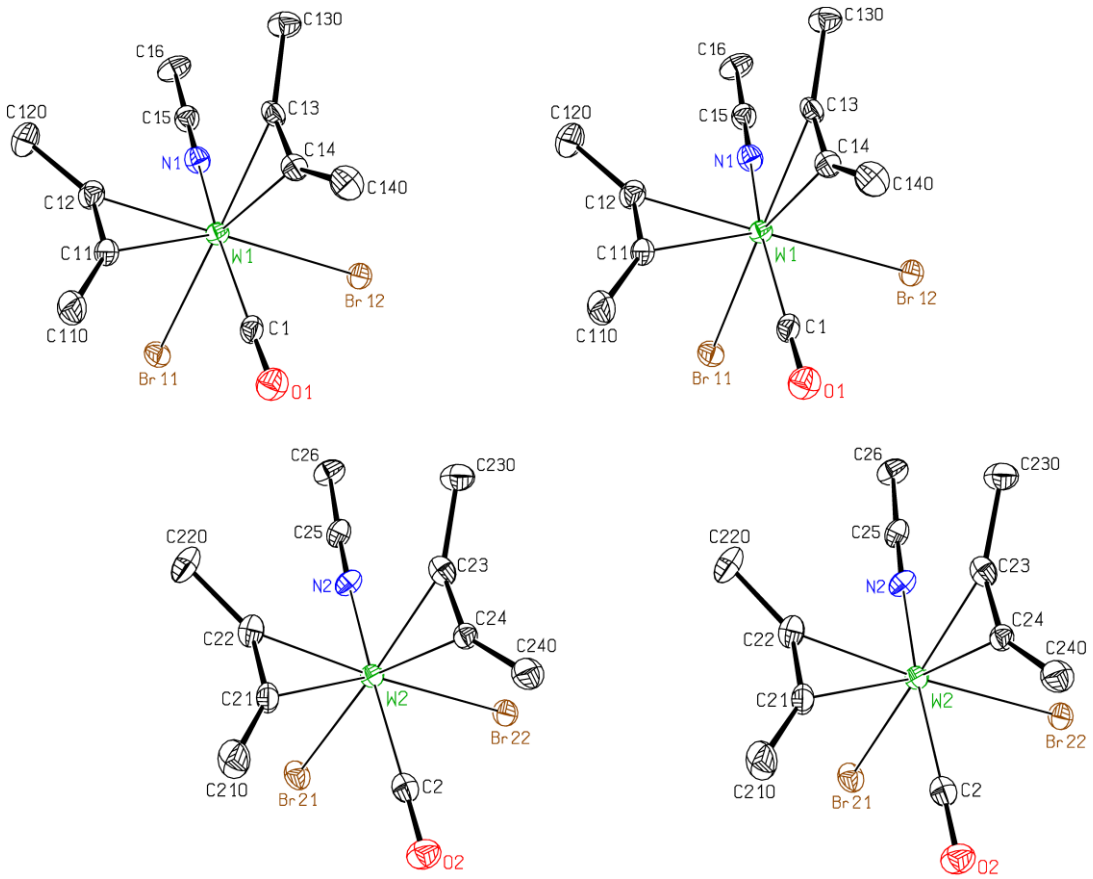

Figure S81: Stereoscopic ORTEP[9] plot of the two complexes of the asymmetric unit of **[W(CO)(C₂Me₂)₂(MeCN)Br₂]'** showing the atomic numbering scheme. The probability ellipsoids are drawn at the 50% probability level. The H atoms and the solvent molecule were omitted for clarity.

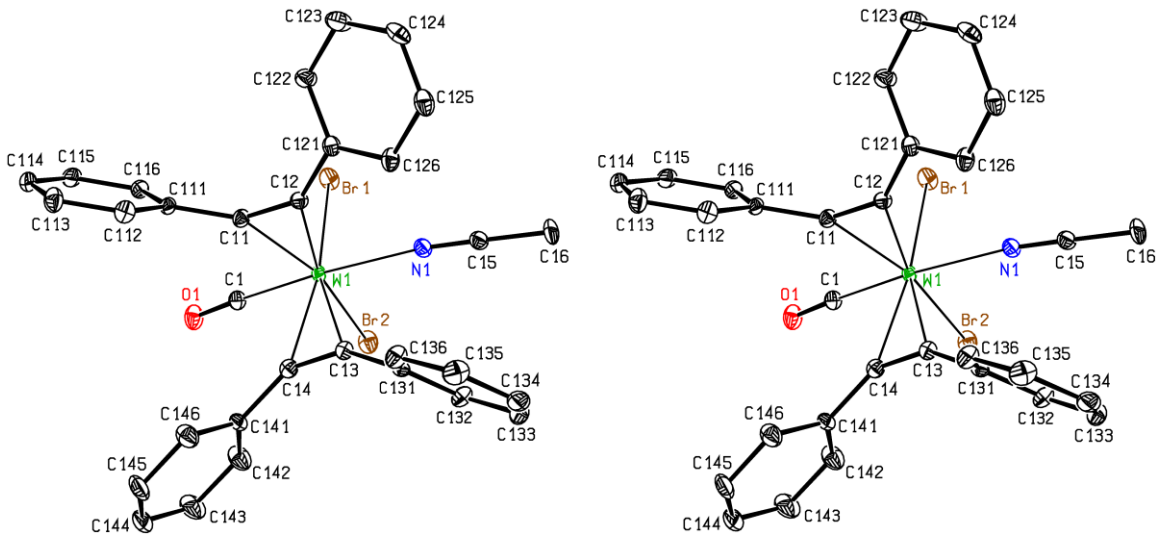

Figure S82: Stereoscopic ORTEP[8] plot of **[W(CO)(C₂Ph₂)₂(MeCN)Br₂]** showing the atomic numbering scheme. The probability ellipsoids are drawn at the 50% probability level. The H atoms were omitted for clarity reasons.

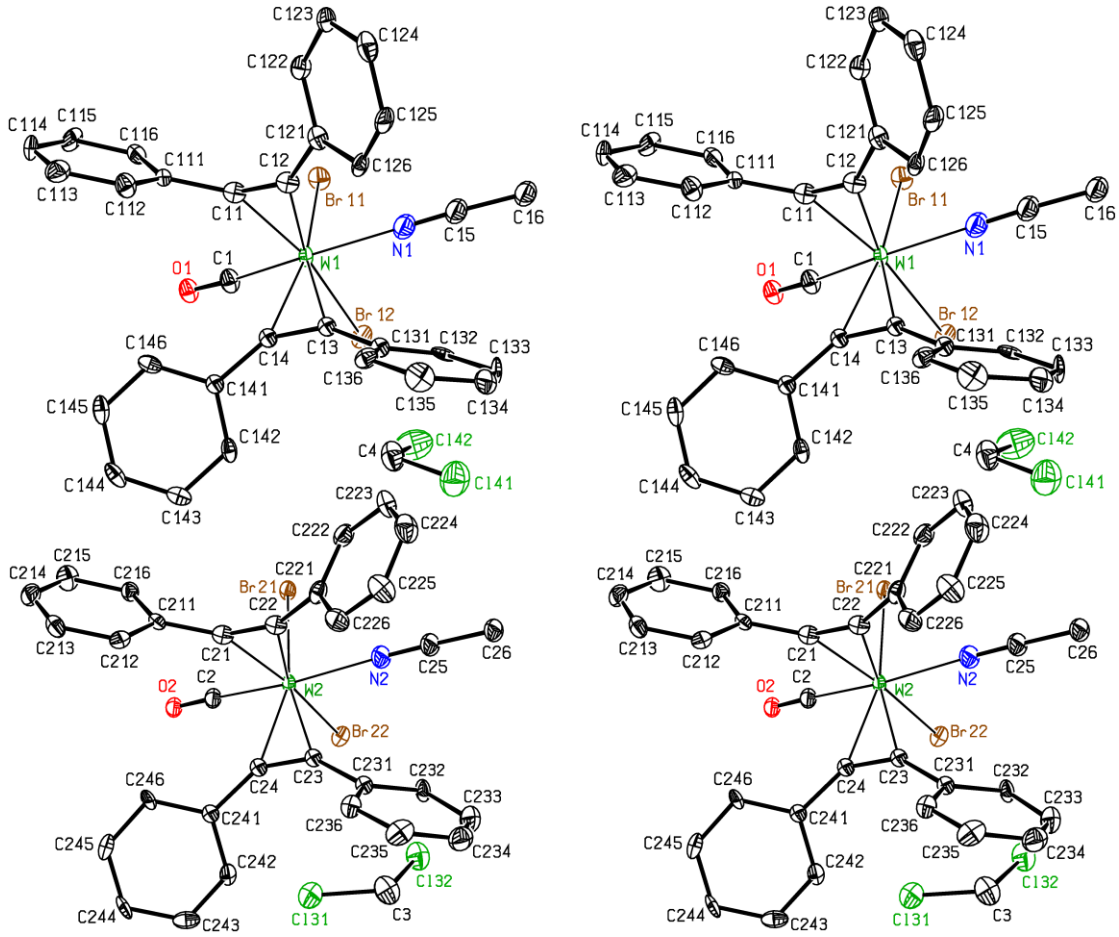

Figure S83: Stereoscopic ORTEP[8] plot of **[W(CO)(C₂Ph₂)₂(MeCN)Br₂]'** showing the atomic numbering scheme. The probability ellipsoids are drawn at the 50% probability level. The H atoms were omitted for clarity reasons.

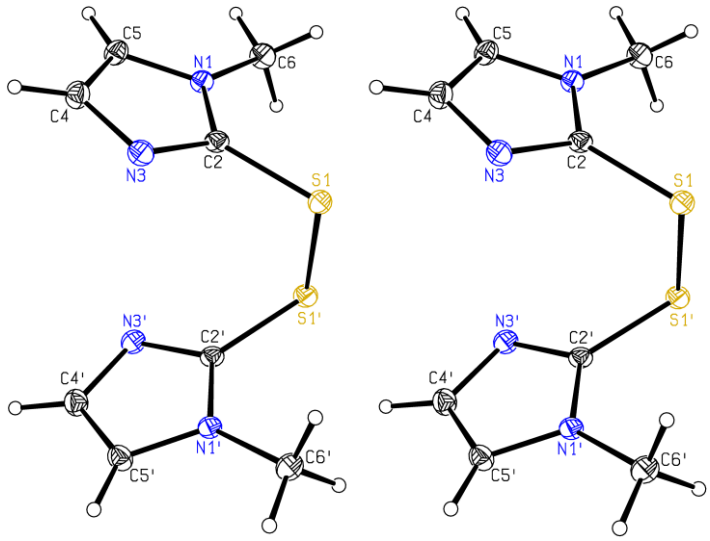

Figure S84: Stereoscopic ORTEP[9] plot of **mt-S-S-mt** showing the atomic numbering scheme. The probability ellipsoids are drawn at the 50% probability level. The H atoms are drawn with arbitrary radii.

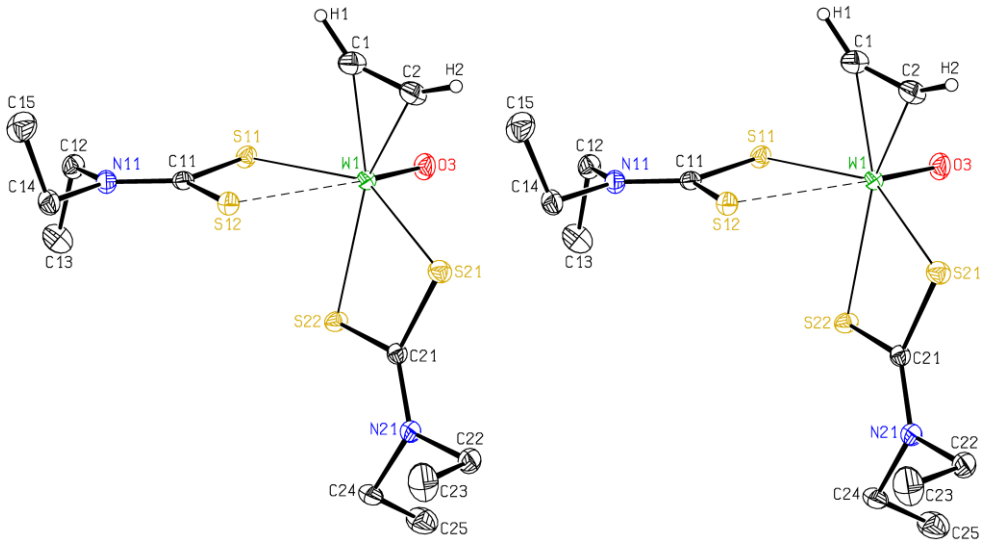

Figure S85: Stereoscopic ORTEP[9] plot of **[WO(C_2H_2)(S_2CNEt_2)$_2$]** showing the atomic numbering scheme. The probability ellipsoids are drawn at the 50% probability level. The H atoms of the acetylene ligand are drawn with arbitrary radii, the other H atoms were omitted for clarity. The rather long W–S bond [2.6962(7)Å] is plotted with a dashed line.

4.2 Selected bond lengths and angels

Table S8: Selected bond lengths [Å] and angles [°] for **1**.

W1-C1	2.055(4)	S3-C32	1.727(6)	C15-N11-B1	120.7(5)
W1-C2	2.050(5)			C22-S2-W1	108.13(19)
W1-C3	2.002(8)	C3-W1-S1	171.5(3)	C22-N21-C25	106.7(6)
W1-S1	2.5808(16)	S2-W1-Br1	162.19(5)	C22-N21-B1	130.8(5)
W1-S2	2.3907(15)	C1-W1-S3	155.76(16)	C25-N21-B1	121.7(6)
W1-S3	2.6137(18)	C2-W1-S3	163.80(14)	C32-S3-W1	107.0(2)
W1-Br1	2.6089(7)	C2-C1-H1	147.1(7)	C32-N31-C35	107.5(5)
C1-C2	1.252(7)	W1-C1-H1	140.6(6)	C32-N31-B1	130.1(5)
C3-O3	1.191(11)	C1-C2-H2	140.5(10)	C35-N31-B1	122.5(5)
B1-N31	1.543(8)	W1-C2-H2	146.4(9)		
B1-N21	1.550(8)	O3-C3-W1	179.0(9)	C1-C2-W1-S1	-177.1(4)
B1-N11	1.560(7)	C12-S1-W1	107.1(2)	C1-C2-W1-C3	1.1(7)
S1-C12	1.729(8)	C12-N11-C15	108.3(5)		
S2-C22	1.746(7)	C12-N11-B1	130.6(5)		

Table S9: Selected bond lengths [Å] and angles [°] for **1'**.

W1-C1	2.0531(18)	S3-C32	1.727(2)	C12-S1-W1	108.07(6)
W1-C2	2.0315(18)			C22-S2-W1	105.99(7)
W1-C3	1.954(2)	C3-W1-S1	170.34(6)	C32-S3-W1	105.62(7)
W1-Br1	2.5991(2)	Br1-W1-S2	162.525(13)		
W1-S1	2.6034(5)	C1-W1-S3	155.67(5)	C1-C2-W1-Br1	95.18(12)
W1-S2	2.4065(5)	C2-W1-S3	164.51(6)	C2-C1-W1-Br1	-89.38(12)
W1-S3	2.6287(5)	C2-C1-H1	144.0(8)	C1-C2-W1-C3	-0.2(5)
C1-C2	1.306(3)	W1-C1-H1	145.1(7)	C2-C1-W1-C3	179.8(4)
C3-O3	1.156(2)	C1-C2-H2	139.7(4)	C1-C2-W1-S1	178.20(17)
S1-C12	1.723(2)	W1-C2-H2	148.0(3)	C2-C1-W1-S1	-1.98(16)
S2-C22	1.7431(19)	O3-C3-W1	179.17(19)		

Table S10: Selected bond lengths [Å] and angles [°] for **2**.

W1-C1	2.050(6)	C3-O3	1.134(7)	C1-W1-S3	154.75(15)
W1-C2	2.029(6)	B1-N11	1.543(7)	C2-W1-S3	164.79(14)
W1-C3	1.971(6)	B1-N21	1.551(6)	C2-C1-C10	141.2(6)
W1-S1	2.5936(12)	B1-N31	1.571(6)	C1-C2-C20	138.5(5)
W1-S2	2.4043(13)	S1-C12	1.725(5)	O3-C3-W1	177.7(6)
W1-S3	2.6330(13)	S2-C22	1.758(5)	C12-S1-W1	110.43(16)
W1-Br1	2.6325(6)	S3-C32	1.726(6)	C22-S2-W1	107.55(17)
C1-C2	1.314(7)			C32-S3-W1	107.22(18)
C1-C10	1.484(7)	C3-W1-S1	171.22(18)		
C2-C20	1.503(7)	Br1-W1-S2	162.13(4)		

Table S11: Selected bond lengths [Å] and angles [°] for **3**.

W1-C1	2.053(5)	S3-C32	1.719(9)
W1-C2	2.036(6)	C1-C2	1.343(8)
W1-C3	1.944(7)	C1-C101	1.458(6)
W1-S1	2.595(2)	C2-C201	1.455(7)
W1-S2	2.395(2)		
W1-S3	2.612(2)	C3-W1-S1	169.2(2)
W1-Br1	2.5832(7)	Br1-W1-S2	161.35(19)
C3-O3	1.164(8)	C1-W1-S3	150.5(2)
B1-N11	1.560(16)	C2-W1-S3	160.2(2)
B1-N21	1.566(12)	O3-C3-W1	179.8(7)
B1-N31	1.541(15)	C12-S1-W1	106.2(6)
S1-C12	1.722(9)	C22-S2-W1	109.4(6)
S2-C22	1.744(8)	C32-S3-W1	104.7(8)

Table S12: Selected bond lengths [Å] and angles [°] for the two molecules of **4**.

W1-O1	1.723(6)	W2-O2	1.726(5)
W1-C1	2.096(7)	W2-C4	2.097(8)
W1-C2	2.106(7)	W2-C5	2.100(8)
W1-Br1	2.6171(8)	W2-Br2	2.6164(10)
W1-S1	2.6210(17)	W2-S4	2.5871(19)
W1-S2	2.4394(19)	W2-S5	2.493(2)
W1-S3	2.6786(17)	W2-S6	2.635(2)
C1-C2	1.262(12)	C4-C5	1.242(11)
S1-C12	1.732(7)	S4-C42	1.736(7)
S2-C22	1.769(7)	S5-C52	1.752(8)
S3-C32	1.704(8)	S6-C62	1.726(8)
C1-W1-S1	162.3(2)	C4-W2-S4	161.5(2)
C2-W1-S1	162.3(2)	C5-W2-S4	163.5(2)
Br1-W1-S2	159.81(5)	Br2-W2-S5	161.21(5)
O1-W1-S3	164.65(18)	O2-W2-S6	163.60(18)
C12-S1-W1	110.1(2)	C42-S4-W2	109.0(2)
C22-S2-W1	109.1(2)	C52-S5-W2	107.2(2)
C32-S3-W1	107.1(3)	C62-S6-W2	106.4(2)
C1-C2-W1-Br1	-14.3(5)	C4-C5-W2-Br2	-10.6(5)
C2-C1-W1-Br1	166.6(5)	C5-C4-W2-Br2	169.9(5)
C1-C2-W1-O1	89.4(5)	C4-C5-W2-O2	94.3(5)
C2-C1-W1-O1	-97.3(5)	C5-C4-W2-O2	-93.8(5)
C1-C2-W1-S2	-174.2(5)	C4-C5-W2-S5	-172.1(5)
C2-C1-W1-S2	5.9(5)	C5-C4-W2-S5	8.1(5)

Table S13: Selected bond lengths [Å] and angles [°] for **5**.

W1-O1	1.791(4)	C1-W1-S1	162.12(17)	C1-C2-W1-Br1	-16.9(4)
W1-C1	2.077(6)	C2-W1-S1	162.86(16)	C2-C1-W1-Br1	164.2(4)
W1-C2	2.114(5)	Br1-W1-S2	160.13(4)	C1-C2-W1-O1	87.8(4)
W1-Br1	2.5984(6)	O1-W1-S3	162.07(14)	C2-C1-W1-O1	-99.0(4)
W1-S1	2.6847(15)	C2-C1-C10	142.8(6)	C1-C2-W1-S2	-177.7(4)
W1-S2	2.4343(13)	C10-C1-W1	143.0(5)	C2-C1-W1-S2	2.4(4)
W1-S3	2.6501(13)	C1-C2-C20	144.3(6)		
C1-C2	1.255(8)	C20-C2-W1	144.7(4)		
B1-H10	1.04(6)	C12-S1-W1	111.23(18)		
S1-C12	1.720(6)	C22-S2-W1	107.26(17)		
S2-C22	1.750(6)	C32-S3-W1	107.14(17)		
S3-C32	1.737(5)				

Table S14: Selected bond lengths [Å] and angles [°] for **6**.

W1-C1	2.098(7)	C1-W1-S2	163.8(2)	C1-C2-W1-Br1	7.3(5)
W1-C2	2.132(6)	C2-W1-S2	159.20(19)	C2-C1-W1-Br1	-173.4(5)
W1-S1	2.3907(10)	S3-W1-S4	164.61(5)	C1-C2-W1-S4	-93.3(4)
W1-S2	2.6328(10)	S1-W1-Br1	160.97(5)	C2-C1-W1-S4	94.5(4)
W1-S3	2.6398(10)	C3-W2-S3	155.0(8)	C1-C2-W1-S1	168.2(5)
W1-S4	2.1497(13)	C4-W2-S3	167.3(9)	C2-C1-W1-S1	-11.7(5)
W1-Br1	2.6490(9)	S1-W2-S5	161.8(10)	C3-C4-W2-Br2	7.9(20)
C1-C2	1.248(9)	S2-W2-Br2	162.19(13)	C4-C3-W2-Br2	-172.0(19)
B1-N11	1.547(5)	C12-S1-W1	110.32(13)	C3-C4-W2-S5	-92.1(18)
B1-N21	1.545(5)	C22-S2-W1	110.31(13)	C4-C3-W2-S5	97.1(20)
B1-N31	1.546(5)	C32-S3-W1	105.87(14)	C3-C4-W2-S2	170.5(18)
S1-C12	1.736(4)			C4-C3-W2-S2	-10.2(20)
S2-C22	1.727(4)				
S3-C32	1.730(4)				

Table S15: Selected bond lengths [Å] and angles [°] for **7**.

W1-C1	2.069(7)	B1-N31	1.546(9)	C22-S2-W1	110.6(2)
W1-C2	2.118(7)	S1-C12	1.726(7)	C32-S3-W1	108.3(2)
W1-S10	2.1730(18)	S2-C22	1.739(7)		
W1-Br1	2.6190(8)	S3-C32	1.729(6)	C10-C1-C2-C20	2(2)
W1-S1	2.4384(16)			C1-C2-W1-Br1	27.3(5)
W1-S2	2.6351(17)	S1-W1-Br1	158.11(5)	C1-C2-W1-S1	-174.7(5)
W1-S3	2.6755(18)	S2-W1-C1	161.72(19)	C2-C1-W1-Br1	-154.4(5)
C1-C2	1.240(9)	S2-W1-C2	161.41(19)	C2-C1-W1-S1	5.5(5)
C1-C10	1.483(10)	S3-W1-S10	163.37(6)	W1-S1-C12-N11	84.3(6)
C2-C20	1.444(10)	C2-C1-C10	142.4(7)	W1-S2-C22-N21	74.8(6)
B1-N11	1.567(8)	C1-C2-C20	145.3(7)	W1-S3-C32-N31	73.6(6)
B1-N21	1.557(7)	C12-S1-W1	109.0(2)		

Table S16: Selected bond lengths [Å] and angles [°] for **8**.

W1-O1	1.715(6)	W2-S6	2.611(2)	W1-O2-W2	163.3(4)
W1-C1	2.097(10)	C1-C2	1.265(13)	C2-C1-C10	146.9(10)
W1-C2	2.092(9)	C3-C4	1.256(14)	C1-C2-C20	147.6(9)
W1-O2	2.157(6)			C12-S1-W1	97.9(3)
W1-S1	2.470(3)	O1-W1-O2	165.9(3)	C22-S2-W1	96.5(3)
W1-S2	2.508(2)	S1-W1-S2	150.99(8)	C32-S3-W2	112.3(3)
W1-H1	2.081	C1-W1-H1	148.7	C4-C3-C30	140.4(9)
W2-O2	1.772(6)	C2-W1-H1	150.7	C3-C4-C40	144.5(10)
W2-C3	2.107(9)	B1-H1-W1	131.3	C42-S4-W2	109.2(3)
W2-C4	2.120(10)	S3-W2-S4	155.97(7)	C52-S5-W2	109.2(3)
W2-S3	2.540(2)	C3-W2-S5	166.2(3)	C62-S6-W2	104.7(3)
W2-S4	2.425(2)	C4-W2-S5	158.8(3)		
W2-S5	2.642(2)	O2-W2-S6	159.2(2)		

Table S17: Selected bond lengths [Å] and angles [°] for **9**.

W1-C1	2.072(10)	C10-C1	1.464(15)	S3-W2-S4	162.31(8)
W1-C2	2.078(12)	C2-C20	1.453(17)	S21-W2-S5	173.30(8)
W1-S12	2.326(2)	B1-N11	1.481(11)	S12-W2-S6	160.72(8)
W1-S21	2.380(2)	B1-N31	1.503(13)	C2-C1-C10	146.1(12)
W1-S1	2.510(3)	B1-N21	1.525(10)	C1-C2-C20	149.4(12)
W1-S2	2.502(3)	B2-N41	1.502(13)	W2-S12-W1	75.79(8)
W1-H1	2.129(15)	B2-N51	1.510(10)	W2-S21-W1	74.86(8)
W2-S21	2.254(3)	B2-N61	1.543(10)	C12-S1-W1	101.8(4)
W2-S12	2.262(2)			C22-S2-W1	107.7(4)
W2-S3	2.495(3)	S21-W1-S1	153.38(10)	C32-S3-W2	113.0(4)
W2-S4	2.377(2)	S12-W1-S2	166.78(10)	C42-S4-W2	105.5(3)
W2-S5	2.466(2)	C1-W1-H1	163.2(5)	C52-S5-W2	113.4(3)
W2-S6	2.600(2)	C2-W1-H1	155.0(4)	C62-S6-W2	110.2(4)
C1-C2	1.313(15)	B1-H1-W1	141.2(12)		

Table S18: Selected bond lengths [Å] and angles [°] for **[WCl_3Tm^{Me}]**.

W1-Cl1	2.4354(12)	B1-N21	1.543(7)	Cl1-W1-S1	176.13(5)
W1-Cl2	2.4261(13)	B1-N31	1.564(7)	Cl2-W1-S2	169.52(5)
W1-Cl3	2.3176(16)	S1-C12	1.741(6)	Cl3-W1-S3	170.59(5)
W1-S1	2.5019(14)	S2-C22	1.754(6)	C12-S1-W1	106.3(2)
W1-S2	2.4278(15)	S3-C32	1.732(6)	C22-S2-W1	105.00(19)
W1-S3	2.4949(14)			C32-S3-W1	107.11(19)
B1-N11	1.556(8)				

Table S19: Selected bond lengths [Å] and angles [°] for **[WCl_3Tm^{Me}] · 3 $CDCl_3$**.

W1-Cl1	2.356(4)	B1-N11	1.559(10)	Cl1-W1-S1	170.74(9)
W1-S1	2.488(3)	S1-C12	1.733(10)	C12-S1-W1	107.6(3)

Table S20: Selected bond lengths [Å] and angles [°] for **[$W(CO)(C_2Me_2)_2(MeCN)Br_2$]**.

W1-C1	2.020(3)	W1-Br1	2.6456(4)	C1-W1-N1	163.45(12)
W1-C11	2.114(3)	W1-Br2	2.6817(4)	C13-W1-Br1	162.09(10)
W1-C12	2.070(3)	C1-O1	1.136(4)	C14-W1-Br1	158.25(9)
W1-C13	2.080(3)			C11-W1-Br2	158.64(9)
W1-C14	2.127(3)			C12-W1-Br2	163.35(10)
W1-N1	2.185(3)			O1-C1-W1	177.5(3)

Table S21: Selected bond lengths [Å] and angles [°] for the two complexes of **[$W(CO)(C_2Me_2)_2(MeCN)Br_2$]'**.

W1-C1	2.015(5)	W2-C2	2.000(5)
W1-C11	2.122(4)	W2-C21	2.130(5)
W1-C12	2.069(5)	W2-C22	2.076(5)
W1-C13	2.079(5)	W2-C23	2.070(5)
W1-C14	2.131(5)	W2-C24	2.131(5)
W1-N1	2.166(4)	W2-N2	2.175(4)
W1-Br11	2.6668(5)	W2-Br21	2.6600(5)
W1-Br12	2.6591(5)	W2-Br22	2.6684(5)
C1-O1	1.132(6)	C2-O2	1.142(6)

C1-W1-N1	164.95(17)	C2-W2-N2	164.40(17)
C13-W1-Br11	161.77(13)	C23-W2-Br21	161.63(13)
C14-W1-Br11	159.51(13)	C24-W2-Br21	157.82(12)
C11-W1-Br12	155.44(13)	C21-W2-Br22	157.36(13)
C12-W1-Br12	164.25(14)	C22-W2-Br22	163.84(13)
O1-C1-W1	177.8(4)	O2-C2-W2	178.0(4)
C12-C11-C110	148.3(5)	C22-C21-C210	146.4(5)
C11-C12-C120	144.9(5)	C21-C22-C220	144.5(5)
C14-C13-C130	146.7(5)	C24-C23-C230	145.9(5)
C13-C14-C140	147.8(5)	C23-C24-C240	148.6(5)

C110-C11-C12-C120	-2.1(15)	C210-C21-C22-C220	-1.7(14)
C130-C13-C14-C140	3.2(14)	C230-C23-C24-C240	-1.1(14)

Table S 22: Selected bond lengths [Å] and angles [°] for **[W(CO)(C_2Ph_2)$_2$(MeCN)Br_2]**.

W1-C1	2.026(3)	C1-W1-N1	160.06(12)
W1-C11	2.097(3)	C13-W1-Br1	161.56(9)
W1-C12	2.081(3)	C14-W1-Br1	159.27(8)
W1-C13	2.105(3)	C11-W1-Br2	153.79(8)
W1-C14	2.130(3)	C12-W1-Br2	165.27(9)
W1-N1	2.168(3)	Br1-W1-Br2	82.71(3)
W1-Br1	2.6351(4)	O1-C1-W1	177.3(3)
W1-Br2	2.6455(4)		
C1-O1	1.135(4)	C12-C11-C111	145.8(3)
C11-C12	1.304(4)	C11-C12-C121	141.9(3)
C13-C14	1.283(4)	C14-C13-C131	147.4(3)
N1-C15	1.135(4)	C13-C14-C141	146.7(3)
C15-C16	1.451(5)		

Table S23: Selected bond lengths [Å] and angles [°] for the two molecules of **[W(CO)(C_2Ph_2)$_2$(MeCN)Br_2]'**.

W1-C1	2.039(10)	W2-C2	2.042(10)
W1-C12	2.078(9)	W2-C21	2.125(9)
W1-C13	2.086(9)	W2-C22	2.128(9)
W1-C14	2.107(9)	W2-C23	2.039(9)
W1-C11	2.108(9)	W2-C24	2.106(9)
W1-N1	2.165(8)	W2-N2	2.165(8)
W1-Br11	2.6359(10)	W2-Br21	2.6678(10)
W1-Br12	2.6714(10)	W2-Br22	2.6339(10)
C1-O1	1.147(10)	C2-O2	1.137(10)
C11-C12	1.279(12)	C21-C22	1.302(12)
C13-C14	1.309(11)	C23-C24	1.270(11)
N1-C15	1.120(11)	N2-C25	1.142(11)
C15-C16	1.462(13)	C25-C26	1.466(12)
C1-W1-N1	157.3(3)	C2-W2-N2	160.3(3)
C13-W1-Br11	161.2(2)	C23-W2-Br21	165.2(3)
C14-W1-Br11	156.0(2)	C24-W2-Br21	156.4(2)
C11-W1-Br12	160.0(3)	C21-W2-Br22	161.4(3)
C12-W1-Br12	163.4(3)	C22-W2-Br22	159.9(2)
Br11-W1-Br12	83.20(3)	Br21-W2-Br22	85.17(3)
O1-C1-W1	175.8(8)	O2-C2-W2	176.1(9)
C12-C11-C111	143.5(9)	C22-C21-C211	144.5(9)
C11-C12-C121	141.9(9)	C21-C22-C221	153.2(9)
C14-C13-C131	146.5(9)	C24-C23-C231	141.1(9)
C13-C14-C141	142.3(9)	C23-C24-C241	143.2(9)

Table S24: Selected bond lengths [Å] and angles [°] for **mt-S-S-mt**.

S1-C2	1.7389(9)	N3-C2-N1	111.64(8)	C2-S1-S1$^{i)}$-C2$^{i)}$	-62.29(4)
S1-S1$^{i)}$	2.1003(5)	N3-C2-S1	123.75(6)	S1$^{i)}$-S1-C2-N3	101.18(8)
C2-S1-S1$^{i)}$	101.60(3)	N1-C2-S1	124.59(7)	S1$^{i)}$-S1-C2-N1	-77.03(8)

Symmetry transformations used to generate equivalent atoms:
$^{i)}$ 1-x, y, 3/2-z

Table S25: Selected bond lengths [Å] and angles [°] for **[WO(C_2H_2)(S_2CNEt_2)$_2$]**

W1-C1	2.092(2)	S11-W1-S21	146.764(18)
W1-C2	2.112(2)	C1-W1-S22	160.06(7)
W1-O3	1.7137(16)	C2-W1-S22	148.79(6)
W1-S11	2.5302(6)	O3-W1-S12	159.20(6)
W1-S12	2.6962(7)	S12-W1-S22	79.37(2)
W1-S21	2.4379(6)	C2-C1-H1	141.6(8)
W1-S22	2.5397(6)	C1-C2-H2	148.2(5)
C1-C2	1.282(3)	C11-S11-W1	91.31(7)
S11-C11	1.737(2)	C11-S12-W1	86.45(7)
S12-C11	1.710(2)	C21-S21-W1	90.22(7)
S21-C21	1.743(2)	C21-S22-W1	87.46(7)
S22-C21	1.717(2)		

5 REFERENCES

[1] J. S. Figueroa, K. Yurkerwich, J. Melnick, D. Buccella, G. Parkin, *Inorg. Chem.* **2007**, *46*, 9234–9244.

[2] L. M. Peschel, J. A. Schachner, C. H. Sala, F. Belaj, N. C. Mösch-Zanetti, *Z. anorg. allg. Chem.* **2013**, *639*, 1559–1567.

[3] A. Braendle, C. Vidovič, N. C. Mösch-Zanetti, M. Niederberger, W. Caseri, *Polymers* **2018**, *10*, 881.

[4] P. K. Baker, D. J. Muldoon, A. J. Lavery, A. Shawcross, *Polyhedron* **1994**, *13*, 2915–2921.

[5] C. Vidovič, L. M. Peschel, M. Buchsteiner, F. Belaj, N. C. Mösch-Zanetti, *Chem. Eur. J.* **2019**, *25*, 14267–14272.

[6] M. Garner, M.-A. Lehmann, J. Reglinski, M. D. Spicer, *Organometallics* **2001**, *20*, 5233–5236.

[7] Sheldrick, G. M. A short history of SHELX. *Acta Crystallogr. Sec. A, Found. Crystallogr.* **2008**, *64*, 112–122.

[8] Sheldrick, G. M. Acta Cryst. **2015**, *C71*, 3-8.

[9] Johnson, C. K. ORTEP. Report ORNL-3794. Oak Ridge National Laboratory, Tennessee, USA, **1965**.